

THE FUNCTION OF THE INFLUENZA A VIRUS M2 PROTEIN

BY

CAROL ANN THOMPSON

A thesis submitted in part fulfillment of the requirements of the University of London for the Degree of Doctor of Philosophy.

Division of Virology,
National Institute for Medical Research,
Mill Hill,
London NW7 1AA.

JANUARY 1994

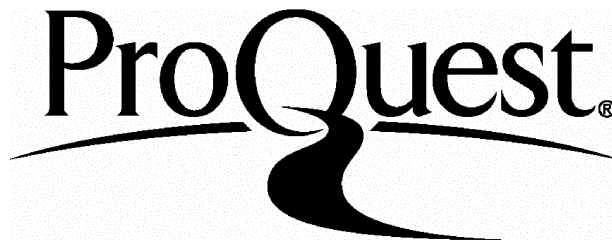
ProQuest Number: 10106924

All rights reserved

INFORMATION TO ALL USERS

The quality of this reproduction is dependent upon the quality of the copy submitted.

In the unlikely event that the author did not send a complete manuscript and there are missing pages, these will be noted. Also, if material had to be removed, a note will indicate the deletion.



ProQuest 10106924

Published by ProQuest LLC(2016). Copyright of the Dissertation is held by the Author.

All rights reserved.

This work is protected against unauthorized copying under Title 17, United States Code.
Microform Edition © ProQuest LLC.

ProQuest LLC
789 East Eisenhower Parkway
P.O. Box 1346
Ann Arbor, MI 48106-1346

TO MUM AND DAD

ABSTRACT

The influenza A virus M2 protein is a 70kDa transmembrane protein which forms an ion permeable channel. The specific inhibition of M2 by the antiviral drug amantadine has identified two roles of the protein, in virus uncoating and in the maturation of haemagglutinin (HA). With respect to the latter M2 has been shown to have the ability to modify pH.

Immunofluorescence studies using monoclonal antibodies specific for the native and low pH forms of HA showed that the inhibition of M2 causes a pH-induced conformational change in HA within the trans-Golgi or trans-Golgi network (TGN). Consistent with its role in modifying the pH of transport vesicles transferring native HA to the cell surface, M2 was found to colocalize with both conformations of HA.

In view of the pH changes observed within the vesicles of the transport pathway, the pH of the cell cytoplasm was studied directly using the fluorescent pH probe SNARF-1. Influenza virus infection was shown to reduce the pH of the cell cytoplasm. At 6 hours p.i. a 0.4pH unit difference was observed between the pH of uninfected and Rostock virus-infected MDCK cells, which effectively abolished the pH gradient across the plasma membrane. The change in cytoplasmic pH was shown to be M2-dependent by its specific reversal by amantadine and inhibition by antiserum against the exposed N-terminus of M2. Similar M2-induced changes in pH were also observed in M2-expressing MEL cells. Further evidence suggests that M2 located in the plasma membrane is responsible for these effects. In addition to its role in modifying the pH within the transport pathway, these studies show that M2 can also affect the pH of the cell cytoplasm, in a manner which is consistent with the transfer of protons.

CONTENTS

	<u>Page</u>
Abstract	iii
Contents	iv
List of Tables	vii
List of Figures	viii
Acknowledgements	xi
Abbreviations	xii

INTRODUCTION

Introduction	2
1.1 Classification	3
1.2 Virion structure	3
1.3 Genetic and antigenic variation	12
- Antigenic drift	13
- Antigenic shift	15
1.4 Viral replication	18
- Attachment and entry	18
- Gene expression and replication	21
- Protein synthesis, assembly and release	26
1.5 Prevention and treatment of influenza	30
- Vaccination	30
- Antiviral agents	32
i) Attachment and entry	33
ii) Viral replication	35
iii) Assembly and release	38
iv) Amantadine and rimantadine	39
1.6 The ion channel activity of the M2 protein and its role in viral replication	41
1.7 Project aims	46

MATERIALS AND METHODS

2.1 Virus growth and titration	49
- Virus growth	49
- UV-inactivation of virus	49
- Plaque assay	49
2.2 Tissue culture	50

- Cells	50
- Infection of cells	51
2.3 Radiolabelling of cells	52
- [³⁵ S] pulse-chase labelling	52
- [³ H] palmitic acid labelling	52
2.4 Immunological methods	53
- Antibodies	53
- Immunofluorescence	53
- Enzyme-linked immunosorbant assay (ELISA)	55
- Immunoblotting	55
- Immunoprecipitation	56
2.5 Polyacrylamide gel electrophoresis	56
2.6 Determination of cytoplasmic pH	57
2.7 Flow cytometric measurement of cytoplasmic pH	58
2.8 Materials	59

RESULTS

3.1 Conformational changes in HA and the pH of transport vesicles	61
- The effect of brefeldin A on HA and M2 protein	72
3.2 Cytoplasmic pH changes within virus-infected cells	80
- Reduction in the cytoplasmic pH of virus-infected MDCK cells	87
- Evidence for the involvement of M2 in the cytoplasmic pH reduction	91
- The relationship between M2 and the cytoplasmic pH	100
- Differences in the drug sensitivity of different M2 proteins	108
- The effect of varying ionic conditions on the M2-specific pH change in virus-infected cells	115
- M2-specific pH changes within other influenza virus-infected cell systems	121
3.3 Cytoplasmic pH changes within M2-expressing cells	128

- M2-expressing baculovirus-infected cells	128
- M2-expressing MEL cells	129
- The inhibition of Weybridge M2 protein expressed in MEL cells	137
- Flow cytometric analysis of the pH changes within M2-expressing MEL cells	141

DISCUSSION

4.1 pH changes within HA-containing transport vesicles	147
4.2 Cytoplasmic pH changes within virus-infected cells	153

REFERENCES

171

LIST OF TABLES

<u>INTRODUCTION</u>	<u>Page</u>
I Influenza virus RNA segments and coding assignments	22
 <u>RESULTS</u>	
1 The inactivation of Rostock virus by ultraviolet light (254nm), as determined by plaque assay	92
2 The effect of 5 μ M amantadine on the cytoplasmic pH of MDCK cells infected with amantadine-resistant viruses	95
3 Inhibition of the M2-mediated change in cytoplasmic pH by anti-M2 antiserum	98
4 The effect of BFA on the cytoplasmic pH of Rostock-infected MDCK cells	99
5 The composition of Gey's, 0mM Na ⁺ , 30mM Na ⁺ , 0mM Cl ⁻ and 30mM Cl ⁻ media	116
6 The cytoplasmic pH of MDCK cells incubated under different ionic conditions	118
7 The cytoplasmic pH of various cell types infected with Rostock virus (6 hours p.i.)	122
8 The effects of amantadine and rimantadine on cytoplasmic pH changes within MDCK cells infected with different influenza viruses	126
9 The effects of nigericin, rimantadine and R53 antiserum on the cytoplasmic pH of MEL cells	136

LIST OF FIGURES

<u>INTRODUCTION</u>		<u>Page</u>
I	A schematic representation of the structure of the influenza A virion	5
II	A schematic representation of the 3-D structure of the Hong Kong virus HA monomer	8
III	A representation of the splicing events required for the synthesis of the M2 polypeptide from RNA segment 7	25
IV	The structures of the anti-influenza compounds amantadine, rimantadine and ribavirin	36
V	A schematic representation of the proposed roles of the influenza A M2 protein in the viral replication cycle	42
VI	A. The primary structure of the A/Chicken/Germany/34 ('Rostock') virus M2 protein B. A representation of the proposed channel structure of the A/chicken/Germany/27 ('Weybridge') M2 transmembrane domain (residues 24-44)	45
<u>RESULTS</u>		
1	The effects of amantadine on the expression of HA in Rostock-infected CEF cells	62
2	The effects of amantadine on the expression of HA in Rostock-infected MDCK cells	64
3	The effect of amantadine on the distribution of HA in MDCK cells infected with the amantadine-resistant 08 virus	65
4	The distribution of HA within Rostock-infected MDCK cells with respect to WGA	68
5	The effect of amantadine on the distribution of M2 protein in Rostock-infected MDCK cells	69
6	The distribution of M2 protein within Rostock-infected MDCK cells with respect to HA and WGA	71
7	The distribution of HA and M2 protein in Rostock-infected MDCK cells in the presence of BFA, as observed by immunofluorescence	73
8	The effect of BFA on the amount of HA detected in Rostock-infected MDCK cells by ELISA	75

9	The effect of BFA on palmitoylation and HA0 cleavage in Rostock-infected MDCK cells	77
10	The effect of BFA on the distribution of HA and M2 protein within amantadine-treated cells	79
11	Calibration curves for BCECF and SNARF-1	82
12	The reduction in the cytoplasmic pH of uninfected MDCK cells in Gey's+20mM Hepes, pH7.10 by the addition of various concentrations of nigericin	84
13	Comparison of the 'in vitro' and 'in vivo' calibration of SNARF-1	85
14	The distribution of SNARF-1 in uninfected and infected MDCK cells as observed by fluorescence microscopy	88
15	The effect of amantadine on the emission spectra (excitation 534nm) of SNARF-1, in uninfected and infected MDCK cells	89
16	The effect of cycloheximide on the cytoplasmic pH decrease observed in Rostock-infected MDCK cells	90
17	The specific reversal by amantadine of the reduced cytoplasmic pH in Rostock-infected MDCK cells	94
18	Reversal of the M2-mediated change in cytoplasmic pH by anti-M2 antiserum	97
19	Comparison between the synthesis of M2 and the reduction in cytoplasmic pH in Rostock-infected MDCK cells	101
20	Comparison between the synthesis of M2 and the reduction in cytoplasmic pH in 039-infected MDCK cells	102
21	Comparison between the synthesis of M2 and the reduction in cytoplasmic pH in 08-infected MDCK cells	103
22	The ratio of the change in cytoplasmic pH to the change in the amount of M2 protein, with respect to time p.i.	106
23	Comparison between the synthesis of M2 and the reduction in cytoplasmic pH in Weybridge-infected cells	107
24	The effect of various concentrations of amantadine and rimantadine on the cytoplasmic pH of Rostock-infected MDCK cells	110
25	The effect of various concentrations of amantadine and rimantadine on the cytoplasmic pH of Weybridge-infected MDCK cells	112
26	Reversal of the reduced cytoplasmic pH in Rostock and Weybridge-infected MDCK cells, by amantadine, rimantadine	114

	and cyclooctylamine	
27	The cytoplasmic pH of uninfected and Rostock-infected MDCK cells incubated in Gey's, adjusted to various pHs	120
28	The production of M2 protein in various Rostock-infected cell types, as detected by immunoblotting	124
29	M2 production in MDCK cells infected with different influenza A viruses as detected by immunoblotting	127
30	Calibration curve for SNARF-1 in Sf9 spodoptera cells	130
31	The distribution of SNARF-1 in control and M2-expressing MEL cells, as observed by fluorescence microscopy	132
32	Calibration curve for SNARF-1 in MEL cells	133
33	M2 production in DMSO-induced C39 MEL cells in relation to the reduction in cytoplasmic pH	134
34	The effect of various concentrations of amantadine and rimantadine on the cytoplasmic pH of M2-expressing C39 MEL cells	138
35	Inhibition of the M2-specific decreases in the cytoplasmic pH of C39 MEL cells, by amantadine, rimantadine and cyclooctylamine	140
36	Flow cytometric analysis of the pH changes in SNARF-1 loaded MEL cells	142
37	Comparison of the 640/580nm emission ratios of SNARF-1 loaded MEL cells, as determined by flow cytometry	145

ACKNOWLEDGEMENTS

I wish to thank and acknowledge the help of the following people:-

my supervisor Dr. Alan Hay for his advice and helpful discussions over the past three years

my colleagues in the laboratory, in particular Seti Grambas for all her help and technical advice, Finola Geraghty for supplying the MEL cells and Cornelia Schroeder for supplying the M2-expressing baculovirus.

Chris Atkins for carrying out the EPICS analysis

Neil Papworth and Jim Burt for their technical assistance with the fluorescence microscope

all the members of the Photography and Graphics Department who have helped in the production of the figures for this thesis

the Medical Research Council for their financial support

my parents and Euan for their support and encouragement over the past three years.

ABBREVIATIONS

anti-DNP	Anti-dinitrophenol antibody
BCECF	2',7'-bis-(2-carboxyethyl)-5-carboxyfluorescein
BCECF-AM	2',7'-bis-(2-carboxyethyl)-5-carboxyfluorescein acetoxymethyl ester
BFA	Brefeldin
BHK cells	Baby hamster kidney cells
BSA	Bovine serum albumin
CD	Circular dichroism
CEF cells	Chick embryo fibroblast cells
cRNA	Complementary RNA
CS	Calf serum
DAMP	3-(2,4-dinitroanilino)-3'-amino-N-methyldipropylamine
DMSO	Dimethyl sulphoxide
dH ₂ O	Distilled water
EDTA	Ethylenediaminetetraacetic acid
ELISA	Enzyme-linked immunosorbant assay
ER	Endoplasmic reticulum
FCS	Foetal calf serum
FITC	Fluorescein isothiocyanate
FSC	Forward light scatter
GAR-FITC	Goat anti-rabbit IgG-FITC conjugate
GAR-TRITC	Goat anti-rabbit IgG-TRITC conjugate
HA	Haemagglutinin
KLH	Keyhole limpet haemocyanin
M1 protein	Matrix protein
MDCK cells	Madin-Darby canine kidney cells
MEL cells	Murine erythroleukaemia cells

MEM	Minimal essential medium
m.o.i.	Multiplicity of infection
mRNA	Messenger RNA
NA	Neuraminidase
NMDG	N-methyl-D-glucamine
NP	Nucleoprotein
PBS	Phosphate buffered saline
p.f.u.	Plaque forming units
p.i.	Post infection
PMSF	Phenylmethanesulphonyl fluoride
RAM-FITC	Rabbit anti-mouse IgG-FITC conjugate
RAM-TRITC	Rabbit anti-mouse IgG-TRITC conjugate
RER	Rough endoplasmic reticulum
RNP	Ribonucleoprotein
RT	Room temperature
SDS	Sodium dodecyl sulphate
SNARF-1	Seminaphthorhodafluor-1
SNARF-1-AM	Seminaphthorhodafluor-1-acetoxymethyl ester
SSC	Side light scatter
TRITC	Tetramethylrhodamine isothiocyanate
TGN	Trans-Golgi network
TMB	Tetramethyl benzidine dihydrochloride
vRNA	Viral RNA
WGA-TRITC	TRITC-labelled wheatgerm agglutinin

INTRODUCTION

INTRODUCTION

Influenza is an acute respiratory disease which results in considerable human morbidity and mortality. It is the most significant cause of viral respiratory disease in humans and throughout history worldwide pandemics and epidemics have claimed millions of lives.

The disease is usually mild in otherwise healthy individuals, severe illness and death largely being confined to the elderly and immunocompromised. The impact of influenza in economic terms is however considerable. New pandemic strains also pose a much more serious threat having the potential to decimate whole populations regardless of age or immune status. Over 20 million deaths worldwide resulted from the 'Spanish flu' outbreak of 1918 alone. The ability of the influenza viruses to alter their antigenic makeup and avoid the immune response poses problems for vaccine production as vaccines must reflect the current circulating strains. At present the antiviral agent amantadine and its close relative rimantadine are the only effective prophylactic and therapeutic drugs available for use against influenza.

1.1 CLASSIFICATION

The group of viruses responsible for influenza belong to the orthomyxovirus group of enveloped RNA viruses. They are divided into three main types (A, B and C) on the basis of antigenic differences between their nucleoproteins (NP) and matrix (M1) proteins. Influenza B and C viruses are primarily human pathogens. There are however exceptions as an influenza C virus has been isolated from swine in China (Guo et al., 1983) and more recently from dogs (Manuguerra and Hannoun, 1992). Influenza B virus has also been isolated from swine (Takatsy et al., 1967). Type A influenza viruses infect a number of other animal species including swine, horses, seals and birds. They are further subdivided on the basis of fourteen haemagglutinin (HA) and nine neuraminidase (NA) subtypes.

Influenza viruses are designated on the basis of type, host, geographical origin, strain number and year of isolation e.g. A/Equine/Miami/1/63 (Human subtypes omit their host origin e.g. A/Singapore/1/57). The majority of work contained within this thesis relates to type A influenza viruses unless otherwise stated.

1.2 VIRION STRUCTURE

Influenza virions, with the exception of certain filamentous forms found in fresh isolates (reviewed by Wrigley, 1979), are roughly spherical in shape with a

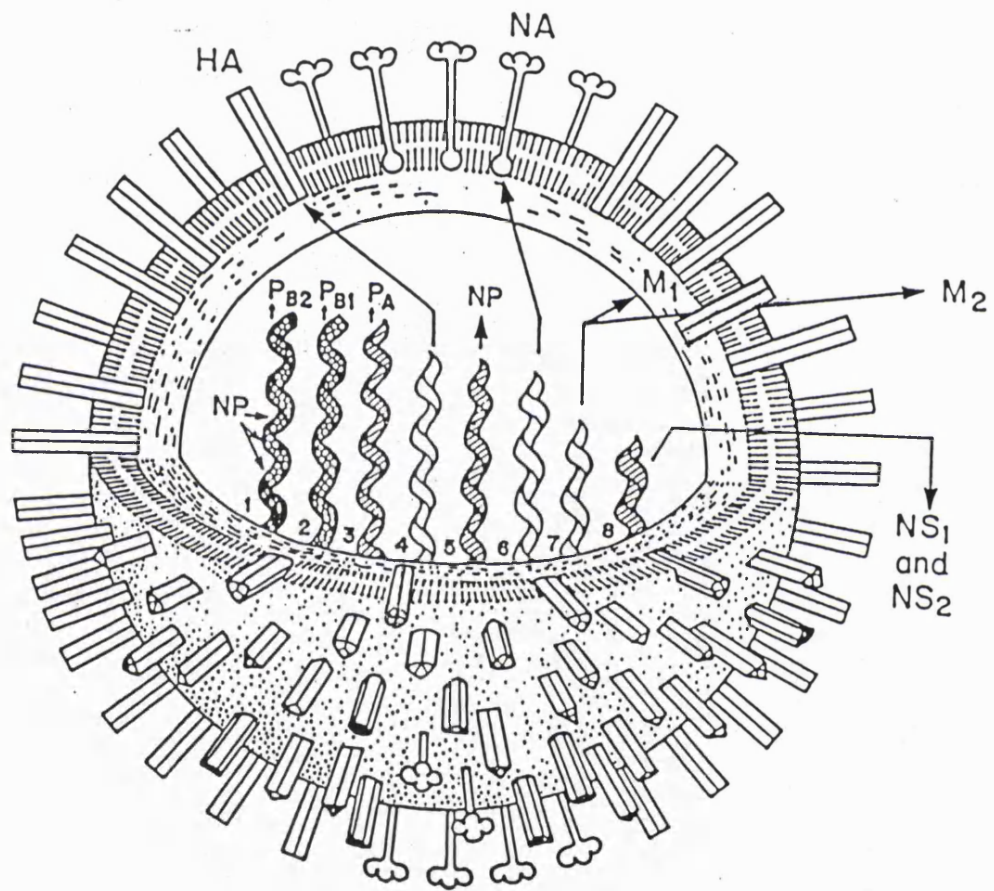
diameter of approximately 100nm. Located in the centre of the virus particle is the ribonucleoprotein (RNP) core. This appears helical in structure when observed by electron microscopy (Murthi et al., 1980; Murthi et al., 1992; Wrigley, 1979) and consists of four virally encoded proteins in close association with the RNA genome. The genome is comprised of eight single stranded segments of negative sense RNA which form a complex with nucleoprotein (NP) (Pons, 1975). NP is an arginine rich, basic protein (Hoyle and Davis, 1961) that binds to viral RNA, having a structural role in forming the RNP core and a putative role in RNA replication. The latter is indicated by the defects in RNA synthesis exhibited by temperature-sensitive mutants and by the inhibition of virion transcriptase activity by NP-specific monoclonal antibodies (Almond and Felsenreich, 1982; Beaton and Krug, 1986; Hamaguchi et al., 1985; van Wyke et al., 1981). NP is also one of four phosphoproteins found within the virion, although the significance of this feature remains to be determined (Almond and Felsenreich, 1982; Petri and Dimmock, 1981).

Associated with the end of each RNA segment is a RNA dependent RNA polymerase (Murthi et al., 1988) which is composed of the three largest viral polypeptides. Two of the polypeptides are basic (PB1 and PB2) and the other acidic (PA) (Horisberger, 1980). Each virion contains 12-15 copies of each the three polymerase proteins (Inglis et al., 1976; Skehel and Schild, 1971).

Surrounding and intimately associated with the RNP core

Figure I:

A schematic representation of the structure of the influenza A virion. The internal RNP core contains the 8 vRNA segments (each of which encode one or two proteins), NP and the three polymerase proteins (PB1, PB2 and PA). Surrounding the core and in close association with the viral envelope is the M1 protein shell. Embedded within the envelope are small amounts of M2 protein and the two major glycoproteins HA and NA.



is an electron dense layer of matrix (M1) protein approximately 6nm thick (Apostolov and Flewett, 1969; Kawakami and Ishihama, 1983; Rees and Dimmock, 1981; Ruigrok et al., 1989). M1 is the smallest and yet most abundant of the viral proteins accounting for approximately 40% of the virion mass. It is hydrophobic in nature and subject to phosphorylation (Gregoriades et al., 1984; Gregoriades et al., 1990), the significance of which is not understood. M1 is involved structurally in maintaining the integrity of the virion core and may also have a number of other functions including a role in the regulation of transcription (Hankins et al., 1990; Ye et al., 1987). Recently it has been reported that M1 is involved in the nuclear-cytoplasmic transport of the negative-sense viral RNAs (Enami et al., 1993; Martin and Helenius, 1991b).

The virion is ultimately surrounded by a lipid envelope derived from the host cell plasma membrane. This is acquired during virus budding and as such its lipid composition reflects that of the host cell (reviewed by Choppin and Compans 1975; Kates et al., 1961). Embedded in the envelope are the two major viral glycoproteins haemagglutinin (HA) and neuraminidase (NA). These appear in electron micrographs as distinctive 'spike' and 'mushroom' shaped structures respectively, protruding from the virion surface in a ratio of approximately 5:1 (Laver and Valentine, 1969; Wrigley, 1979).

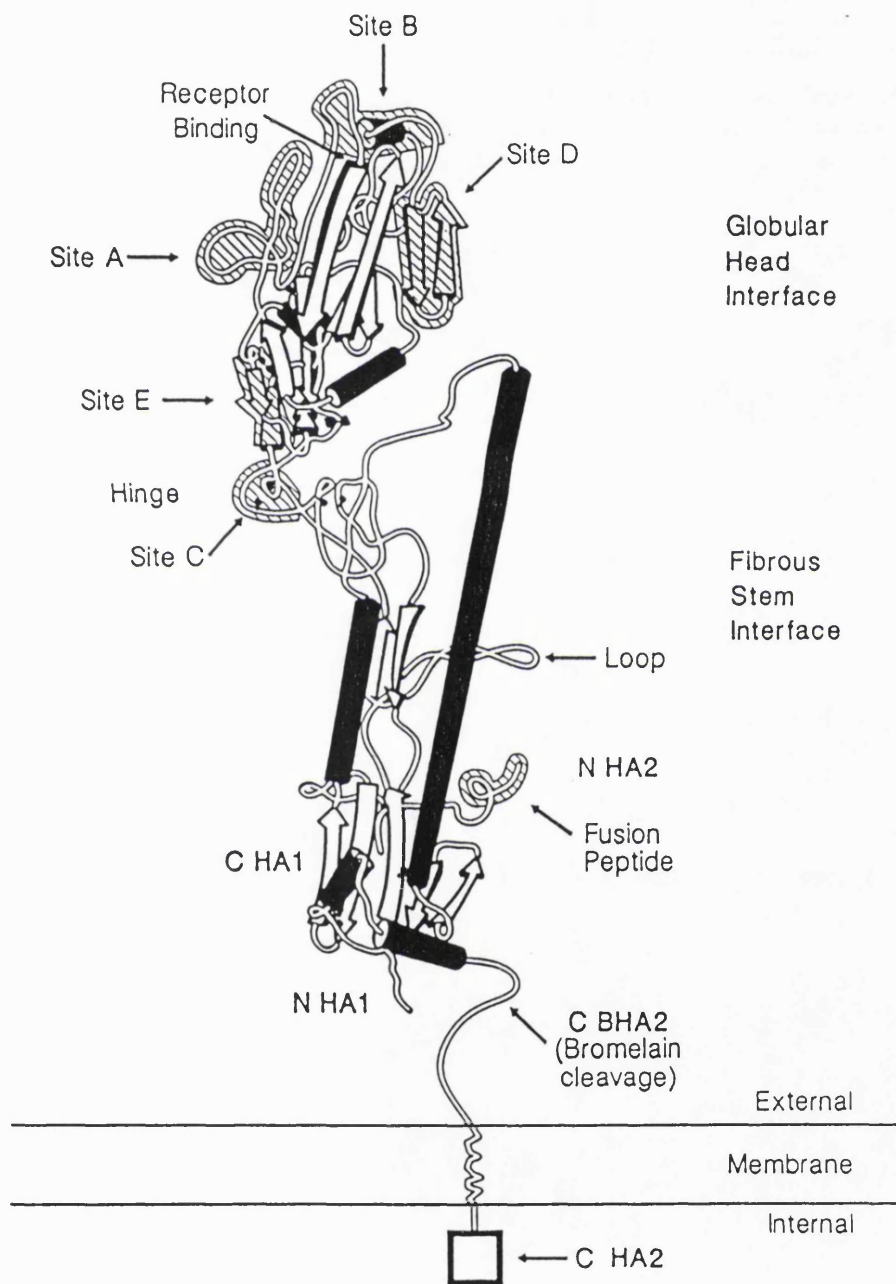
HA is distributed evenly across the virion surface and accounts for 25% of viral protein (Murti and Webster,

1986). It binds to sialic acid-containing receptors on the cell surface, allowing virus attachment and subsequent entry into the host cell cytoplasm by a HA-mediated membrane fusion event (see 1.5, pp.19-20). HA is also the major surface antigen against which neutralizing antibodies are produced (reviewed by Wiley and Skehel, 1987). Thus variation in the antigenicity of HA is primarily responsible for the emergence of new epidemic strains (see 1.4).

The HA protein is a 224,640 Dalton trimer (Wiley et al., 1977; reviewed by Wiley and Skehel, 1987). Each monomeric unit is synthesized as a single polypeptide chain HA0, which is subsequently cleaved into two disulphide linked subunits HA1 (36,334 Daltons) and HA2 (25,750 Daltons) (Wiley et al., 1977). Postranslational cleavage of HA is necessary for its fusion activity (Wiley and Skehel, 1987), but not for the binding of sialic acid (Klenk et al., 1975; Larowitz et al., 1973). Other postranslational modifications include the removal of a 16 amino acid N-terminal signal sequence, palmitoylation (Naeve and Williams, 1990; Veit et al., 1990) and glycosylation (Ward, 1981; Waterfield et al., 1980; Wiley and Skehel, 1987).

The three dimensional structure of HA has been determined by X-ray crystallography (Figure II) and found to consist of two structurally distinct regions (Wilson et al., 1981). A long fibrous 'stalk' (HA1 and HA2) extends

Figure II: A schematic representation of the 3-D structure of the Hong Kong virus HA monomer, showing the folding of the HA1 and HA2 polypeptides. The globular head region of anti-parallel β sheets (flat arrows) contains the receptor binding site surrounded by five antigenic sites A to E (shaded areas). Supporting the head is an α -helical (black cylinders) stem region which is anchored into the membrane by the C-terminus of HA2. The N-terminal or fusion peptide of HA2 is usually buried within the trimer, but extruded during low pH fusion (see 1.5).



from the membrane containing a triple coiled coil of α -helices, attached to a globular 'head' (HA1) containing β -pleated sheets. The structure of the protein complexed with its sialic acid receptor has been determined (Weis et al., 1988) and from this the receptor binding region identified. This exists as a 'pocket' or 'depression' of conserved amino acids, within the region of the proteins globular head. The C-terminus of HA2 anchors the protein into the virus envelope with 15 C-terminal residues on the cytoplasmic side.

Neuraminidase accounts for 5-10% of the virus protein and exists as a disulphide linked tetramer (reviewed by Air and Laver, 1989). Each of the monomeric units consists of a single polypeptide chain of approximately 60kD which is anchored in the virus envelope by a N-terminal hydrophobic sequence (Fields and Winter, 1981; Blok et al., 1982). The three dimensional structure of two neuraminidase subtypes N2 (A/Tokyo/3/67) (Varghese and Colman, 1991; Varghese et al., 1983) and N9 (A/tern/Australia/G70c/75) (Tulip et al., 1991) have been determined. Both have similar box-shaped heads (100x100x60 A) composed of four coplanar roughly spherical subunits attached centrally to a 'stalk' embedded in the viral membrane. The length of the stalk is highly variable and may influence the virus host range (Castrucci and Kawaoka, 1993).

NA catalyses the cleavage of the α -ketosidic linkage between terminal sialic acids and their adjacent sugar residues (Gottschalk, 1957; Klenk et al., 1955). The

structure of the neuraminidase-sialic acid complex has been determined (Varghese et al., 1992) and the sialidase activity located to the head region (Colman et al., 1983; Laver, 1978).

The role of NA in the viral replication cycle remains unclear. In general it may facilitate the movement of virus to and from the site of infection, influencing the spread of the infection (Gottschalk, 1966). The removal of sialic acid probably aids the transport of virus through the mucin layer of the respiratory tract. Mutants of NA (Palese et al., 1974) and also the presence of NA inhibitors (Palese and Compans, 1976) causes the formation of virus aggregates on the surface of infected cells. These observations suggest that the removal of sialic acid from HA, NA itself and cell surface receptors is necessary to prevent self aggregation (Griffin et al., 1983) and to promote the release of viral progeny (Griffins and Compans, 1979; Palese et al., 1974). Antibodies directed against NA are not neutralizing but do restrict the release of virus. The three dimensional structure of an antibody-neuraminidase complex has been determined (Colman et al., 1987).

Also located within the viral envelope is the M2 protein which is the focus of this investigation. It has been proposed that the M2 protein is an ion permeable channel which plays an important role in virus uncoating and maturation (refer 1.7, pp.41-44). The protein is a 70 kDa transmembrane protein encoded by a spliced mRNA of the

M gene (RNA segment 7) (Lamb et al., 1981). Although only a minor component of the influenza A virus envelope (Jackson et al., 1991; Zebedee and Lamb, 1988), considerable amounts of M2 are found within the plasma membranes of virus-infected cells (Lamb et al., 1985). The protein spans the membrane in the form of a homotetramer with two disulphide linked dimers held together non-covalently (Holsinger and Lamb, 1991; Sugrue and Hay, 1991). Each monomer possesses a N-terminal domain (23 residues) external to the virion or host cell cytoplasm, a transmembrane region (19 residues) and an internal cytoplasmic domain (54 residues). The N-terminal domain contains cysteine residues at positions 17 and 19, both of which are capable of forming disulphide linkages (Holsinger and Lamb, 1991; Sugrue and Hay, 1991). Conservation of the cysteine at position 17 (Sugrue et al., 1990b; Zebedee & Lamb, 1988) suggests that this is essential for disulphide linkage.

The C-terminal domain undergoes postranslational modification with the addition of palmitate to Cys 50 (Sugrue et al., 1990b; Veit et al., 1991) and phosphate to Thr 65 (Sugrue et al., 1991). The significance of these modifications is unknown. For instance in certain H3N8 equine viruses such as A/Equine/Fontainebleau/79, a phenylalanine is found at position 50 resulting in the absence of palmitate (Sugrue et al., 1990b).

In addition to the structural proteins of the virion, influenza A viruses encode two proteins:- NS1 and NS2 which

are considered to be non-structural. A recent report however suggests that virions do contain small amounts of NS2 (Richardson and Akkina, 1991). Both proteins are encoded by the NS gene on RNA segment 8 and are phosphorylated (Privalsky and Penhoet, 1981; Richardson and Akkina, 1991). NS1 is synthesized in the early stages of infection. It accumulates in the infected host cell nucleus and is also found in close association polysomes (Shaw et al., 1982). NS2 in contrast is produced late in infection and accumulates in the cytoplasm (Greenspan et al., 1985). Both proteins migrate into the infected cell nucleus and are believed to be involved in virus replication although their precise roles are unclear. NS1 has been reported to be involved in the post-transcriptional control of gene expression (Alonso-Caplen et al., 1992; Hatada et al., 1990; Hatada et al., 1992) and a role for NS2 in the replication of vRNA has been suggested (Odagiri and Tobita, 1990).

1.4 GENETIC AND ANTIGENIC VARIATION

The great diversity of influenza strains and their ability to produce successive epidemics and pandemics is dependent on their genetic variability. Variability can arise through a number of different mechanisms whereby mutations are introduced into the influenza genome. Changes in the genome may lead to variation in the antigenicity of the virus proteins. The two major

mechanisms involved in antigenic variation are known as shift and drift.

Antigenic drift

Antigenic drift refers to minor changes in the antigenic character of a virus, which arise through the gradual accumulation of point mutations (substitutions, deletions or insertions) within the virus genome. Viral RNA polymerases are inherently prone to producing replication errors of the order of 1 base in every 10^4 (Holland et al., 1982; Steinhauer and Holland, 1987). Consequently each successive round of influenza virus replication produces a number of variant viruses which may or may not possess proteins with altered amino acid sequences. A number of the amino acid changes will not be tolerated due to the functional and structural constraints placed on the viral proteins. Consequently the majority of variants will not be viable. Occasionally however mutations may arise which offer the virus a selective advantage and this can result in the appearance of a new dominant strain.

A number of factors may influence this selection process. Probably one of the most important is the host immune system. Strains possessing mutations which alter the antigenicity of their proteins, are able to avoid the immune response enabling them to become dominant and resulting in antigenic drift. Similarly mutations which produce resistance to antiviral drugs may also confer a selective advantage. The rate at which the different

influenza proteins evolve or 'drift' depends on the selective pressures involved. The viral surface proteins NA and in particular HA, undergo greater variation than the internal proteins, possibly because they are subject to stronger selective pressure from the host immune system. Immunity to influenza virus infection is associated with the presence of antibody capable of neutralizing virus infectivity. Antibodies directed against HA are capable of neutralizing virus infectivity, whereas antibodies directed against NA do not. Instead they inhibit sialidase activity and this interferes with the release of viral progeny and effectively blocks multiple cycle viral replication. Drift within the antigenic sites of NA is less frequent than that observed for HA. This may be due to the fact that antibodies against NA are not directly neutralizing or alternatively there may be greater structural and functional constraints on NA variation.

The internal proteins (e.g. NP) are not subject to such strong selective pressure from the host immune system. They still undergo variation but at a somewhat slower rate. In addition variation within proteins such as the PB1, PB2 and PB3 is not as extensive, possibly due to the need to conserve amino acid residues important to the function of the proteins. The M1 and M2 proteins are both encoded by the M gene (segment 7) and yet they possess very different rates of variation (Ito et al., 1991). M2 which is a minor surface protein has evolved much more rapidly over the past 55 years than M1 which is an internal protein. There has

been almost no accumulation of amino acid changes in M1 over this period.

The process of drift can be mimicked in laboratory strains by their growth in the presence of monoclonal antibody. Evidence for the mechanism of antigenic drift has been obtained from the sequence analysis of both naturally occurring 'drift' isolates and laboratory escape mutants. It may occur in any of the three influenza virus types but is most pronounced in type A viruses. Soon after the appearance of a new subtype, antigenic changes in NA and HA can be detected, giving rise to new strains. On the basis of the clustering of sequence variations in natural isolates and laboratory isolates, five antibody-binding sites have been proposed for HA (Figure II) (Wiley and Skehel, 1987). These are predominantly located on the distal surface of HA1, surrounding the conserved sialic acid binding site. The analysis of NA variants shows a similar pattern of three antigenic sites around the rim of the conserved sialidase active site (Colman and Ward, 1985). These sites overlap however and are less well defined than those suggested for HA.

Antigenic shift

Sudden and dramatic changes predominantly in HA but also in NA, give rise to antigenic shift. The segmented nature of the influenza genome is critical to the shift process which occurs by the genetic reassortment of the RNA segments. Coinfection of cells by two antigenically different strains enables the 'shuffling' or reassortment

of RNA segments to produce 'mixed' progeny viruses. Again however only certain combinations will be viable and only very rarely will a recombinant give rise to a new pandemic subtype. Genetic reassortment has been demonstrated between influenza viruses in the laboratory and ample evidence exists for the occurrence of genetic reassortment between human viruses and also between human and animal viruses 'in vivo' (Cox et al., 1983; Webster et al., 1971).

Since the first human influenza virus was isolated in 1933 three antigenic shifts have occurred in the influenza A virus population, each resulting in the appearance of a new pandemic subtype. In 1957 the then current H1N1 'Swine' viruses were replaced by H2N2 'Asian' viruses and similarly in 1968 the 'Hong Kong' H3N2 viruses appeared. H1N1 viruses showing similar antigenic characteristics to the pre-1957 strains reappeared in 1977 and both subtypes (H1N1 and H3N2) have subsequently cocirculated in the human population.

Genetic reassortment can occur between viruses with different host specificities giving rise to dramatically different new subtypes. This however is a rare event as the influenza viruses show host-restricted growth and so the viability of the reassortant is dependent on the combination of host-adapted genes present. The 1968 'Hong Kong' H3N2 subtype is believed to have been the result of such an event. Identical to the 'Asian' H2N2 viruses in all but its HA (which is antigenically related to that of the avian H3N8 strain A/Duck/Ukraine/63) and PB1 (Kawaoka

et al., 1989), the 'Hong Kong' virus is believed to be an avian-human reassortant (Laver and Webster, 1973; Ward and Dopheide, 1981). Animal reservoirs may therefore play an a role in the emergence of new pandemic subtypes. More recently evidence has been obtained to suggest that pigs may behave as 'mixing' vessels for the reassortment of avian and human viruses (Castrucci et al., 1993). They harbour both human and avian strains and have frequently been associated with the interspecies transmission of type A viruses. 'Swine' H1N1, 'avian-like' H1N1 and 'human-like' H3N2 viruses are all found to circulate in pigs worldwide. The relative conservation of the antigenic characteristics of the viruses within swine and avian hosts (Bean et al., 1992; Noble et al., 1993) has led to the suggestion that they may act as 'hiding' places for type A viruses which disappear from human circulation only to reappear in later years. Such an event occurred in 1977 with the reappearance of H1N1 viruses which varied little from the strains isolated 27 years previously.

The emergence of new pandemic strains may also be due to animal influenza strains becoming infectious to man. Such transmissions between animals and humans are documented periodically (Kendal et al., 1977; Bearle and Webster, 1991). The majority of these transmission are however a 'dead end' for the virus, which has no or very little capacity to undergo human to human transmission. The nature of the genetic changes required to permit such cross-species infection to occur are unknown.

Influenza C viruses have not been found to undergo antigenic shift. Reassortment between influenza B viruses has been demonstrated in the laboratory, but is not found to be important in nature, as indicated by the absence of other influenza B subtypes. This may be due to the lack of animal reservoirs for the influenza B and C viruses.

1.5 VIRAL REPLICATION

Attachment and entry

Virus infection is initiated by the binding of HA to sialylglycolipids or sialylglycoproteins on the surface of susceptible cells. The affinity of binding to α 2-6 and α 2-3 linked sialic acid residues is found to vary between strains and between human, avian and swine subtypes (Rogers *et al.*, 1985; Rogers *et al.*, 1983; Underwood, 1985). This is probably a determining factor in the host specificity and tissue tropism of influenza viruses. X-ray crystallography studies of the HA-sialic acid complex show that the sialic acid occupies a 'pocket' in the distal globular region of the HA (Weis *et al.*, 1988). This binding site is inaccessible to antibody and lined by the conserved residues tyr 98, trp 153, his 183, glu 190 and leu 194 (Wilson *et al.*, 1981). Presumably due to the cooperativity of binding between large numbers of HA molecules, virus binding to the cell surface is effectively irreversible.

Once bound the virus is internalized through coated

pits and vesicles into endosomes by receptor-mediated endocytosis (Matlin et al., 1981). The low pH encountered within late endosomal compartments initiates virus uncoating by triggering the HA-mediated fusion of viral and endosomal membranes (Yoshimura and Ohnishi, 1984). For this to occur HA must be present in its cleaved (HA1-S-S-HA2) form (Wiley and Skehel, 1987). Hence the requirement of certain viruses for trypsin when replicating in cell culture.

At a pH specific to each influenza strain (usually between 5.5 and 6.0) HA undergoes irreversible changes in its conformation, accompanied by an increase in its hydrophobicity. The exposure of hydrophobic regions within the molecule is evident from the aggregation at low pH of bromelain-cleaved HA ectodomains (BHA) (Figure II), accompanied by their ability to bind detergent and associate with liposomes (Skehel et al., 1982; Doms et al., 1985). The removal by thermolysin of the conserved hydrophobic N-terminal of HA2 results in the solubilization of BHA aggregates, low pH apparently revealing this otherwise hidden region of the molecule (Daniels et al., 1983a; Ruigrok et al., 1988). It is thought that the extrusion and interaction of the HA2 N-terminus with membranes results in their destabilisation and fusion. This is supported by the observation that synthetic peptides corresponding to the region interact and fuse artificial membrane vesicles (Lear and DeGrado, 1987; Wharton et al., 1988a).

An accompanying reduction in the association of the distal globular regions of the HA trimer, is apparent at low pH from the increased susceptibility of HA and BHA to the actions of reducing agents and proteinases (Doms et al., 1985; Graves et al., 1983; Skehel et al., 1982). Antibody-binding sites at the trimeric interface of the HA molecule are destroyed (Daniels et al., 1983b; Webster et al., 1983) and sites within the interface become accessible to anti-peptide antibodies (White and Wilson, 1987), indicating that the distal portions of the trimer move apart. The stalk of the trimer however appears to remain intact (Ruigrok et al., 1988) showing negligible alterations in its α -helical secondary structure as determined by circular dichroism (Skehel et al., 1982). Some rearrangement in the tertiary structure may occur (Wharton et al., 1988b). Additional information concerning the regions important for the low pH conformational changes, has been obtained from the analysis of amino acid substitutions within mutant HA viruses. These were selected in the presence of high concentrations of amantadine (500 μ M) which increase the internal pH of cell compartments (Daniels et al., 1985). These HA molecules undergo fusion at elevated pHs presumably because the amino acid alterations destabilize the regions involved, making the transition from the native to low pH conformation more favourable. Such viruses exhibit mutations within either the intersubunit region of the trimer or in regions which destabilize the N-terminal of HA2.

Believed to be simultaneous with the fusion of viral and endosomal membranes is the dissociation of the M1 protein from the viral RNP core. The removal of the M1 shell is required before the RNP can pass through nuclear pores into the nucleus to initiate viral replication (Martin and Helenius, 1991b). The normally close interaction of M1 and RNP has been shown to be readily disrupted at low pH (Zhirnov, 1990). It has been proposed that the viral M2 protein facilitates this process by allowing the acidification of the virus particle interior (see 1.7, pp.41-43).

Gene expression and replication .

Influenza virus transcription, translation and replication requires the activities of both cellular and viral enzymes (reviewed by Krug et al., 1989). Upon entry into the cell nucleus the viral polymerase complex directs the transcription of the eight negative sense viral RNA (vRNA) segments. The segments range in size from 890 to 2341 nucleotides, each encoding at least one viral protein (shown in Table I) and possessing identical conserved 3' and 5' terminal sequences.

Two types of structurally and functionally distinct transcripts are synthesized:- messenger RNA (mRNA) transcripts and complementary (positive strand) transcripts (cRNA), which are required for the replication of the viral genome. The mRNAs are capped, polyadenylated and internally methylated, incomplete transcripts lacking the sequences complementary to the vRNA 5' regions (Etkind and

Table I: Influenza virus RNA segments and coding assignments

<u>RNA</u> <u>segment</u>	<u>Size</u> <u>(nucleotides)</u>	<u>Protein</u> <u>encoded</u>	<u>MW</u> <u>(Kd)</u>	<u>Function</u>
1	2341	PB1	96	Polymerase complex
2	2341	PB2	87	Polymerase complex
3	2233	PA	85	Polymerase complex
4	1778	HA	64	Attachment, fusion
5	1565	NP	50-60	Component of RNP
6	1413	NA	48-63	Sialidase activity
7	1027	M1	28	Structure, assembly
		M2	17	Ion channel
8	890	NS1	25	Unknown
		NS2	12	Unknown

Krug, 1975; Krug et al., 1976; Hay et al., 1977a and 1977b). In contrast cRNAs lack cap and polyadenylation modifications and are complete complementary copies of the vRNAs (Hay et al., 1977b; Hay et al., 1980; Hay et al., 1982). Both the synthesis of mRNA and the replication of vRNA are catalysed by the viral RNA polymerase complex, which consists of PB1, PB2 and PA. Three nucleotide residues (9-11) of the vRNA promoter region have been identified as crucial for the binding of the polymerase complex (Fodor et al., 1993).

The synthesis of mRNA is dependent on the activities of the host cell RNA polymerase, which provides mRNA primers in the form of 5' capped and methylated host cell transcripts. The PB2 component of viral polymerase binds to the host mRNA cap structure (Blass et al., 1982; Braam et al., 1983; Ulmanen et al., 1981) and is believed to be responsible for the cleavage of 10-15 residues from the 5' end of the mRNA. The cleavage is dependent on the presence of a cap structure and occurs preferentially on the 3' side of a purine residue (Plotch et al., 1981). The resultant oligonucleotide is used directly to prime the addition of the first nucleotide, a G residue. PB1 contains the nucleotide binding site (Romanos and Hay, 1984) and along with the virus NP protein is believed to be involved in primer elongation (Braam et al., 1983; Honda et al., 1988; Ulmanen et al., 1981). The function of PA in the transcription process is obscure. Studies of temperature-sensitive mutations in PA suggest that it may be important

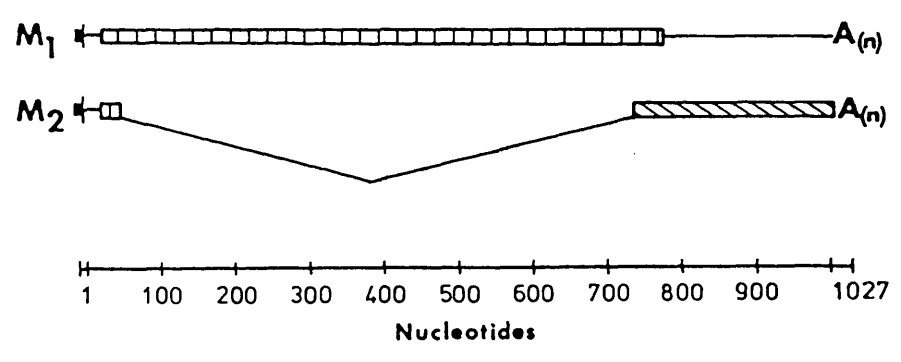
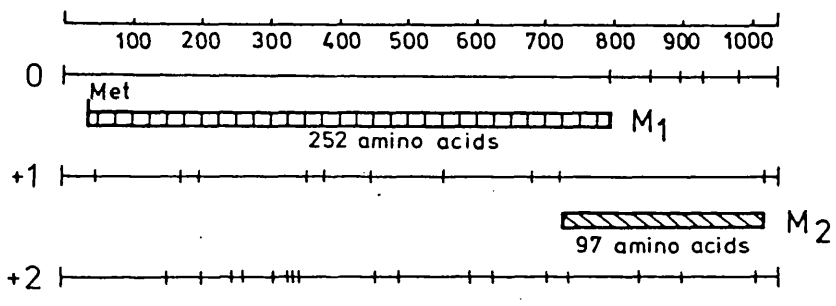
for vRNA replication but not for transcription. However along with PB1 and PB2, PA is essential for the assembly of an active polymerase complex (Kobayashi et al., 1992).

The polymerase complex proceeds along the template RNA until transcription is terminated at a site 15-22 bases from the end of the template where a polyadenylated 3' terminus is formed. This occurs by the repetitive use of the template oligo U sequence (Luo et al., 1991).

RNA segments 1-6 of the influenza A virus genome are transcribed to produce a single mRNA product, whilst segments 7 and 8 give rise to spliced transcripts. The M2 protein is encoded by a spliced mRNA product of the M gene (segment 7), the unspliced transcript coding for the M1 matrix protein (Lamb et al., 1981). Except for a short region at the 5' end of the transcript (corresponding to 9 amino acids), the spliced M2 mRNA is transcribed in a +1 reading frame relative to the unspliced M1 transcript (Figure III). The subsequent 689 nucleotides are spliced out of the M2 message. The extent of the splicing appears to be regulated so that some of the unspliced product is preserved while a sufficient amount of the spliced transcript is produced (Lamb et al., 1981; Volcàrcel et al., 1991).

The processes involved in the synthesis of vRNA copies still remain to be determined however evidence suggests that NS1 and NP, in addition to the three polymerase proteins are required for viral genome replication (Beaton and Krug, 1986; Buonaguirio et al., 1984; Shapiro and Krug,

Figure III: A representation of the splicing events required for the synthesis of the M2 polypeptide from RNA segment 7. The two coding regions (0 and +1) are represented by crosshatched areas, non-coding regions (3' and 5') by thin lines and spliced out regions by the V-shaped thin lines. M2 mRNA is transcribed using a different reading frame (+1) to M1 messenger RNA in the region 740-1004. The scale is in nucleotides from the 5' end of the mRNA. The black boxes at the 5' termini represent the heterologous host derived priming sequences.



1988).

Protein synthesis, assembly and release

Protein synthesis appears to be principally controlled at the transcriptional level and is dependent on the levels of mRNA present (Hay et al., 1977a; Inglis and Mahy, 1979). Different cells vary in their patterns of gene expression, however the early predominance of NP and NS1 protein synthesis correlates with their proposed involvement in vRNA synthesis. In permissive cells the later stages of viral replication are subsequently denoted by the preferential synthesis of the structural proteins NA, HA and M1 involved in virion assembly. PB1, PB2 and PA polymerase proteins are synthesized in relatively low amounts, which correlates with their low abundance in virions. The three polymerase proteins in addition to the NS1, NS2 and NP proteins, have been found to be transported into the infected cell nucleus. The proteins when expressed independently from cloned cDNA have been shown to accumulate within the cell nucleus and nuclear localization signals have subsequently been identified in each of the proteins (Davey et al., 1985; Greenspan et al., 1988; Mukaigawa and Nayak, 1991; Nath and Nayak, 1990).

Virion assembly can effectively be divided into two stages involving the formation of the RNP cores (vRNA, NP and the polymerase proteins) within the nucleoplasm and the incorporation of viral cores into the virus envelope, which forms at the cell surface prior to budding. M1 protein is closely associated with both the RNPs and the viral

envelope during budding and in mature virions, suggesting it plays a key role in assembly. Indeed the association of M1 in the nucleus with the newly formed RNP cores has been shown to be necessary for their export into the cytoplasm (Martin and Helenius, 1991b). One intriguing question concerning the assembly of the viral core which remains to be answered is how the vRNAs, which possess the same 3' and 5' terminal sequences, are packaged so as each virion contains a full complement of eight segments.

The second stage of virus assembly occurs at the plasma membrane where the viral envelope proteins (HA, NA and M2) are transported and inserted into the lipid bilayer. HA, NA and M2 are synthesized on membrane bound ribosomes. They are subsequently targeted to and translocated across the membrane of the endoplasmic reticulum (ER) into the lumen of the ER, by virtue of signal sequences. The signal sequence of NA is found near its N-terminus (Blok et al., 1982) and also serves to anchor the polypeptide into the ER membrane, unlike the HA N-terminal signal sequence which is subsequently cleaved away. M2 becomes located within the ER membrane by its hydrophobic transmembrane domain (Hull et al., 1988). Upon entry into the ER the polypeptides undergo several modifications including the formation of disulphide bonds, protein folding and trimerization. These processes have been extensively studied for HA (Gething et al., 1986; Segal et al., 1992), as has the trimerization of the protein (Copeland et al., 1986; Copeland et al., 1988). The HA trimers are selectively transported to the Golgi

complex (Braakman et al., 1991; Copeland et al., 1986; Gething et al., 1986) and misfolded HA retained in the ER (Garten et al., 1992; Gething et al., 1986; Gething and Sambrook, 1989).

During their passage through the ER, HA and NA are also glycosylated. Branched GlcNAc₂Man₆Glc₃ oligosaccharides are transferred *en bloc* to the polypeptides, as glycosylation sites specified by the amino acid sequence Asn-X-Ser/Thr are revealed. These oligosaccharide units are subsequently trimmed and modified by various enzymes as they pass through the ER and into the Golgi.

After exiting the ER the HA, NA and M2 proteins enter the Golgi complex. The Golgi is a highly organized structure comprising various morphologically and functionally distinct compartments. Proteins enter at the cis-face and proceed through the medial-Golgi to the trans-face. During this time the structures of the proteins are modified further by the actions of a variety of different Golgi enzymes. Palmitate groups are added to both HA and M2 upon their entry into the cis-Golgi (Naeve and Williams, 1990; Sugrue et al., 1990b; Veit et al., 1990; Veit et al., 1991) and M2 is modified further by phosphorylation (Sugrue et al., 1991). Whilst in the Golgi the mannose rich oligosaccharide side chains previously added to HA and NA in the ER, are further trimmed and terminal glycosylation occurs. Removal of the terminal mannose units renders HA insensitive to the actions of endoglycosidase-H, which can be used as a marker for the entry of HA into the trans-

Golgi. Subsequent to its entry into this final Golgi compartment galactose and sialic acid residues are added to the HA molecule (Basak et al., 1985). Mature HA within the newly formed virions however has no bound sialic acid due to the action of NA (Klenk et al., 1970). The extent of HA glycosylation is dependent on the particular HA and the cell type (Nakamura and Compans, 1979). Glycosylation but not palmitoylation also appears to be involved in the effective translocation of HA to the cell surface (Gallagher et al., 1992; Naim et al., 1992; Roberts et al., 1993).

Proteolytic cleavage of HA₀ into HA₁ and HA₂ is necessary for HA fusion and virus infectivity. The majority of influenza viruses have HA's that are only cleaved in a restricted number of cell types, hence they require the addition of trypsin in order to replicate in cell culture (Klenk and Rott, 1988). Certain pathogenic H5 and H7 avian viruses however possess HA's that are cleavable in a wide range of cell types. The consensus sequence R-X-K/R-R has been shown to be critical for this cleavage activation (Vey et al., 1992). Such a site has been identified in the HA of fowl plague virus (FPV), which has recently been shown to be cleaved by the protease furin (Stieneke-Gröber et al., 1992). Cleavage probably occurs within the trans-Golgi compartment.

HA, NA and M2 are eventually inserted into the plasma membrane. In the case of polarized cells such as MDCK cells the proteins are expressed only on the apical cell

surface (Rodriguez-Boulan et al., 1984; Rodriguez-Boulan and Sabatini, 1979; Roth et al., 1979). HA, NA and M2 appear to be distributed evenly across the plasma membrane (Amano et al., 1992; Hughey et al., 1992; Murti et al., 1986). The glycoproteins are then rapidly recruited into the budding virions. The earliest stage in budding, as apparent by electron microscopy, is the appearance of RNP core particles below a thickened area of membrane containing the envelope glycoproteins. Mutations in HA, NP and M protein which block virus assembly have been identified suggesting that the process involves all three proteins (reviewed by Compans and Klenk, 1979). One interesting question that is evident from the assembly process is the relative exclusion of M2 protein from mature virions. Only 14-68 molecules of M2 are present per virion (Zebedee and Lamb, 1988) and yet the protein is abundantly expressed at the infected cell surface (Lamb et al., 1985). It has been suggested that M2 may play a role in the assembly and budding process, but this still remains to be determined.

1.6 PREVENTION AND TREATMENT OF INFLUENZA

Vaccination

Despite the availability of a vaccine for the past 50 years the antigenic variability of the influenza virus still presents a formidable challenge to vaccine design. Protection against the virus is afforded by antibodies

against the two major surface glycoproteins HA and NA and is primarily associated with the presence of serum neutralizing antibody against HA. Currently licensed vaccines in the UK and the USA are based on inactivated whole virus (WV) or split product (SP) vaccines containing NA and standardized quantities of immunoreactive HA. However due to the continual appearance of new strains which quickly spread and replace circulating variants, antibodies directed against the antigenic sites of a single influenza virus have little protective value. Consequently new vaccines are produced each year on the basis of recommendations made by the World Health Organization (WHO), who continuously monitor the prevalence of circulating strains. The format adopted in recent years is to include one type B virus and two type A virus strains from the previous winter's outbreaks. Efficacy levels against antigenically similar viruses range from 70-90% (Meiklejohn et al., 1978; Meyer, 1978; Ruben 1987). Vaccination is currently recommended for persons who because of age or an underlying medical condition are at an increased risk of developing complications associated with influenza infection. This includes the elderly and people with chronic cardiopulmonary disorders. Health care workers and others who may spread influenza to high risk patients are also prime candidates for vaccination. However the uptake of vaccines outside these groups is generally poor as the disease is not judged to be life threatening to otherwise healthy individuals. Early forms

of the vaccine were associated with some side effects, though complications with current vaccines are rare. The need to constantly update the vaccine strains and the requirement for annual vaccinations, however has fuelled the search for alternative approaches to the problems of vaccination.

Inactivated vaccines fail to induce significant cell-mediated and local IgA immune responses which may have an important role in infection. In addition there have been a number of reports suggesting that efficacy of the vaccines is reduced in elderly recipients (reviewed by Beyer et al., 1989). As a result research is currently underway into the use of live vaccines based on temperature-sensitive, cold-adapted and host-restricted avian-human attenuated viruses (Clements et al., 1990; Murphy et al., 1979; Murphy et al., 1981; Sears et al., 1988; Snyder et al., 1986). Although early trials offer some promise, as yet there are no licensed live vaccines.

Antiviral agents

The absence of influenza vaccines offering broad spectrum, long-lasting immunity, means that there is a need for the development of effective chemotherapeutic agents. The influenza virus replication cycle offers many potential sites for the specific action of such an antiviral agent and indeed a number of compounds have been shown to have anti-influenza virus activity '*in vitro*'. However toxicity and the lack of specific '*in vivo*' activity have resulted in the limited availability of effective prophylactic and

therapeutic agents. At present only two antiviral drugs, amantadine and its close relative rimantadine are licensed for use against influenza A (Bektimirov et al., 1985; Dolin et al., 1982; Douglas, 1990; Tominack and Hayden, 1987).

The following section briefly outlines some of the chemotherapeutic agents which show selective antiviral activity against the influenza viruses and provides examples of the search for potential anti-influenza agents using new computer assisted design methods.

i) Attachment and entry

The binding of viral HA to cell surface sialylglycolipids and sialylglycoproteins is essential for virus infectivity. Compounds therefore which inhibit this interaction are potential candidates for influenza chemotherapy. The inhibition of binding and in some cases infection has been demonstrated using natural sialylglycoproteins, such as are found in serum (Rogers et al., 1983; Ryan-Poirier and Kawaoka, 1991; Wakamiya et al., 1992). The investigation of low molecular mass sialic acid derivatives however has shown that their inhibitory activity is too low for practical use (Pritchett et al., 1987; Sauter et al., 1989). More recently in an attempt to mimic the multivalent cooperative nature of virus binding to the cell, polyvalent compounds have been synthesized (Matrosovich et al., 1990; Spaltenstein and Whitesides, 1991; Sebesan et al., 1992). These show higher binding affinities for HA and may offer possibilities as chemotherapeutic agents.

Synthetic oligopeptides which mimic the hydrophobic N-terminus of the influenza A virus HA2 molecule, have been shown to be effective at inhibiting the multiple cycle replication of the virus (Richardson et al., 1980). These sequence specific peptides appear to act early in the infection process interfering with the HA fusion process. Though their precise mechanism of action is unknown it is most probably related to the fusogenic properties of the HA2 N-terminal peptide (Murata et al., 1987). A peptide corresponding to the C-terminal domain of HA2 has also been shown to inhibit single cycle virus replication. This appears to be due to a more specific inhibition effect on the release of biologically active of viral progeny (Collier et al., 1991). Problems exist with the development of this approach for clinical use however with the low solubility of the peptides in aqueous solution and the risk of proteolytic degradation. Indeed subsequent studies in animal models have failed to detect any antiviral activity with the HA2 N-terminal peptides (Choppin et al., 1983).

More recently computer assisted methods have been used to select and test benzoquinone and hydroquinone compounds for their ability to stabilize the non-fusogenic conformation of HA and so inhibit the conformational changes required for fusion (Bodian et al., 1993). This offers a promising approach to the development of new therapeutic agents.

Amantadine and rimantadine also inhibit a stage early

in the influenza A virus infection process, involved in the uncoating of virus. This is discussed in a later stage (see 1.7, pp.41-43)

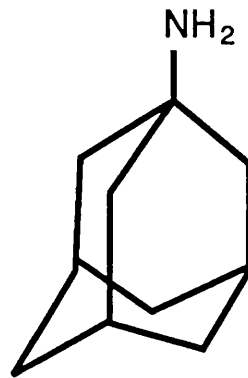
ii) Viral replication

Compounds which inhibit the replication of the influenza virus include the nucleoside analogues. These compounds specifically inhibit RNA virus replication. Ribavirin (1- β -D-ribofuranosyl-1H-1,2,4-triazole-3-carboxamide) a purine nucleoside analogue (Figure IV) has been shown to be clinically active against both influenza A and B infections in man (Knight et al., 1981; McClung et al., 1983; Gilbert et al., 1985). However the treatment regime is too intensive and costly to be of general clinical benefit. The precise mechanism of ribavirin action '*in vivo*' is unknown but three possible mechanisms have been proposed. The monophosphate derivative is a potent inhibitor of inosine monophosphate (IMP) dehydrogenase resulting in the depletion of cellular GTP pools (Stridh, 1983; Wray et al., 1985) and the triphosphate (RTP) form inhibits the GTP-dependent 5' capping of viral mRNA's (Goswani et al., 1979). RTP has also been shown to directly inhibit the influenza virus RNA polymerase complex (Eriksson et al., 1977; Wray et al., 1985). Any combination of these effects may play a role in its anti-influenza activity. Recently a number of other promising purine nucleosides have been synthesized and evaluated in cell culture and '*in vivo*' in the mouse model (Tisdale et al., 1993). However it still remains to be seen

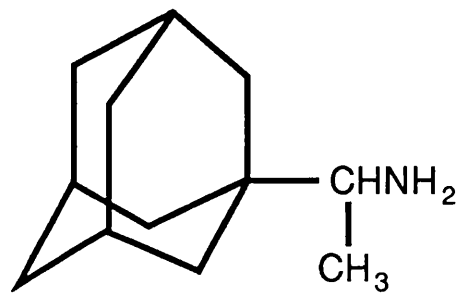
Figure IV:

The structures of the anti-influenza compounds amantadine, rimantadine and ribavirin.

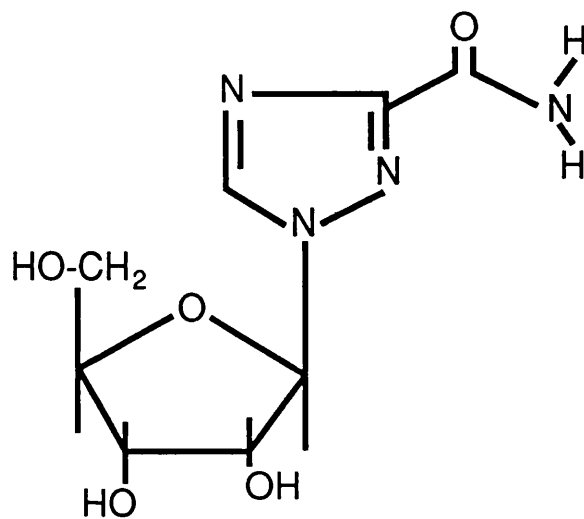
Amantadine



Rimantadine



Ribavirin



whether these will ever be of clinical value. A number of compounds exhibiting anti-influenza activity have an inhibitory effect on the virus RNA dependant RNA polymerase. Lignin-like compounds isolated from pine cone extracts are one such group which markedly suppress influenza growth in cells (Nagata et al., 1990), inhibiting viral polymerase activity and protein synthesis. Their mechanism of action is unknown but appears to be structurally dependent. Synthetic phenylprenoids polymers display similar properties (Sakagami et al., 1990). The increased solubility of these synthetic lignin compounds is advantageous, but the further investigation of their precise mode of action is required before they can be considered in clinical terms.

Antisense oligonucleotides with sequences complimentary to viral mRNAs offer a more specific approach to the inhibition of viral replication. Potential targets include the 3'-terminal sequence common to all eight of the influenza A RNA segments (Stridh et al., 1981) and sequences on the viral polymerase RNAs (Leiter et al., 1990; Kabanov et al., 1990). Cell entry and degradation problems however need to be addressed before this approach can be considered feasible. Modifications including the use of phosphorothioate derivatives (Leiter et al., 1990) and the addition of intercalating agents (Zerial et al., 1987) or hydrophobic groups (Kabanov et al., 1990) may offer potential solutions to these problems.

iii) Assembly and release

Many questions still remain as to the nature of this final stage of the viral replication cycle, however two main antiviral targets are evident. The first is the proposed activity of NA in the release of viral progeny from the cell membrane, raising the possibility that sialidase inhibitors may be potentially useful as antiviral agents. One important factor to be considered in this approach is the specificity of the inhibitor, as many cellular processes also rely on similar enzymes.

Until recently the most potent known inhibitor of NA was 2-deoxy-2,3-dehydro-N-trifluoroacetylneuraminic acid (FANA), a derivative of N-acetylneuraminic acid. Although FANA inhibits influenza virus replication '*in vitro*' (Schulman and Palese, 1975), its effects '*in vivo*' are disappointing. Subsequently certain plant flavonoids have been shown to possess both '*in vitro*' and '*in vivo*' activity in mice without any apparent toxic side effects (Nagai et al., 1990; Nagai et al., 1992). The determination of the crystal structure of NA (see 1.1, pp.9-10) and the use of computer-assisted drug design methods, has recently enabled the development of a number of potent specific sialidase inhibitors (Von Itzstein et al., 1993). The compounds exhibit both '*in vitro*' and '*in vivo*' anti-influenza activity and at present no resistant viral mutants have been isolated, suggesting that this approach offers useful leads for the future development of anti-influenza drugs.

In order for the effective release of budding virus from the infected cell surface HA must be in its native non-fusogenic form. The antiviral agents amantadine and rimantadine prevent the replication of certain influenza A viruses by blocking the release of budding particles from the plasma membrane. This is discussed in greater detail in the next section.

Amantadine and rimantadine

Amantadine (1-amino adamantane hydrochloride) and rimantadine (α -methyl-1-adamantane methylamine hydrochloride) are tricyclic amines (Figure IV) which possess similar structural and antiviral properties. Amantadine was first licensed for prophylactic and therapeutic use against influenza A in 1966 and has been used in the USA and UK. The use of rimantadine has largely been confined to what was the Soviet Union (Zlydnikov et al., 1981), although it has more recently been licensed in France and the USA. Both agents specifically inhibit influenza A viruses but have no effect on influenza B viruses and this has limited their usage. Amantadine has however been used successfully to contain influenza outbreaks within schools and nursing homes (Atkinson et al., 1986; Payler and Purdham, 1984).

A further consideration in the widespread and long-term usage of the drugs is the isolation of drug-resistant mutant viruses. These have been isolated '*in vitro*' and '*in vivo*' in the presence of drug (Appleyard, 1977; Belshe et al., 1988; Hayden et al., 1989; Mast et al., 1991). The

viruses exhibit cross resistance to both agents, however when compared to the corresponding wildtype viruses, they show no obvious differences in their pathogenicity (Bean et al., 1989; Beard et al., 1987; Sweet et al., 1991). At present such strains have only been isolated from patients undergoing treatment and have not been found to spread to the wider population. Without the more widespread use of the drugs though the true impact of resistance cannot be assessed.

The analysis of mutations conferring resistance identified the influenza M2 protein as the drug target (Belshe et al., 1988; Hay et al., 1979; Hay et al., 1985; Hay et al., 1986; Lubeck et al., 1978). Drug resistance is specifically due to single point mutations in the M2 transmembrane residues 27, 30, 31 and 34 (Bean et al., 1989; Belshe et al., 1988; Hay et al., 1991; Hay et al., 1985; Kendal and Klenk, 1991; Mast et al., 1991), suggesting that amantadine interacts within this region to block the ion channel.

Amantadine and rimantadine are not viricidal. Millimolar concentrations of the drugs act in a non-specific manner to block membrane fusion and the removal of the virus envelope (Marsh and Helenius, 1989; White, 1990). Consequently such high concentrations of amantadine and rimantadine have a similar effect on a number of other enveloped RNA viruses e.g. alphaviruses and rhabdoviruses. They behave as weak bases, reducing the acidity of endosomes and so preventing the low pH-induced uncoating of

the virus.

1.7 THE ION CHANNEL ACTIVITY OF THE M2 PROTEIN AND ITS ROLE IN VIRAL REPLICATION

Micromolar concentrations of amantadine and rimantadine specifically inhibit the M2 protein of influenza A viruses. The specific inhibition of M2 by amantadine has identified two roles of the protein in virus infection: during virus uncoating (Bukrinskaya et al., 1982a; Burkrinskaya et al., 1982b; Martin and Helenius, 1991a; Wharton et al., 1990) and in certain avian H7 and H5 viruses, during viral maturation (Sugrue et al., 1990a) (Figure V). Both of these suggest that M2 has the ability to modify pH.

In the early stages of viral replication amantadine inhibition of M2, appears to prevent the dissociation of the virus M1 protein shell from the RNP core. Studies suggest that this dissociation occurs readily around pH6 (Gregoriades, 1973; Zhirnov, 1990) and that the presence of drug blocks this event, trapping the RNP core with its M1 protein shell, within the cell cytoplasm (Bukrinskaya et al., 1982a; Bukrinskaya et al., 1982b; Martin and Helenius, 1991a). The exact role of M2 in this uncoating stage remains to be determined. It has been proposed that M2 can modify the pH within the virus by allowing protons to pass (in a N to C-terminal direction) from the acidic interior of the endosome into the virus particle, creating the necessary acidic conditions for M1 protein dissociation.

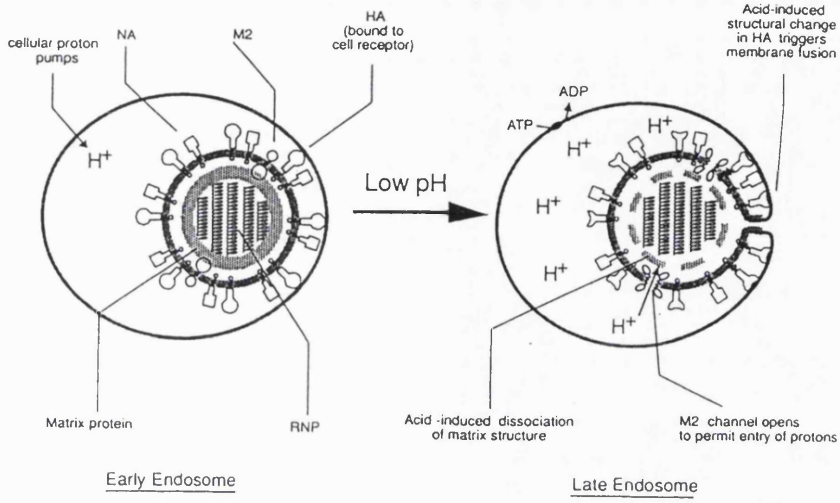
Figure V:

A schematic representation of the proposed roles of the influenza A M2 protein in the viral replication cycle.

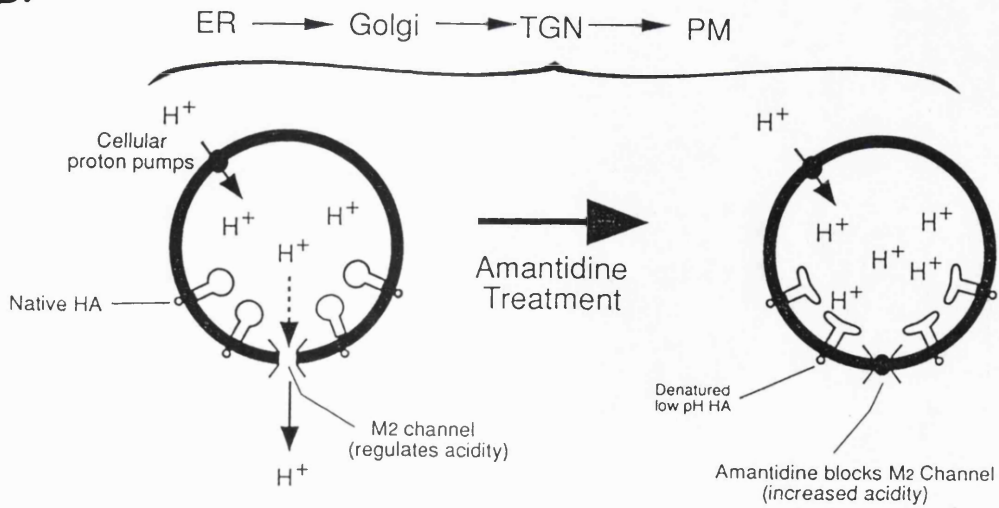
A. shows the involvement of M2 protein in the low-pH dependent uncoating of virus particles. M2 (orientated with its N-terminus external to the virion) is proposed to allow the entry of protons into the virion interior, initiating the acid-induced dissociation of M1 protein from the RNP core, which is required for its transport into the cell nucleus.

B. represents the role of M2 in the maturation of HA. M2 (orientated with its N-terminus facing into the lumen of the vesicle) counteracts the acidification of the TGN, preventing the low pH-induced conformational change in HA.

A.



B.



Amantadine inhibits M2 function and so prevents this occurring. Consistent with this is the observation that proton ionophores (e.g. monensin), which dissipate pH gradients counteract the drug inhibition of M2 and accelerate membrane fusion 'in vitro'. Recent studies investigating the kinetics of virus-liposome fusion, also suggest that M2 may influence the fusion process (Bron et al., 1993; Wharton et al., in press). This is unlikely however to be the primary role of M2 in the uncoating process.

The inhibition of virus maturation by amantadine appears to act through a related activity of the M2 protein in modifying the pH of HA-containing transport vesicles. Electron microscopy revealed that in the presence of drug viral buds are formed on the cell surface but fail to be released (Ruigrok et al., 1991). This is a consequence of the increased expression of low pH form of HA, as defined by its susceptibility to proteolytic digestion and its recognition by monoclonal antibodies specific for acid-treated HA (Sugrue et al., 1990a). Pulse-chase experiments suggest that temporally HA drug sensitivity coincides with its cleavage from HA0 to HA1 and HA2 (Sugrue et al., 1990a). This is consistent with the observation that only cleaved HA can undergo low pH-induced conformational changes (Wiley and Skehel, 1987) and points to amantadine exerting its effects late in the transport pathway, in TGN vesicles (Sugrue et al., 1990a). Experiments using the immunocytochemical pH probe DAMP showed that in the

presence of drug the TGN vesicles do become more acidic (Ciampor et al., 1992a). Agents which elevate the pH of the vesicles, e.g. amines and ionophores such as monensin, can counteract this effect of drug. Mutations which affect the acid stability of HA also affect the sensitivity to drug (Steinhauer et al., 1991). These observations implicate M2 in vesicle pH regulation as M2 is the specific target of micromolar concentrations of drug.

M2 is synthesized in the ER and transported to the cell surface via a similar route to HA (Hull et al., 1988). One hypothesis to explain the role of M2, is that it is present in the membranes of HA-containing vesicles and acts to protect native HA, by counteracting the acidifying effects of vesicular proton pumps. Amantadine inhibition of M2 would result in the acidification of the vesicle interior leading to low pH conformational changes in HA.

From studies of the effects of M2 within the trans-Golgi it has been proposed that M2 has ion channel activity. The position of single point mutations conferring drug resistance suggest that amantadine interacts with the transmembrane domain (Figure VIB). The transmembrane domain has the potential to form an amphiphilic α -helix within membranes, the drug resistance mutations lying on the polar face (Hay, 1991; Hay et al., 1985). The α -helical nature of a peptide containing the transmembrane domain within liposomes has recently been demonstrated by circular dichroism (CD) (Duff et al., 1992).

Figure VI:

A. shows the primary structure of the A/Chicken/Germany/34 ('Rostock') virus M2 protein, highlighting the 3 domains and the attachment sites of palmitate and phosphate groups.

B. is a representation of the proposed channel structure of the A/chicken/Germany/27 ('Weybridge') M2 transmembrane domain (residues 24-44). Two of the α -helices of the tetramer are shown with their hydrophilic faces forming the interior of the channel. Highlighted in boxes are the sites of single amino acid changes associated with resistance to amantadine. On the basis of these resistance mutations the proposed interaction of amantadine within the channel is shown.

It has been proposed that within the M2 tetramer the monomers associate with their hydrophilic faces forming an ion permeable channel, with which amantadine interacts (Hay, 1989; Sugrue and Hay, 1991). This appears analogous to the interaction of amantadine with the ion channel of the nicotinic acetylcholine receptor (Warnick et al., 1982). It has recently been demonstrated using a two-electrode voltage clamp procedure, that M2 protein expressed in *Xenopus* oocytes exhibits Na⁺/K⁺ activity (Pinto et al., 1992). In addition a proton translocation activity has been identified for the M2 transmembrane domain when incorporated into single-channel, voltage-clamped, planar lipid bilayers (Duff and Ashley, 1992). In both cases amantadine was seen to block the M2 channel activity.

1.8 PROJECT AIMS

The aim of this project was to further investigate the ion channel activity of the M2 protein of influenza A viruses and more precisely its role in modulation of pH within virus-infected cells. The project was initially based on observations made by F. Ciampor, concerning the regulation of pH within cytoplasmic vesicles. Using the immunocytochemical pH probe DAMP, virus infection was shown to cause an increase in the number of acidic cytoplasmic vesicles. In addition the specific inhibition of M2 by amantadine resulted in the appearance of large acidic

vesicles within the cell cytoplasm. The initial aim of this project was to investigate further these changes in vesicular pH using DAMP. By monitoring the changes in the vesicle pH immediately after the addition of amantadine, the intention was to try and determine more precisely the location of the pH changes and how subsequently these changes in vesicular pH related to the conformational changes observed in HA by immunofluorescence.

In view of the apparent increase in the acidity of virus-infected cells, fluorescent pH probes were used to monitor changes within the pH of the cell cytoplasm. Using the probe SNARF-1, a decrease in the cytoplasmic pH of virus-infected MDCK cells was observed and this was subsequently found to be M2-specific. The remaining part of the project has concentrated on developing further this assay system and using it to study in greater detail the nature of the M2-specific changes in cell pH.

MATERIALS AND METHODS

MATERIALS AND METHODS

2.1 VIRUS GROWTH AND TITRATION

Virus growth

All viruses were grown in the allantoic cavity of 11 day old embryonated hens eggs. Strains A/chicken/Germany/34 (H7N1, "Rostock" strain), A/chicken/Germany/27 (H7N7, "Weybridge" strain) and the amantadine-resistant mutant viruses were grown for 26 hours at 37°C. Human strains A/Singapore/1/57 (H2N2), A/Beijing/32/92 (H3N2), A/Victoria/36/88 (H1N1) and B/Panama/45/90 were grown for 72 hours at 33°C.

Amantadine-resistant "Rostock" mutants R41R (M2, I27T), 08 (M2, A30T) and 039 (M2, I27T) were selected for resistance to 5 μ M amantadine as described elsewhere (Hay *et al.*, 1985; Steinhauer *et al.*, 1991). In a similar manner the amantadine resistant "Weybridge" mutant GC16 (M2, G34E) was selected for resistance to 5 μ M amantadine.

Infectivities of virus stocks as determined by plaque assay were between 5x10⁸ and 7x10⁸ p.f.u./ml in each case.

UV-inactivation of virus

Allantoic fluid (1ml in a 5cm petri dish) was irradiated with varying doses of 254nm UV light (0.1-4J). The extent of inactivation was assessed by plaque assay.

Plaque assay

Primary chick embryo fibroblast (CEF) cell monolayers were infected with ten-fold serial dilutions of virus in

0.2% bovine serum albumin (BSA) in saline. These were overlaid with 199 medium containing 0.75% Noble's agar, 1% calf serum (CS), 5% BSA and 0.001% dextrose. Plaques were counted after staining with 0.01% neutral red in saline for 3 hours at 37°C and fixing in 10% formol saline.

2.2 TISSUE CULTURE

Cells

Madin-Darby canine kidney (MDCK) cells and Hela cells were propagated at 37°C in minimum essential medium (MEM) supplemented with 5% foetal calf serum (FCS) and gassed with 3-5% CO₂. VERO cells were propagated at 37°C in H21 medium supplemented with 5% FCS and 5mM sodium pyruvate, gassed with 3-5% CO₂.

Confluent cell monolayers were grown on coverslips treated with 5µg/cm poly-L-lysine (Sigma Chemical Co.) for 5 minutes, prior to use. For immunofluorescence 20mm diameter, No.1 coverslips (Chance Propper Ltd.) were used and for measurements in the fluorescence spectrophotometer 9x35mm, No.1½ coverslips (Horwell) were used.

For radiolabelling and immunoblotting cell monolayers were grown in 3cm petri dishes (~2x10⁶ cells).

For ELISA studies MDCK cells were grown in 96-flat-bottomed well microtitre plates (~2x10⁵ cells/plate).

Primary CEF cells were prepared by a method modified from Porterfield (1960). The tissue (~40g) from 11 day old chick embryos with the eyes and guts removed, was

macerated and treated with 200ml of trypsin (1.25g/l) for 30 minutes. After subsequent centrifugation (2000g, 10 mins, 4°C), the cells were resuspended ($\sim 1.5 \times 10^6$ cells/ml) in Tris-buffered Gey's medium supplemented with 10% CS and filtered through a fine wire gauze. 2ml of cell suspension was added per 3cm petri dish 24 hours prior to use and incubated at 37°C.

Mouse erythroleukaemia (MEL) cells expressing the "Weybridge" M2 protein (a gift from F. Geraghty) were maintained at 37°C (3-5% CO₂) in MEM supplemented with 10% FCS and 2mM glutamine. The cells were induced to produce M2 protein by the addition of 2% dimethyl sulphoxide (DMSO) 4 days prior to use. Before attachment to coverslips (treated as previously described) the cells were washed twice (300g, 5 minutes) and resuspended in PBS ($\sim 1 \times 10^7$ cells per ml). 0.2ml of cell suspension was added to each coverslip and a monolayer allowed to form over a period of 20 minutes at RT.

Sf9 spodoptera cells were maintained in TC100 medium (Gibco BRL) supplemented with 10% FCS at 27°C. Exponentially growing cells ($\sim 1 \times 10^6$ cells/ml) were seeded onto coverslips and allowed to adhere for a period of 1-3 hours. The coverslips were then washed once in TC100 and incubated at 27°C in TC100.

Infection of cells

MDCK, VERO, Hela and CEF cell monolayers were infected with virus at approximately 50 p.f.u. per cell for 30 minutes at RT. After washing twice in MEM (time p.i.=0)

the cells were incubated in MEM for 5-6 hours at 37°C.

Sf9 cell monolayers were infected with "Weybridge" M2-expressing baculovirus (a gift from C. Schroeder) at a multiplicity of 2 p.f.u./ml for 1 hour at RT. The coverslips were then washed with TC100 and incubated in TC100 supplemented with 10% FCS for 40-48 hours at 27°C.

2.3 RADIOLABELLING OF CELLS

[³⁵S] pulse-chase labelling

MDCK cells in 3cm petri dishes were incubated in 200 μ l of MEM without methionine or cysteine, containing 0.15mCi/ml [³⁵S] Trans label (ICN Biomedicals, Inc.; 10.9mCi/ml; 1164Ci/mmol) for 15 minutes, from 6 hours p.i.. The label was removed by washing twice in MEM and chased for a further 1 hour. After washing twice in ice cold phosphate buffered saline (PBS) the cells were lysed in 200 μ l of cold lysis buffer (50mM NaCl, 50mM Tris-HCl pH8, 100 μ g/ml phenylmethylsulphonyl (PMSF), 1% NP40) and stored at -20°C.

[³H] palmitic acid labelling

MDCK cells in 3cm petri dishes were incubated in 200 μ l of MEM supplemented with 5mM sodium pyruvate, containing 25 μ Ci/ml of [9,10(n)-³H] palmitic acid (Amersham; 1mCi/ml; 40-60Ci/mmol) from 5-7 hours p.i.. The cells were washed twice in ice cold PBS and lysed in 200 μ l of cold lysis buffer (50mM NaCl, 50mM Tris-HCl pH8, 100 μ g/ml PMSF, 1% NP40). Samples were stored at -20°C.

2.4 IMMUNOLOGICAL METHODS

Antibodies

Monoclonal anti-HA antibodies against whole virus (HC2 and HC58) and low pH HA (H9) were prepared in BALB/C mice using SP20/0-Ag14 myeloma cells as described by Sugrue et al., (1990a).

Rabbit antisera were prepared against M2 peptides conjugated to keyhole limpet haemocyanin (KLH), R53 against residues 1-24 and R54 against residues 82-97. R53 was purified using a peptide (residues 1-24)-Amino Gel (Pierce) affinity column.

Protein A-purified anti-dinitrophenol (anti-DNP) monoclonal antibody (clone HDP1) was obtained from Oxford Biomedical Research Inc.

Polyclonal anti-rat TGN38 antibody was kindly supplied by G. Banting.

Immunofluorescence

Infected MDCK cells on glass coverslips were incubated in MEM for 5½ hours at 37°C. 5µM amantadine was added from 1 hour p.i.. Monolayers were washed with ice cold PBS and treated with methanol (-20°C) for 5 minutes. A 15 minute incubation at RT with 3% BSA was carried out, before applying a 1/50 dilution of rhodamine-labelled wheatgerm agglutinin (WGA-TRITC; Sigma Chemical Co.) in 0.2% BSA in PBS (PBS/BSA). After 1 hour at 37°C the coverslips were washed with PBS/BSA, before applying monoclonal antibodies HC58 or HC2 diluted to 1/100 or H9 diluted 1/50, with

PBS/BSA. Polyclonal antisera R53 and R54 were diluted to 1/50 , with PBS/BSA. The cells were washed with PBS/BSA after 1 hour at 37°C and HC58, HC2 and H9-treated cells incubated with a 1/125 dilution of rabbit anti-mouse IgG-fluorescein conjugate (RAM-FITC, Sigma Chemical Co.). Cells treated with R53 or R54 were incubated with a 1/80 dilution of goat anti-rabbit IgG-rhodamine (GAR-TRITC, Sigma Chemical Co.). After 1 hour at 37°C the samples were washed thoroughly with PBS, mounted in Uvinert™ (BDH) and observed using a Zeiss Photomicroscope III equipped for epifluorescence.

Cells labelled with polyclonal anti-TGN38 antibody (1/1000 dilution) were treated in a similar way to that described above using GAR-TRITC..

To visualize acidic compartments, monolayers were incubated (5-5½ hours) in MEM with 30µM DAMP (Oxford Biomedical Research, Inc.) as described by Anderson et al., (1984). Cells were fixed for 15 minutes at RT in 3% paraformaldehyde, washed once in 50mM ammonium chloride and twice in PBS with 2mM magnesium chloride. Permeabilization was carried out in pre-cooled (0°C) 0.1% Triton X-100 for 5 minutes. After a 15 minute incubation at RT with 3% BSA, a 1/10 dilution of anti-DNP antibody (Oxford Biomedical Research, Inc.) in 0.2% BSA in PBS (PBS/BSA) was added. The cells were washed in PBS/BSA after 1 hour at 37°C and incubated for a further hour with a 1/125 dilution of RAM-FITC at 37°C. The samples were washed in PBS before mounting and viewing as described above.

Enzyme-linked immunosorbant assay (ELISA)

Rostock-infected MDCK cells in 96-well microtitre plates were fixed 6 hours p.i. with 0.05% (w/v) glutaraldehyde in PBS (15 minutes, RT). After incubating with 3% BSA in PBS for 15 minutes at RT, the cells were incubated with monoclonal antibodies HC58 or HC2 diluted to 1/1000 or H9 diluted to 1/50 with 0.2% BSA in PBS (PBS/BSA). After 1 hour at 37°C the cells were washed 6 times in PBS/BSA and incubated for a further hour at 37°C with a 1/2000 dilution of protein A-horseradish peroxidase (Bio Rad Laboratories) in PBS/BSA. Cells were washed 5 times with PBS and treated with citrate buffer (25mM sodium citrate: 25mM citric acid, 4:3 at pH4.5) containing 0.012% (w/v) hydrogen peroxide and 0.03% (w/v) 3, 3', 5, 5'-Tetramethyl benzidine dihydrochloride (TMB; Sigma Chemical Co.). After the sufficient development of a blue colour the reactions were stopped by the addition of 1M sulphuric acid and assessed by their absorbance at 450nm using a Labsystems Multiskan Biochromatic plate reader.

Immunoblotting

Infected cells grown in 3cm petri dishes were washed twice in ice cold PBS and lysed in 200 μ l of cold lysis buffer (50mM NaCl, 50mM Tris-HCl pH8, 100 μ g/ml PMSF, 1% NP40). MEL cells were washed twice in ice cold PBS (300g, 5 minutes) and resuspended in cold lysis buffer (~1x10⁷ cells/ml). Samples were stored at -20°C until required for polyacrylamide gel electrophoresis (see 2.5).

After polyacrylamide gel electrophoresis proteins were

transferred by electroblotting (0.8mA/cm² for 30-60 minutes) onto Immobilon-P (Millipore Ltd.) and blocked for 30 minutes at RT with 1% Marvel in PBS (1% Marvel/PBS). A 1/500 dilution in 1% Marvel/PBS of R53 and/or R54 antiserum was applied and incubated at RT for 1 hour. The blot was washed 5 times with PBS and incubated for a further hour, with a 1/500 dilution of ¹²⁵Iodine-labelled donkey anti-rabbit Ig (Amersham) in 1% Marvel/PBS. The blot was washed 5 times in PBS, dried at 42°C and exposed to photographic film (Fuji) at -20°C, using an intensifying screen.

Immunoprecipitation

100μl samples of ³⁵S-labelled cell lysates (see 2.3) were incubated overnight on ice with 2.5μl of antibody and 600μl of binding buffer (0.5% NP40, 150mM NaCl, 1mM EDTA, 0.25%(w/v) BSA, 20mM Tris-HCl pH8). The immune complexes were isolated by adding 50μl of protein A-Sepharose (Pharmacia LKB Biotechnology) and rotating at 4°C for 2 hours. The protein A-Sepharose was washed 6 times (10,000g, 5 minutes) in high salt buffer (1% Triton X-100, 650mM NaCl, 1mM ethylenediaminetetraacetic acid (EDTA), 10mM sodium phosphate pH7) and once in PBS. Samples were stored at -20°C until required for polyacrylamide gel electrophoresis (see 2.5).

2.5 POLYACRYLAMIDE GEL ELECTROPHORESIS

Immunoprecipitates were resuspended in 50μl of sample buffer (0.0625M Tris HCl pH 6.8, 2% sodium dodecyl sulphate

(SDS), 10% glycerol, 5% 2-mercaptoethanol, 0.001% bromophenol blue) and cell lysates were mixed with an equal volume of sample buffer. After heating for 3 minutes at 95°C, 30 μ l volumes were analysed by electrophoresis at 150 volts for 1½ hours on a gel of 15% acrylamide, 0.1% SDS and 0.38mM Tris-HCl pH8.8, with a stacking gel of 5% acrylamide, 0.1% SDS, 125mM Tris-HCl pH6.8 and 0.001% bromophenol blue. 5 μ l of Rainbow™ protein molecular weight markers (14.3-200 Kd) (Amersham) were used.

Gels of ³⁵S and ³H-labelled samples were fixed in 25% (w/v) propanol and 10% (w/v) acetic acid, for 20 minutes and placed in Amplify (Amersham) for 30 minutes. After drying overnight at 80°C the gels were exposed to photographic film (Fiji) in the presence of an intensifying screen.

2.6 DETERMINATION OF CYTOPLASMIC pH

Virus-infected cells (5 hours p.i.) were incubated at 37°C with 10 μ M SNARF-1-AM for 1 hour or 10 μ M BCECF-AM for 1½ hours. Coverslips were washed and placed in a thermostated cuvette (37°C) containing Gey's medium with 20mM Hepes buffer, pH 7.1 (see 3.2, Table 5). With the coverslips placed at a 65° angle to the incident beam, emission spectra were obtained for SNARF-1 from 550 to 650nm (excitation 534nm) and excitation spectra for BCECF from 400 to 550nm (emission 530nm) using a Perkin-Elmer MPF-4 fluorescence spectrophotometer. Dilutions of drug and antiserum were

added to the cuvette medium. Emission ratios of 634nm to 604nm for SNARF-1 and excitation ratios of 506nm to 455nm for BCECF, were equated to pH values by means of a standard curve.

Cell viability was assessed by the addition of 0.04% trypan blue to cell monolayers for 10 minutes at RT. The uptake of dye was examined using a Nikon TMS inverted microscope.

Standard curves were established by incubating cells with 10 μ M nigericin in high KCl buffer (115mM KCl, 1mM MgCl₂ and 20mM Hepes buffer, adjusted to various pH's).

2.7 FLOW CYTOMETRIC MEASUREMENT OF CYTOPLASMIC pH

MEL cells were washed twice in PBS (300g, 10 minutes) and incubated with 10 μ M SNARF-1-AM in MEM supplemented with 10% FCS and 2mM glutamine. After 1 hour at 37°C the cells were washed and resuspended (~2x10⁶ cells/ml) in Gey's+20mM Hepes, pH7.10.

Flow cytometric analysis of the samples was kindly carried out by C. Atkins, N.I.M.R. using an EPICS V flow cytometer (Coulter). Samples were maintained at 37°C and excited using a 488nm Argon ion laser (200mW). Optical emission filters consisted of a 488nm laser block, 488nm side scatter dichroic, 610nm dichroic long pass, 640 DF35 and a 580 DF30. Fluorescence (640 and 580nm excitation), side scatter (SSC) and forward angle scatter (FSC) data were acquired by MDADS (Multi-parameter Display and Data

Acquisition System) and transferred via NIMR VAX. The data were analysed using FACSplot, a flow cytometry data analysis package (J. Green, N.I.M.R. Computing).

2.8 MATERIALS

Amantadine hydrochloride, rimantadine and brefeldin A (BFA) were obtained from Sigma Chemical Co..

Cyclobutylamine, cyclopentylamine, cyclohexylamine, cycloheptylamine and cyclooctylamine were obtained from Aldrich Chemical Company, Inc..

Monensin, nigericin and valinomycin were obtained from Sigma Chemical Co. and stored at +4°C as 1mM stock solutions in ethanol.

SNARF-1-AM and BCECF-AM were obtained from Molecular Probes Inc. and dissolved in dimethyl sulphoxide (DMSO). 100 μ l aliquots of stock solution (1mM) were protected from the light and stored at -20°C.

RESULTS

RESULTS

3.1 CONFORMATIONAL CHANGES IN HA AND THE pH OF TRANSPORT VESICLES

In view of the ability of M2 to modify the pH within the transport pathway to protect the structural integrity of HA (Sugrue et al., 1990a), experiments were carried out to try to identify the location of the pH-induced conformational changes in HA and to monitor more closely the changes in pH using DAMP. Changes in the conformation of HA were studied by immunofluorescence using the monoclonal antibodies HC58 and H9 to detect the native and low pH conformations of HA respectively. HC2, another monoclonal antibody which recognizes most forms of HA was used to detect any gross changes in the production of HA. Uninfected cells (not shown) showed minimal background fluorescence with all three of the monoclonal antibodies.

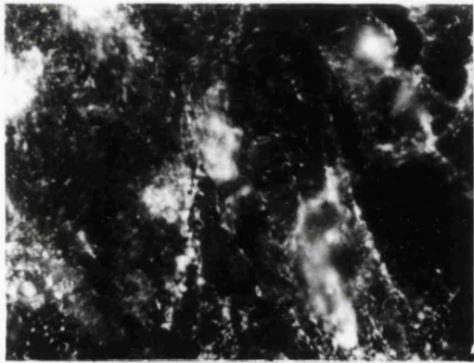
Immunofluorescence staining of virus-infected chick embryo fibroblast (CEF) cells showed that the majority of HA was in the native conformation, as recognized by HC58 (Figure 1A). The HC58 label was distributed both internally and on the cell surface. In contrast very little H9-labelled low pH HA, was observed in these cells (Figure 1C). However following the incubation of the cells in 5 μ M amantadine, significant amounts of low pH HA appeared throughout the cells, both within the cytoplasm and on the cell surface (Figure 1D). Native HA

Figure 1: The effects of amantadine on the expression of HA in Rostock-infected CEF cells.

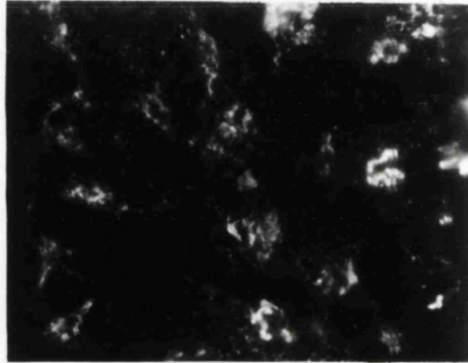
CEF cells were fixed 5½ hours after infection with Rostock virus and incubated with monoclonal anti-HA antibodies HC58 (A and B), H9 (C and D) and HC2 (E and F). All cells were subsequently incubated with RAM-FITC.

Amantadine (5µM) was added to the cells shown in B, D and F, from 1 hour p.i..

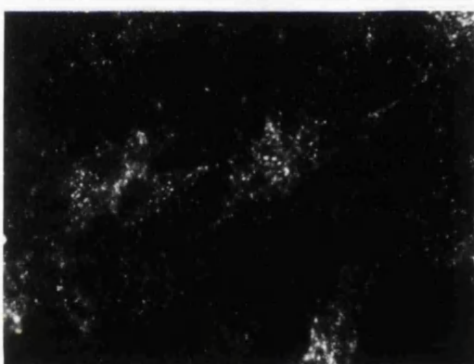
A



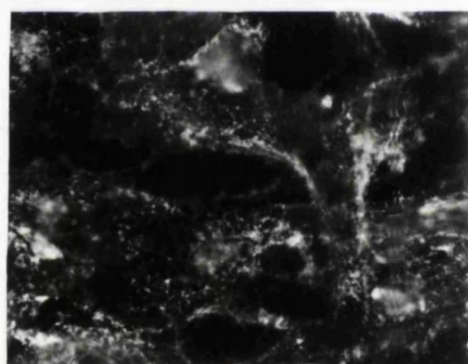
B



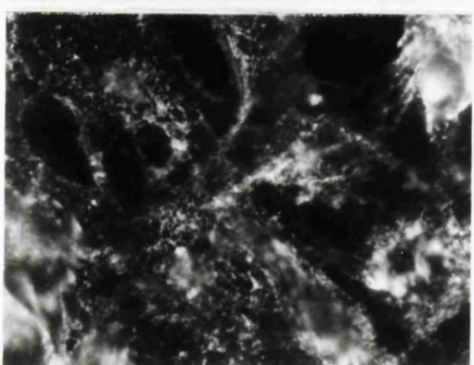
C



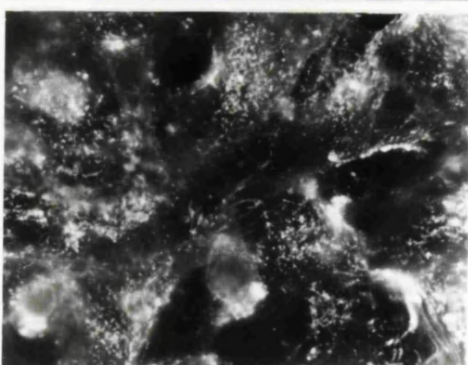
D



E



F



was localized internally with minimal labelling of the cell surface in the presence of amantadine ($5\mu\text{M}$) (Figure 1B). No significant differences in the pattern of HC2 fluorescence were apparent between cells incubated in the absence (Figure 1E) and presence (Figure 1F) of amantadine ($5\mu\text{M}$), indicating that drug treatment had no gross effect on the production of HA.

Similar distribution patterns of HA were observed in Rostock-infected MDCK cells (Figure 2). Cells labelled with HC58 monoclonal antibody indicated that native HA was present within the cell cytoplasm and on the cell surface (Figure 2A), whilst very little fluorescence was observed in cells labelled with the low-pH HA specific antibody H9 (Figure 2C). However in the presence of $5\mu\text{M}$ amantadine large, H9-labelled vesicles (as highlighted in Figure 2D) were observed in the infected cell cytoplasm, in addition to H9-labelling of cell surface HA. Native HA was exclusively located internally in amantadine-treated cells, with very little fluorescent labelling of the cell surface (Figure 2B). No change in HC2 fluorescence was observed in the presence of amantadine ($5\mu\text{M}$) (Figure 2F). Changes in the distribution of HA were more clearly visible in MDCK cells as opposed to CEF cells and consequently MDCK cells were used in subsequent studies.

The distribution of HC58 (Figure 3A), H9 (Figure 3C) and HC2 (Figure 3E and F) fluorescence in MDCK cells infected with the amantadine-resistant mutant 08, was similar to that observed in the Rostock-infected cells.

Figure 2: The effects of amantadine on the expression of HA in Rostock-infected MDCK cells.

Rostock-infected MDCK cells were fixed 5½ hours p,i, and incubated with anti-HA monoclonal antibodies HC58 (A and B), H9 (C and D) and HC2 (E and F), followed by RAM-FITC.

The cells shown in B, D and F were incubated with 5µM amantadine from 1 hour p.i..

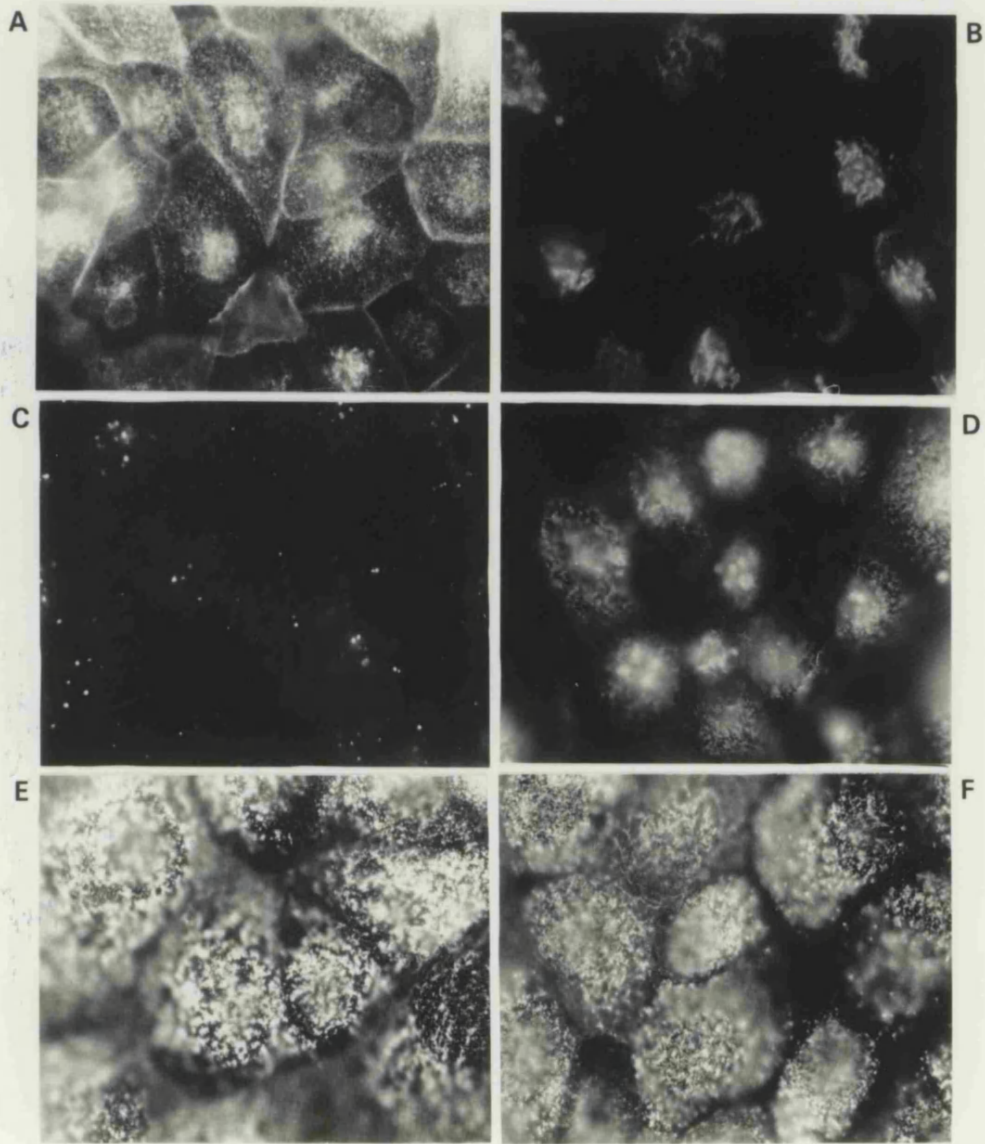


Figure 3: The effect of amantadine on the distribution of HA in MDCK cells infected with the amantadine-resistant 08 virus.

MDCK cells infected with the amantadine-resistant virus 08 were fixed 5½ hours p.i. and incubated with monoclonal antibodies HC58 (A and B), H9 (C and D) and HC2 (E and F) specific for the various forms of HA. All cells were subsequently incubated with RAM-FITC.

Amantadine (5µM) was added to the cells shown in B, D and F from 1 hour p.i..

The distribution of 25 labeled amino acids in the
tissues of the rat (Figure 10, 11 and 12) is

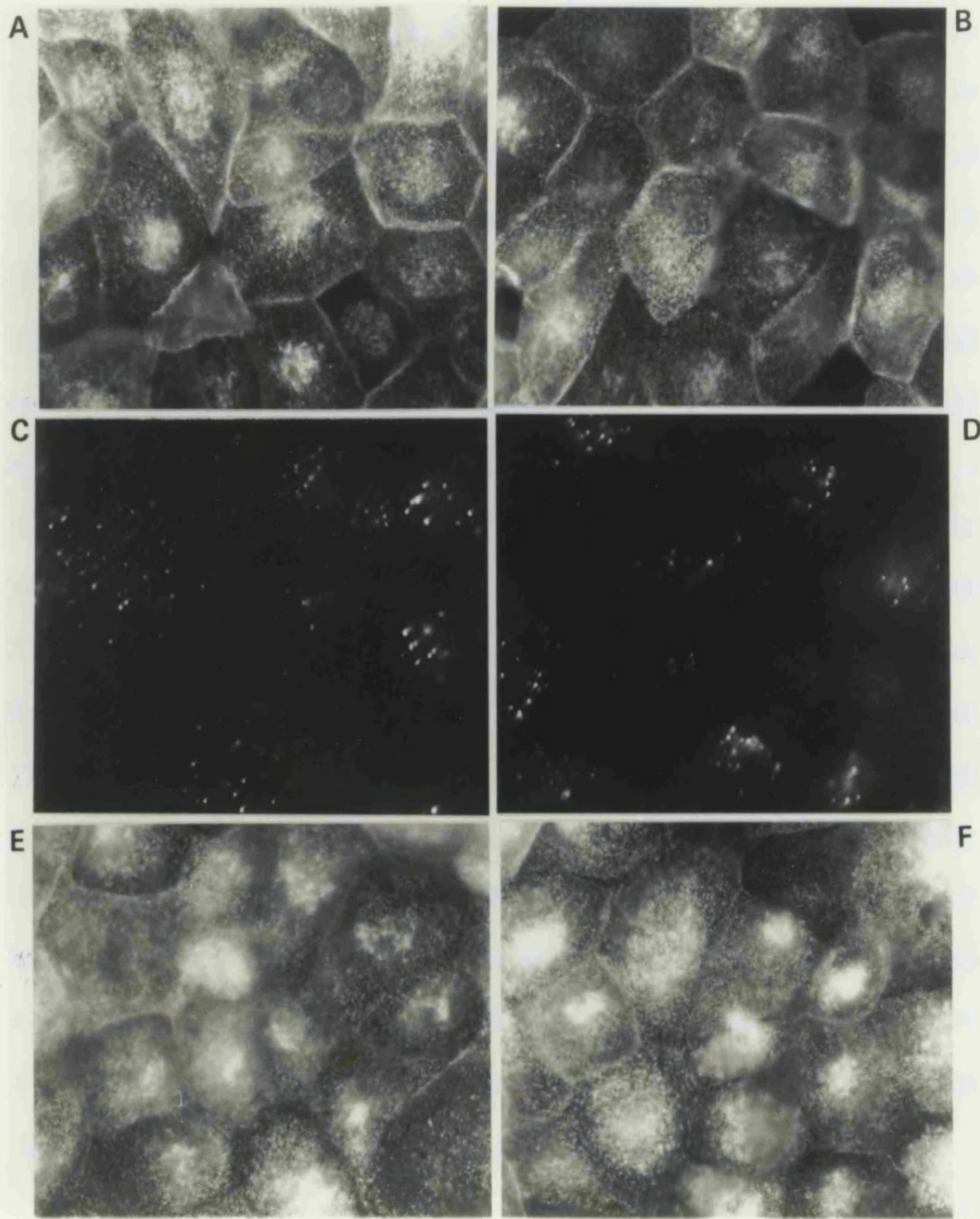


Figure 10. Distribution of 25 labeled amino acids in the
tissues of the rat. (A) Liver, (B) Kidney, (C) Heart,
(D) Spleen, (E) Lung, (F) Pancreas.

The distribution of HA however remained unchanged in the presence of 5 μ M amantadine (Figure 3B, D and F) and no characteristic amantadine-associated changes were observed.

In order to identify the location of the amantadine-induced changes in the HC58 and H9 labelling of Rostock-infected MDCK cells, a number of markers for the trans-Golgi were used. The fluorescent lipids NBD hexanoic ceramide and BODIPY ceramide C₅-DMB-Cer (Molecular Probes Inc., USA) accumulate specifically in the trans-Golgi and can be visualized by FITC fluorescence microscopy (Lipsky and Pagano, 1985; Pagano et al., 1989; Pagano et al., 1991). The use of these probes was unsuccessful however and so a monoclonal antibody against the protein TGN38 (kindly supplied by G. Banting) was used as an alternative marker. TGN38 cycles between the TGN and cell surface but is predominately located within the trans-Golgi (Bos et al., 1993; Ladinsky and Howell, 1992; Luzio et al., 1990; Reaves et al., 1993). Despite observing clear staining of the trans-Golgi in Normal Rat Kidney (NRK) cells, no staining was observed in MDCK cells, despite reports that the antibody could recognize the MDCK cell protein (personal communication G. Banting).

A rhodamine-labelled form of wheatgerm agglutinin (TRITC-WGA) proved to be more successful. WGA is a lectin which binds clustered terminal N-acetylneuraminic acid residues and N-acetylglucosamine-containing oligosaccharides on proteins. As such it labels the distal face of the Golgi (i.e. the trans-Golgi/trans-Golgi network

(TGN)) and the cell surface (Tartakoff and Vassalli, 1983; Virtanen et al., 1980). Double labelling experiments with WGA-TRITC and the three monoclonal anti-HA antibodies were carried out using Rostock-infected MDCK cells (Figure 4). The pattern of fluorescence observed with HC58 (Figure 4A) was similar to that of WGA (Figure 4B) indicating that native HA was located within the trans-Golgi as well as in cytoplasmic vesicles and on the cell surface. In the presence of amantadine (5 μ M) HC58 labelling (Figure 4C) was confined to the trans-Golgi as identified by WGA-TRITC (Figure 4D). The large characteristic H9-labelled vesicles observed in the presence of drug (highlighted in Figure 4E) were also labelled with WGA-TRITC (Figure 4F). The amantadine-induced changes in HA conformation therefore appeared to occur within the trans-Golgi or TGN. The pattern of WGA fluorescence however was more diffuse than that of HA, especially so in the presence of amantadine.

Amantadine (5 μ M) specifically inhibits the M2 protein. The distribution of M2 protein was investigated by immunofluorescence using two polyclonal antisera:- R53 which recognizes the N-terminus of the protein and R54 which recognizes the C-terminus. Similar patterns of fluorescence were observed in Rostock-infected cells, with both R53 and R54. M2 protein was distributed both internally and on the cell surface (Figure 5C and D). The pattern of fluorescence also highlighted the presence of M2 around the edges of the cells. The distribution of M2 protein was unaffected by the addition 5 μ M amantadine

**Figure 4: The distribution of HA within Rostock-
infected MDCK cells with respect to WGA.**

Rostock-infected MDCK cells were fixed (5½ hours p.i.) and labelled with WGA-TRITC, followed by antibodies HC58 (A-D) specific for the native form of HA and H9 (E and F) specific for the low pH form of HA. All cells were subsequently incubated with RAM-FITC. The cells shown in C-F were incubated in the presence of 5µM amantadine from 1 hour p.i..

A, C and E show FITC fluorescence; B, D and F show TRITC fluorescence.

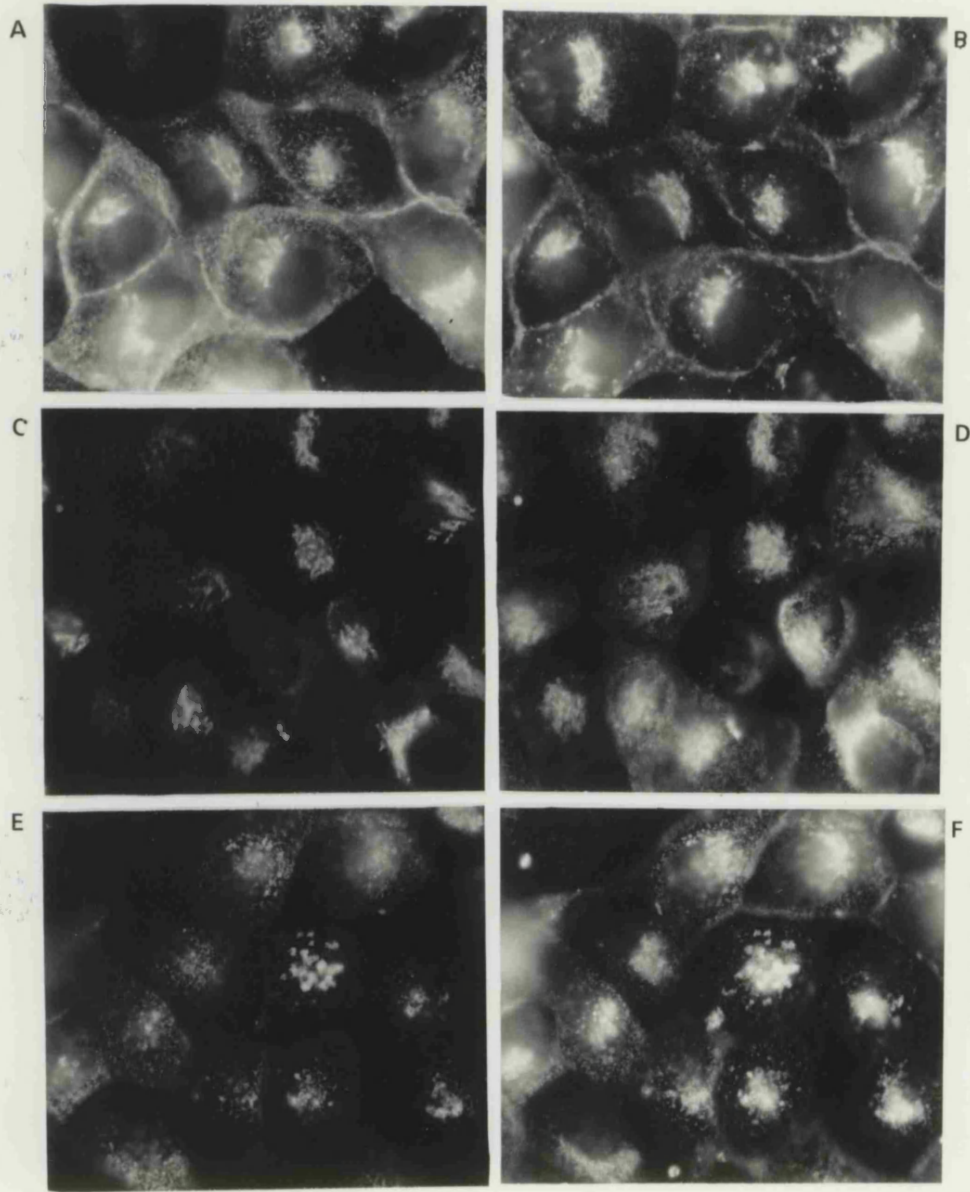


Figure 5: The effect of amantadine on the distribution of M2 protein in Rostock-infected MDCK cells.

Uninfected (A and B) and Rostock-infected (C-E) MDCK cells (5½ hours p.i.) were fixed and incubated with polyclonal antiserum R53 specific for the N-terminus of M2 (A, C and E) and R54 specific for the C-terminus of M2 (B, D and F). All cells were subsequently incubated with GAR-FITC.

5µM amantadine was added to the cells shown in E and F, from 1 hour p.i..

Figure 10 and 11. A higher magnification fluorescence micrograph of the same area shown in Figure 9. The cells are stained with anti-actin (A) and anti-tubulin (B). The actin is stained with rhodamine anti-actin (A) and the tubulin is stained with fluorescein anti-tubulin (B). The cells are shown in phase contrast (C) and fluorescence (D, E, F). The actin is stained with rhodamine anti-actin (A) and the tubulin is stained with fluorescein anti-tubulin (B). The cells are shown in phase contrast (C) and fluorescence (D, E, F).

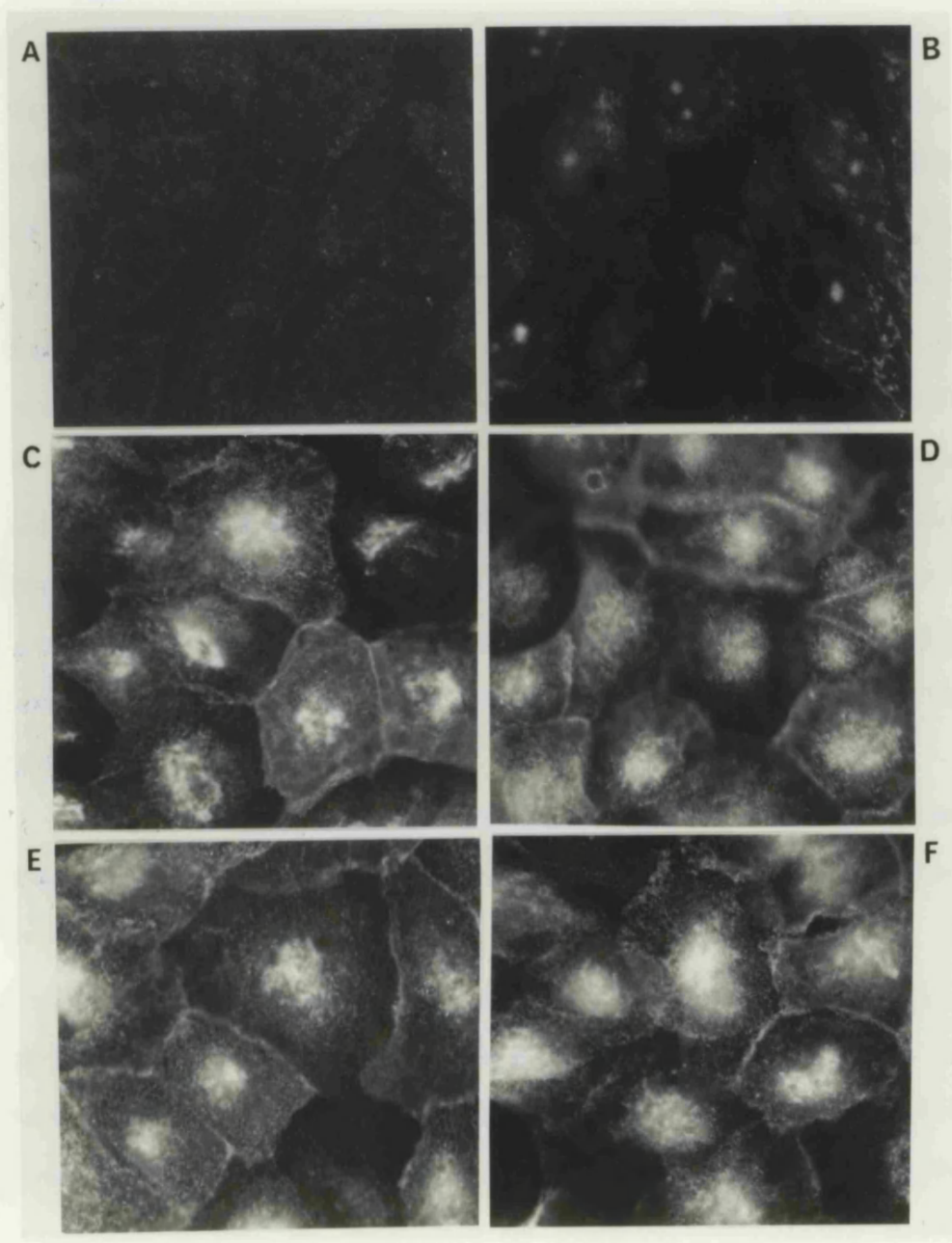


Figure 10 and 11. A higher magnification fluorescence micrograph of the same area shown in Figure 9. The cells are stained with anti-actin (A) and anti-tubulin (B). The actin is stained with rhodamine anti-actin (A) and the tubulin is stained with fluorescein anti-tubulin (B). The cells are shown in phase contrast (C) and fluorescence (D, E, F). The actin is stained with rhodamine anti-actin (A) and the tubulin is stained with fluorescein anti-tubulin (B). The cells are shown in phase contrast (C) and fluorescence (D, E, F).

(Figure 5E and F). A higher background fluorescence was observed in uninfected cells labelled with R54 antiserum (Figure 5B) and for this reason R53 was used in subsequent studies.

Double labelling experiments using the monoclonal anti-HA antibodies and R53 antiserum, were performed to compare the distributions of HA and M2 protein (Figure 6). The pattern of fluorescence observed with R53 (Figure 6D and F) incorporated both the HC58 (Figure 6C) and H9 (Figure 6E) labelling observed in amantadine-treated cells. In addition R53 colocalization with WGA-TRITC (Figure 6A and B) showed that M2 was present in the trans-Golgi as well as at the cell surface and in cytoplasmic vesicles. It would appear from the location of native and low pH HA that amantadine causes a pH-induced conformational change in HA within the trans-Golgi/TGN, where it is colocalized with M2 protein.

Using the immunocytochemical pH probe DAMP, studies have shown that large acidic vesicles similar to the vesicles labelled with H9, appear in the cytoplasm of infected cells treated with 5 μ M amantadine (Ciampor *et al.*, 1991a). DAMP is a basic congener of dinitrophenol which is taken up by viable cells and accumulates within acidic compartments in its protonated form. After aldehyde fixation it can be localized by immunocytochemistry using a monoclonal anti-DNP antibody (Anderson *et al.*, 1984; Anderson and Pathak, 1985). The intention was to use DAMP to further investigate pH changes within the different

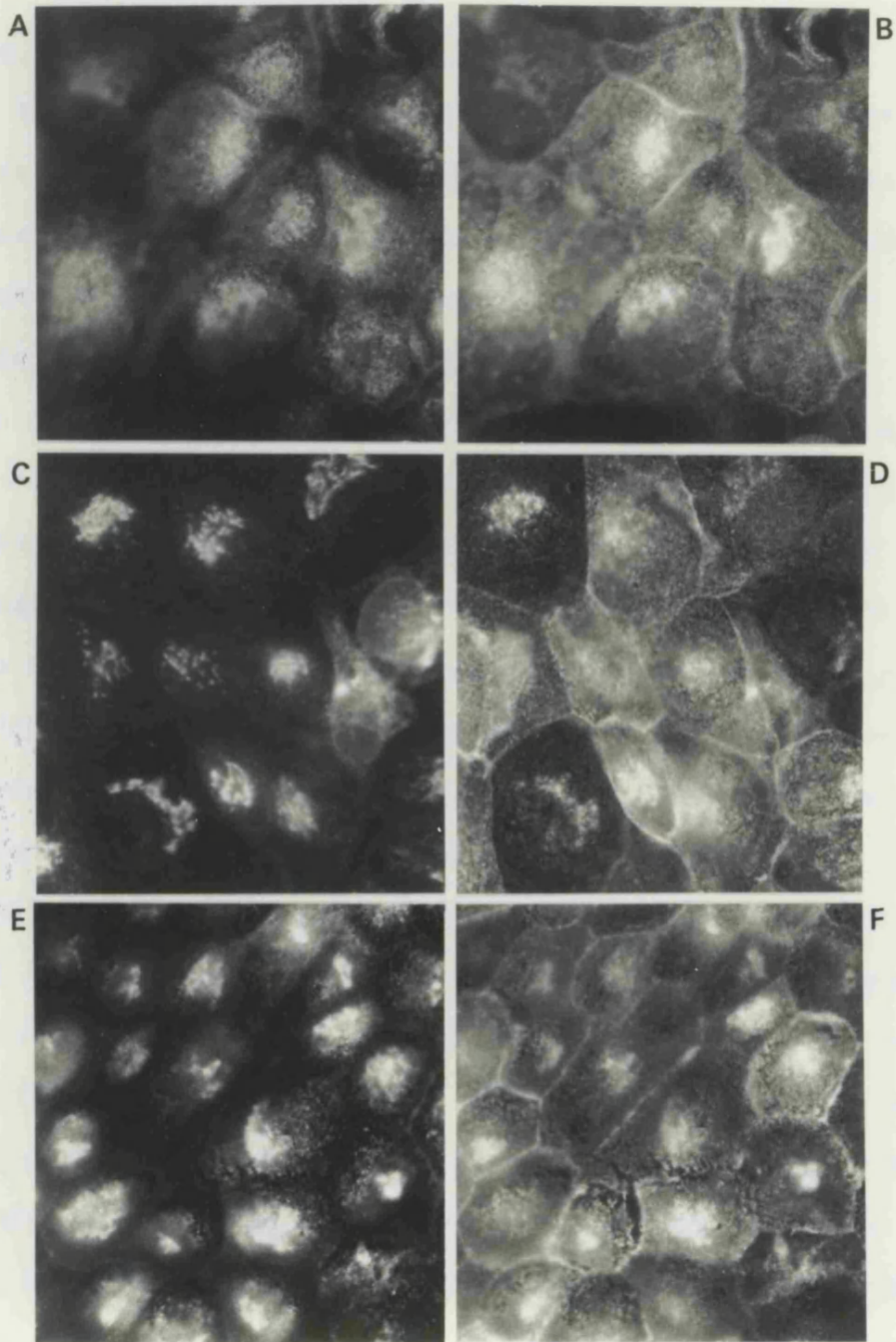
Figure 6: The distribution of M2 protein within Rostock-infected cells with respect to HA and WGA.

Rostock-infected MDCK cells were fixed (5½ hours p.i.) and incubated with R53 anti-M2 antiserum, followed by GAR-FITC. A and B were labelled with WGA-TRITC.

C-F were incubated with monoclonal antibodies HC58 (C and D) specific for the native form of HA and H9 (E and F) specific for the low pH form of HA, followed by RAM-TRITC.

Amantadine (5µM) was added to the cells from 1 hour p.i. (C-F).

A, C and E show TRITC fluorescence; B, D and F show FITC fluorescence.



vesicular compartments and to relate this to the distribution of HA and M2. However the experiments were unsuccessful as only very low levels of fluorescence were observed.

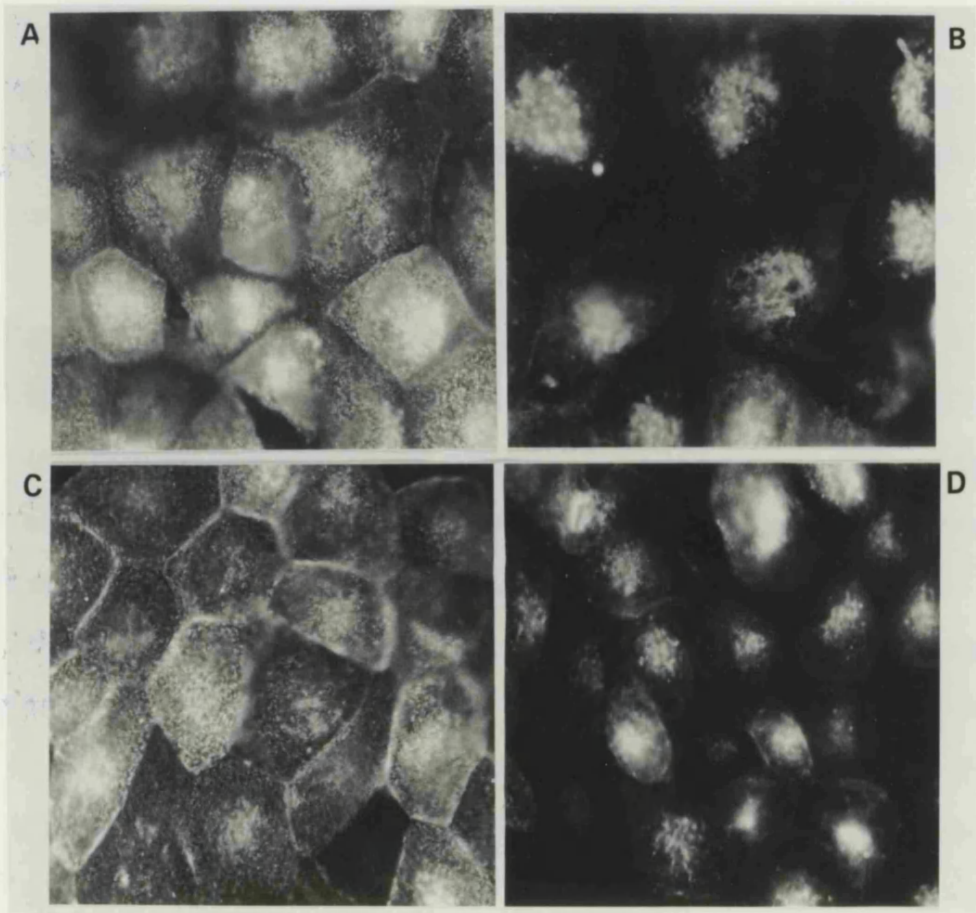
The effect of brefeldin A on HA and M2 protein

The fungal metabolite brefeldin A (BFA) is an important tool in the study of cellular transport mechanisms (Hunziker et al., 1992; Klausner et al., 1992). It has a dramatic effect on both the structure and function of the Golgi apparatus causing its rapid disassembly and the redistribution of Golgi proteins into the ER (Doms et al., 1989; Fujiwara et al., 1988; Lippincott-Schwartz et al., 1989). In contrast to the majority of mammalian cells the Golgi apparatus of MDCK cells appears to be resistant to the effects of BFA (Hunziker et al., 1991; Sandvig et al., 1991). Processes in MDCK cells including transcytosis, endocytosis and the transport of proteins are however affected by the presence of brefeldin A (Hunziker et al., 1991; Low et al., 1991; Prydz et al., 1992). In particular BFA has been found to affect the targeting and subsequent transport of proteins from the TGN to the apical surface, in MDCK cells (Low et al., 1992). Both M2 and HA are expressed apically in MDCK cells (Hughey et al., 1992; Rodriguez-Boulan et al., 1984). The effect of BFA on M2 and HA transport was studied in an attempt to gain further information concerning the pH-induced conformational changes in HA and the alterations in pH caused by M2.

As shown in Figure 7, 5 μ g/ml BFA added from 1 hour p.i.

Figure 7: The distribution of HA and M2 protein in Rostock-infected MDCK cells in the presence of BFA, as observed by immunofluorescence.

Rostock-infected MDCK monolayers were fixed 6 hours p.i.. The cells shown in A and B were incubated with HC2 which recognizes most forms of HA, followed by RAM-FITC. The cells shown in C and D were incubated with anti-M2 antiserum (R53) followed by GAR-FITC. 5 μ g/ml brefeldin A was added to the cells (B and D) from 1 hour p.i..



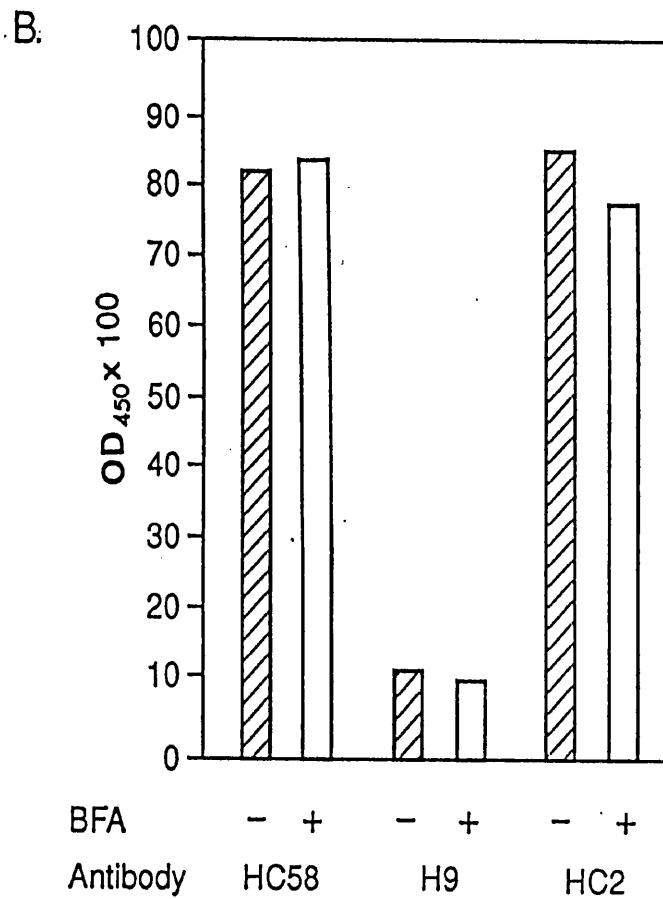
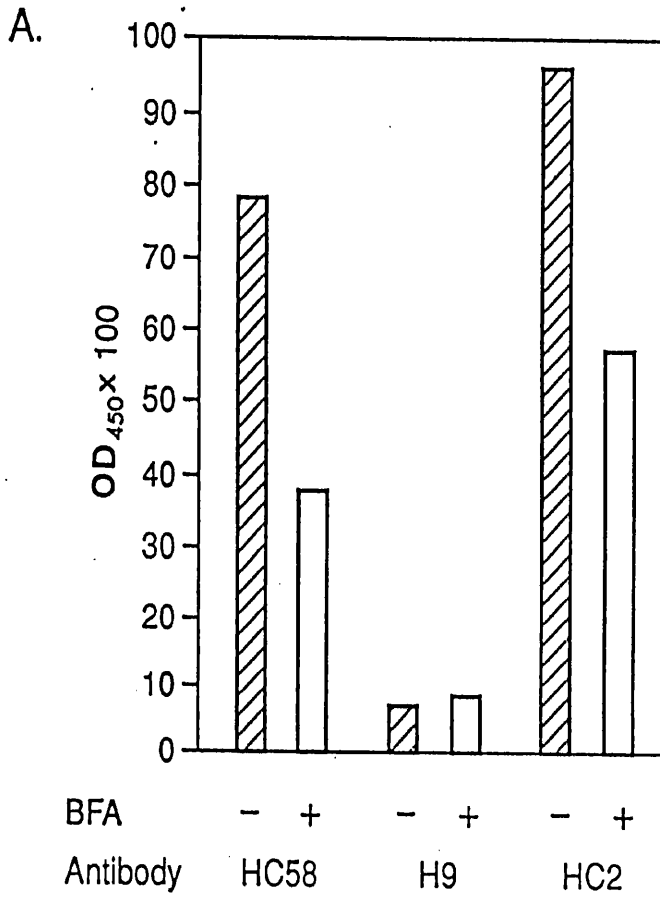
appeared to inhibit the transport of both M2 and HA proteins to the MDCK cell surface. This was indicated by the reduction in speckled surface labelling and the apparent accumulation of internal label, with both the anti-M2 antiserum R53 (Figure 7D) and the anti-HA monoclonal antibody HC2 (Figure 7B).

In order to investigate further the effect of BFA on the distribution of HA, the expression of HA on the cell surface was studied by ELISA (Figure 8). As previously shown the majority of HA detected was in the native conformation and only small amounts of low pH HA were detected. In permeabilized MDCK cells the levels of HC2, HC58 and H9-reactive HA all appeared to be unaffected by BFA, suggesting that HA synthesis was not significantly affected by BFA treatment (Figure 8B). Assuming that only cell surface HA protein can be detected in unpermeabilized cells (due to the exclusion of antibody from the cell interior), cells treated with BFA showed a decrease in the amount of cell surface HA. This was reflected by a reduction in the amount of both HC2 and HC58-reactive HA detected (Figure 8A). In agreement with the previous immunofluorescence observations, the ELISA data therefore showed that BFA affected the transport of HA to the plasma membrane. Unfortunately the cell surface expression of M2 protein could not be studied by ELISA as the polyclonal antisera R53 and R54 produced a high non-specific background signal.

Figure 8: The effect of BFA on the amount of HA detected in Rostock-infected MDCK cells by ELISA.

Rostock-infected MDCK cells were fixed with 0.05% glutaraldehyde 6 hours p.i.. Unpermeabilized (A) and cells permeabilized with 0.1% Triton X-100 for 5 minutes (B) were incubated with anti-HA monoclonal antibodies HC58, H9 and HC2, followed by protein A conjugated to horseradish peroxidase. The cells were incubated with citrate buffer containing TMB (as described in 2.4) and the amount of HA antigen assessed by measuring the optical density (OD) at 450nm.

5 μ g/ml brefeldin A was added to cells from 1 hour p.i. (shaded).



In order to try to determine more precisely the stage at which BFA inhibited the transport of HA and M2, protein-radiolabelling techniques were used. HA and M2 transport through the cell can be monitored by structural modifications which occur to the proteins as they progress through the various cell compartments. Both HA and M2 acquire palmitate groups postrationally. This probably occurs around the time the proteins leave the ER and enter the Golgi. The functional importance of palmitoylation is not known. ³H-labelling of palmitate groups shows that BFA inhibits the palmitoylation of both M2 and HA. The levels of palmitoylated proteins were reduced by 36% and 59%, respectively (Figure 9A).

The cleavage of HA0 into HA1 and HA2 in the case of avian influenza viruses such as Rostock, probably occurs within the trans-Golgi. The effect of BFA on the cleavage process was studied by the immunoprecipitation of ³⁵S-labelled HA with the monoclonal antibody HC2 (Figure 9B). HC2 recognizes both the uncleaved and cleaved forms of HA. The cleavage of HA0 into HA1 and HA2 was reduced by 90% in BFA-treated cells.

In summary BFA appeared to interfere with the transport of M2 and HA proteins to the cell surface. This was associated with the incomplete processing of the proteins, highlighted by the inhibition of palmitoylation and HA cleavage. This suggests that BFA acts at a stage prior to that of amantadine, which in terms of its effect on HA maturation, acts after the cleavage of HA0 into HA1 and

Figure 9: The effect of BFA on the palmitoylation and HA0 cleavage in Rostock-infected MDCK cells

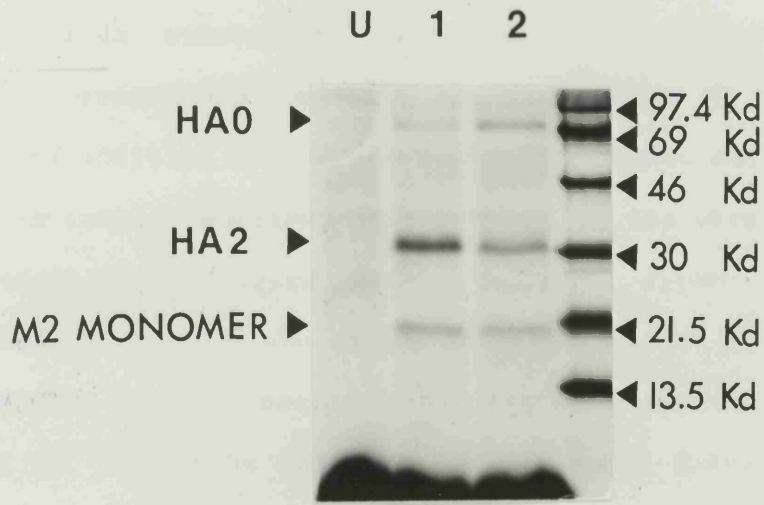
A. Uninfected and Rostock-infected (5 hours p.i.) MDCK cells were labelled with [³H] palmitic acid for 2 hours at 37°C. After washing, the cells were lysed and the lysates subject to polyacrylamide electrophoresis. The gel was exposed to photographic film for 24 hours.

The lanes show (from left to right) uninfected cells (U), Rostock-infected cells (1) and Rostock-infected cells treated with 5µg/ml BFA, added from 1 hour p.i. (2). The amount of palmitoylated HA and M2 was determined by densitometry.

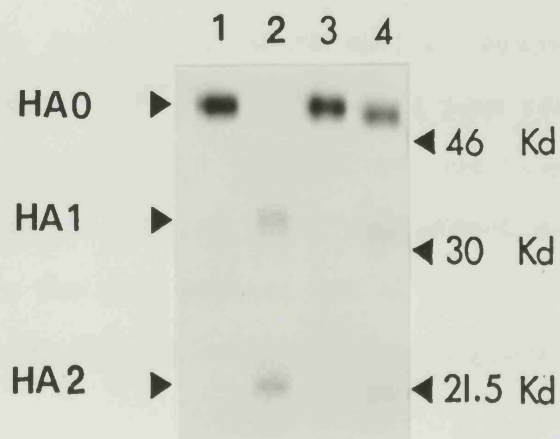
B. Uninfected and Rostock-infected cells (from 6 hours p.i.) were pulse-labelled with [³⁵S]-Trans label for 15 minutes and chased in media without ³⁵S for 1 hour. After this time cell lysates were collected and immunoprecipitated with the monoclonal anti-HA antibody HC2. The samples were then subject to polyacrylamide gel electrophoresis (as in materials and methods). The gel was exposed to film for 48 hours.

The lanes show (from left to right): Rostock-infected cells which have been pulse-labelled (1) and pulse-chase labelled (2); Rostock-infected cells treated with 5µg/ml BFA from 1 hour p.i., which have been pulse-labelled (3) and pulse-chase labelled (4).

A.



B.

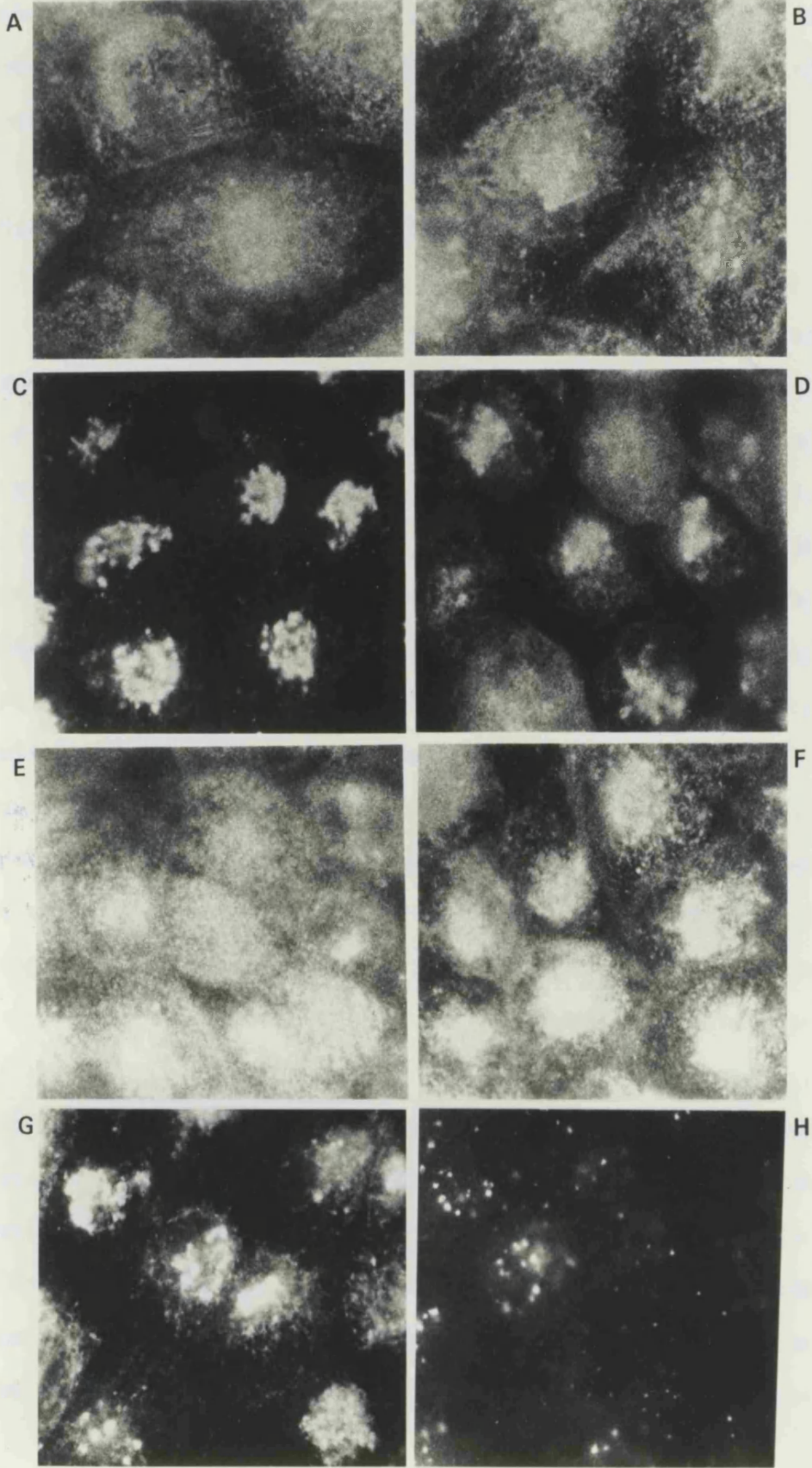


HA2.

The addition of brefeldin ($5\mu\text{g/ml}$) to infected MDCK cells treated with amantadine ($5\mu\text{M}$) was investigated using immunofluorescence to examine the effects on HA (Figure 10). The addition of brefeldin ($5\mu\text{g/ml}$) caused native HA, which is usually confined to the Golgi in the presence of $5\mu\text{M}$ amantadine (Figure 10C), to also appear within cytoplasmic vesicles and on the cell surface (Figure 10D). A reduction in the presence of BFA was also observed in the amount of low pH HA detected in the cells treated with amantadine (Figure 10H). The number of large cytoplasmic vesicles containing low pH HA were reduced and no labelling of the cell surface was observed (Figure 10H). These changes in HA were probably due to the inhibition of HA cleavage which is required before HA can undergo the acid-induced conformational change associated with amantadine treatment. The ability of BFA to inhibit the cell surface transport of HA, as indicated by the accumulation of HC2 within the cell (Figure 10F), also probably contributed to the effects on HA within the amantadine-treated cells, incubated in the presence of BFA. The fact that the small amount of HA which was expressed on the cell surface was predominantly in the native conformation, suggested that although the majority of M2 was prevented from reaching the cell surface it was still capable of modifying the pH within the transport pathway. BFA may affect a number of processes within the cell however and it is not possible to pinpoint precisely its action within the Rostock-infected

Figure 10: The effect of BFA on the distribution of HA and M2 protein within amantadine-treated cells

Rostock-infected MDCK cells were incubated with 5 μ M amantadine from 1 hour p.i.. The cells were fixed at 5 $\frac{1}{2}$ hours p.i. and incubated with the anti-HA monoclonal antibodies HC58 (A-D), H9 (G and H) and HC2 (E and F), followed by RAM-FITC. 5 μ g/ml brefeldin A was added to the cells (D, F and H) from 1 hour p.i..



MDCK cells. It would be of interest however to determine more precisely the effect of BFA on HA and M2, in terms of whether the glycosylation of HA is effected and if the apical targeting of the two proteins is affected.

3.2 CYTOPLASMIC PH CHANGES WITHIN VIRUS-INFECTED CELLS

Using the pH probe DAMP, an increase in the acidity of Rostock virus-infected MDCK cells has been observed (Ciampor et al., 1991a). In view of this observation and the involvement of M2 protein in vesicular pH changes, fluorescent pH probes were used to study directly pH changes within the cytoplasm of virus-infected cells. The recent development of pH-sensitive fluorochromes has provided a non-invasive means of monitoring pH changes within living cells. Two probes were used BCECF and SNARF-1. These were loaded into cells in the form of cell permeant esters BCECF-AM and SNARF-1-AM. Cellular esterases subsequently convert the probes into their cell impermeant fluorescent forms. Changes in the fluorescence spectra of the probes reflect changes in the cytoplasmic pH (Thomas et al., 1979; Rink et al., 1982; Bassnett et al., 1990; Seksek et al., 1991). The pK_a values of BCECF and SNARF-1 are 7.0 and 7.3 respectively making them both suitable for measuring pH within the physiological range. The cytoplasmic pH in BCECF-loaded cells was determined using a ratio of excitation intensities (506/455nm), at an emission wavelength of 530nm and in SNARF-1-loaded cells

using a ratio of emission intensities (634/604nm) at an excitation wavelength of 534nm. The ratios eliminate a number of variables which may perturb the measurements, providing an accurate assessment of the pH. In particular, discrepancies due to non-uniform dye loading, differences in cell thickness, probe bleaching and probe leakage are avoided, as these have a similar effect on the intensities at both wavelengths.

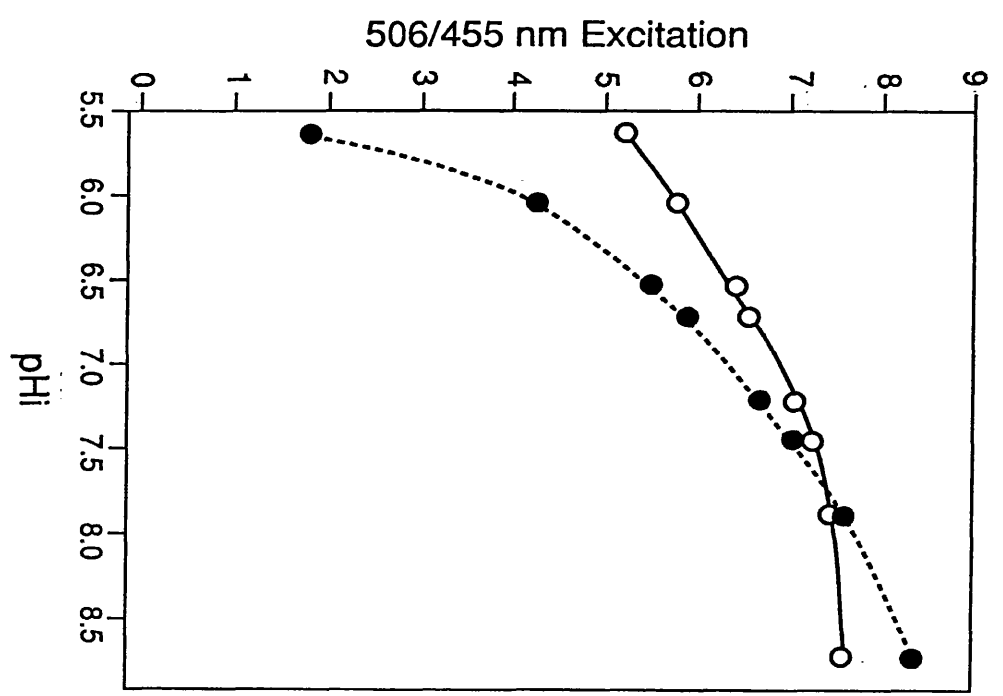
Cytoplasmic pH was determined from the ratios of fluorescence intensities by reference to a calibration curve (Figure 11A for BCECF and Figure 11B for SNARF-1). Nigericin is a K^+H^+ antiporter which allows the cytoplasmic pH to equilibrate with the external pH under conditions where the internal and external K^+ concentrations are equivalent (Thomas et al., 1979). In order to equilibrate the pH of the cell interior with an external solution of known pH, cells were incubated with $10\mu M$ nigericin in high KCl buffer (115mM KCl, 1mM $MgCl_2$ and 20mM HEPES, adjusted to various pH's).

Nigericin caused a decrease in the cytoplasmic pH of BCECF (Figure 11A) and SNARF-1 (Figure 11B) loaded cells exposed to external pHs below 7.6-7.7. This indicated that under these conditions the buffering capacity of the MDCK cell maintained the cell interior at a pH above that of the external medium. Above pH7.6-7.7 the situation was reversed. Initial experiments with MDCK cells indicated that SNARF-1 was the more suitable of the two probes, as the results were more reproducible. Consequently this

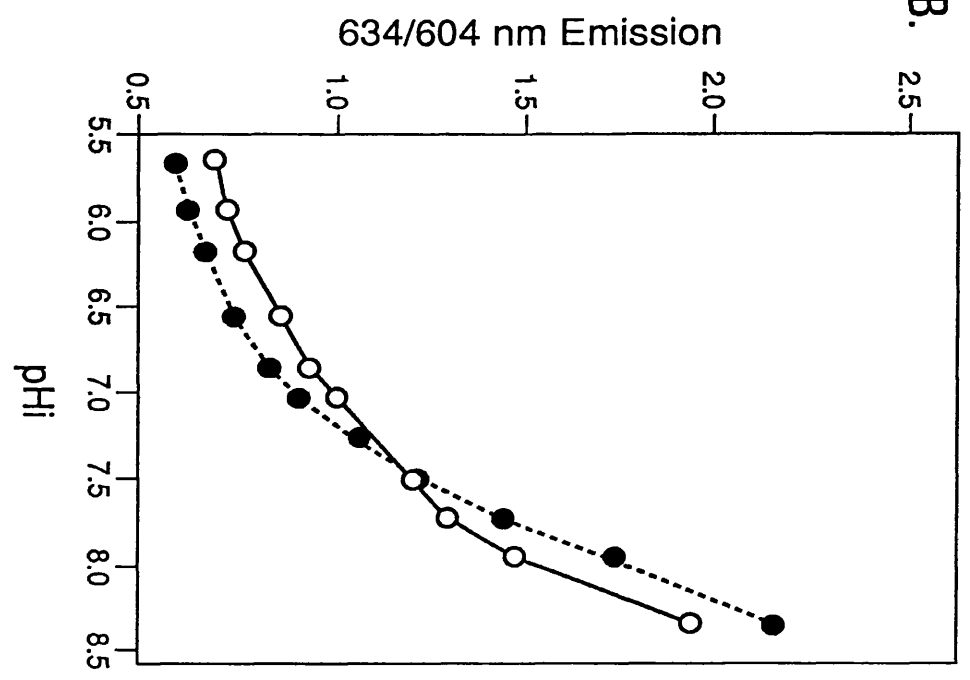
Figure 11: Calibration curves for BCECF and SNARF-1 in MDCK cells.

Uninfected MDCK cells were loaded at 37°C for 1½ hours with 10µM BCECF-AM (A) or for 1 hour with 10µM SNARF-1-AM (B) and placed in a cuvette with 115mM KCl, 1mM MgCl₂ and 20mM Hepes, adjusted to various pHs. 506/455nm excitation ratios (530nm emission) were measured for BCECF and 634/604nm emission ratios (534nm excitation) for SNARF-1. Fluorescence ratios were obtained at each pH before (○) and after (●) the addition of 10µM nigericin (10 minutes).

A.



B.



probe was used in all subsequent experiments. Figure 12 shows the effects of various concentrations of nigericin on the cytoplasmic pH of uninfected cells incubated in Gey's+20mM Hepes, pH7.10. 0.01 μ M nigericin had no significant effect on the cytoplasmic pH, whereas 0.1, 1.0, 10 and 100 μ M concentrations of the ionophore caused the pH to decrease. The addition of 100 μ M nigericin caused the cytoplasmic pH to initially overshoot the pH of the external medium. Such high concentrations of nigericin may also produce cytotoxic effects and so were not used. 10 μ M nigericin is the concentration normally used to calibrate fluorescent pH probes and this reduced the pH to that of the external medium. The pH change produced by 10 μ M nigericin was equivalent in cells incubated in both Gey's buffer and the high KCl calibration buffer. This suggested that in this instance high external concentrations of K⁺ were not necessary to allow nigericin to abolish the plasma membrane pH gradient. Cells incubated with 2 μ M valinomycin (which equilibrates internal and external concentrations of K⁺) in addition to 10 μ M nigericin showed no significant difference in their cytoplasmic pH from cells incubated with nigericin alone (data not shown). This applied to cells incubated in both Gey's and high KCl buffer (pH7.10). SNARF-1-AM may be converted into its pH-sensitive fluorescent form (SNARF-1) in solution by the addition of hog liver esterase. In such a situation the emission ratio of the free probe is shifted from that of the cell-associated form (Figure 13). Similar observations

Figure 12: The reduction in the cytoplasmic pH of uninfected MDCK cells in Gey's+20mM Hepes, pH7.10, by the addition of various concentrations of nigericin.

Uninfected MDCK cells were incubated for 1 hour with 10 μ M SNARF-1-AM. Emission spectra were obtained in Gey's+20mM Hepes, pH7.10, at 2 minute intervals over a period of 20 minutes following the addition of various concentrations of nigericin. Using the SNARF-1 calibration curve (figure 11B) 634/604nm emission ratios (534nm excitation) were converted into cytoplasmic pH values.

0.01 μ M (■), 0.1 μ M (△), 1 μ M (▲), 10 μ M (○) and 100 μ M (●) concentrations of nigericin were used.

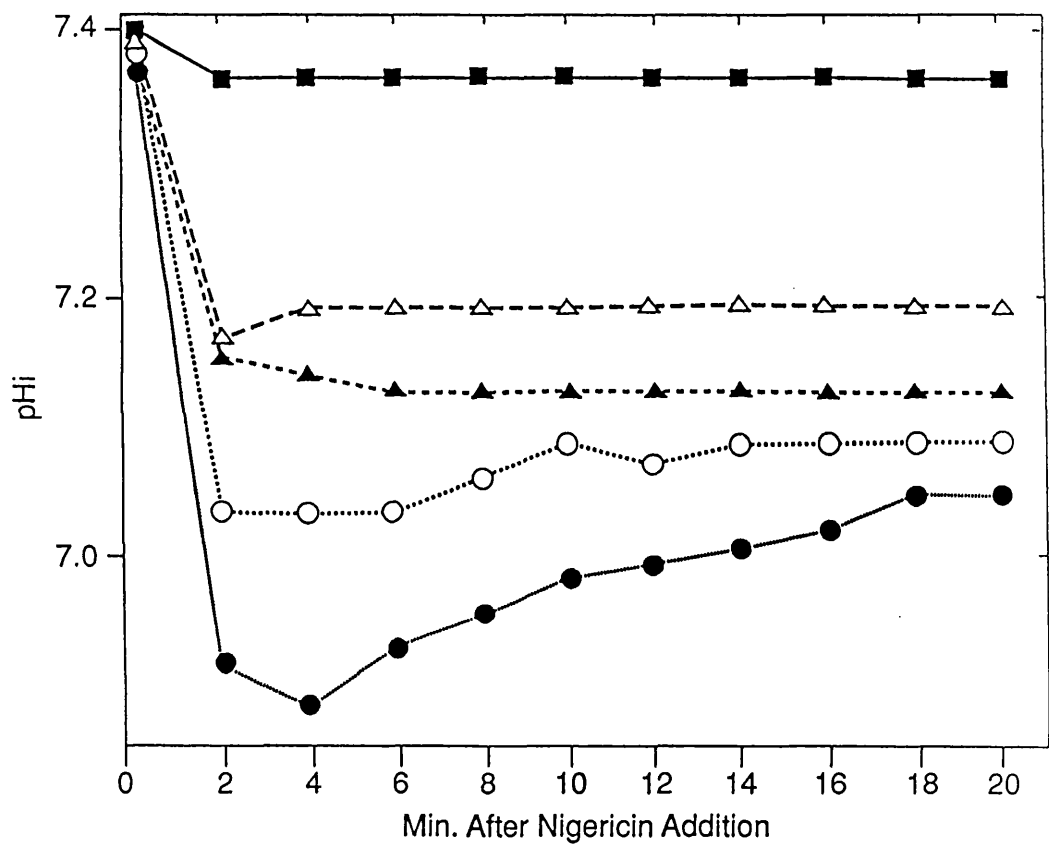
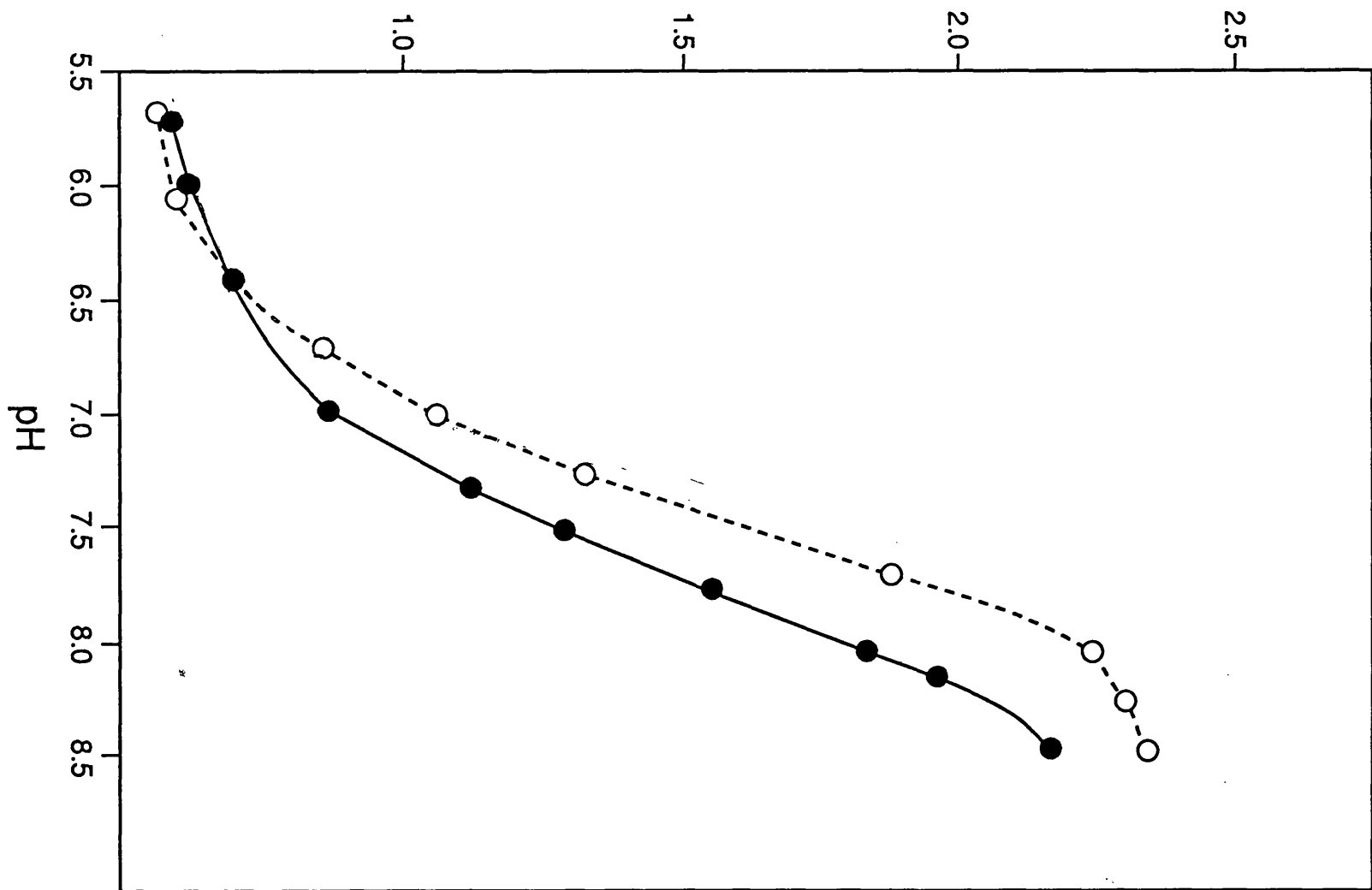


Figure 13: Comparison of the 'in vitro' and 'in vivo' calibration of SNARF-1.

634/604nm emission ratios (534nm excitation) were obtained for SNARF-1-loaded MDCK cells (1 hour) in the presence of 10 μ M nigericin (•) and free SNARF-1 in solution (○), which was converted from SNARF-1-AM by the addition of 30 μ g of hog liver esterase (20 minutes, 37°C). Fluorescence scanning was carried out in 115mM KCl, 1mM MgCl₂ and 20mM Hepes, adjusted to various pHs.

634/604 nm Emission



have also been recently reported by other workers (Bassnett et al., 1990; Blank et al., 1992; Owen, 1992), suggesting that the probe environment influences the fluorescence properties of SNARF-1. Cells loaded with SNARF-1 were washed before use and no significant leakage of the probe into the external solution was detected over periods of up to 2 hours. The viability of the cells after SNARF-1 loading and measurement was also assessed, by the uptake of trypan blue. The proportion of live cells was consistently above 95% with any dead cells (stained blue) been confined to the edges of the coverslip, away from the focus of the incident light beam.

No significant bleaching of the probe fluorescence intensity at the 604nm emission wavelength occurred during periods of up to 40 minutes, where the cells were continuously exposed to the 534nm excitation beam of the spectrofluorimeter. However exposure to the excitation beam was minimized between readings to further ensure that bleaching did not occur. The 604nm emission point represents the isobestic point at which the absorption, excitation and emission intensities of the probe are independent of the concentration of ionic species. This did not vary significantly throughout periods of continuous measurement of up to 45 minutes. The emission intensity at 634nm is dependent on pH and corresponds to the base form of the probe. The 634/604nm emission ratios obtained from SNARF-1-loaded cells on different coverslips varied by ± 0.02 ratio units. When the ratios were converted into pH

using the SNARF-1 calibration curve, this difference had no significant effect on the pH values obtained.

Compartmentalization into lysosomes and mitochondria can be a problem with fluorescent pH probes in certain instances (Thomas et al., 1979). The fluorescent signal from dye localized within these more acidic compartments may interfere with the measurement of the cytoplasmic pH. Figure 14 shows that SNARF-1 in uninfected and virus-infected MDCK cells does not accumulate in any obvious vesicular structures and is distributed throughout the cytoplasm. The central areas of both uninfected and virus-infected cells appear to fluoresce more intensely, due to differences in the thickness of the cells.

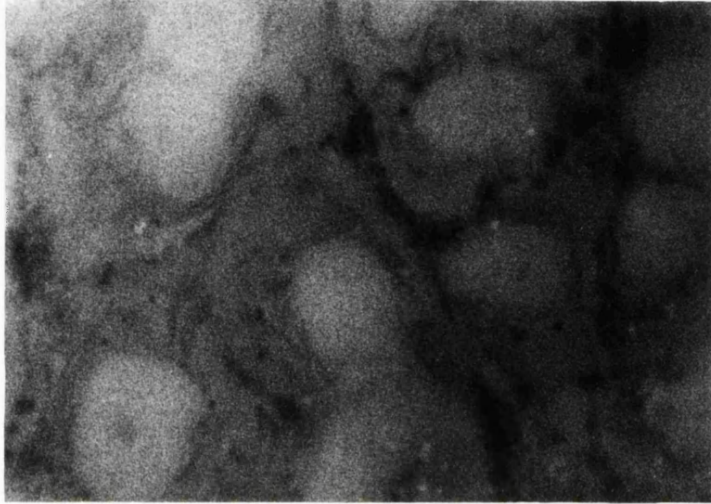
Reduction in the cytoplasmic pH of virus-infected MDCK cells

A clear difference was observed between the emission spectra of uninfected and virus-infected MDCK cells loaded with SNARF-1 (Figure 15). Infected cells (6 hours p.i.) showed a relative decrease in the emission intensity at 634nm as compared to that at 604nm. Changes in the spectra reflected changes in the cytoplasmic pH of the cells, the cytoplasm of the infected cells was more acidic than that of the uninfected cells. This decrease in the cytoplasmic pH of Rostock-infected MDCK cells was observed from 2 hours p.i. (Figure 16). By 6 hours p.i. a 0.4pH unit difference was apparent between the uninfected and infected cells (pH7.4 and pH7.0 respectively). This was equivalent to the change in pH observed in uninfected cells treated with 10 μ M

Figure 14: The distribution of SNARF-1 in uninfected and virus-infected MDCK cells, as observed by fluorescence microscopy.

Uninfected (A) MDCK cells were loaded with 10 μ M SNARF-1-AM for 1 hour. MDCK cells infected with Rostock virus (B) were similarly loaded with SNARF-1-AM, 5-6 hours p.i.. After washing twice with Gey's+20mM Hepes, pH7.10, the coverslips were placed cell surface down onto microscope slides and observed by fluorescence microscopy (FITC filter).

A.



B.

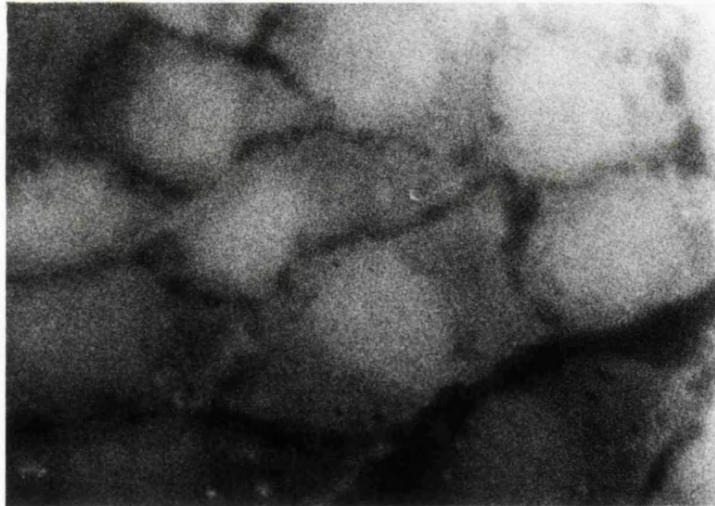


Figure 15: The effect of amantadine on the emission spectra (excitation 534nm) of SNARF-1, in uninfected and virus-infected MDCK cells.

Uninfected (A and B) MDCK cells were incubated with 10 μ M SNARF-1-AM for 1 hour. Cells infected with Rostock virus (C and D) or an amantadine resistant mutant R41R (E and F), were loaded with 10 μ M SNARF-1-AM, 5-6 hours p.i.. Emission spectra (534nm excitation) were scanned from 570nm to 650nm, in Gey's+20mM HEPES, pH7.10.

Amantadine (5 μ M) was added to the cells from 1 hour p.i. (B, D and F).

Emission Intensity

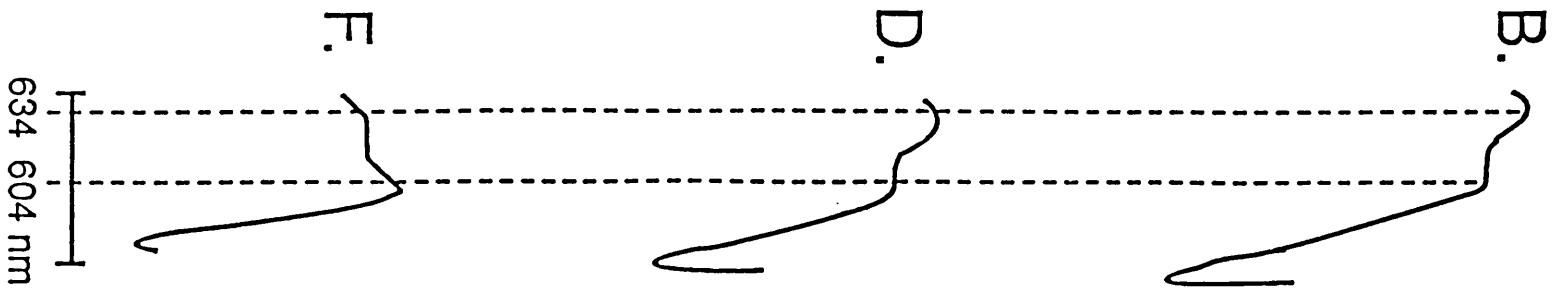
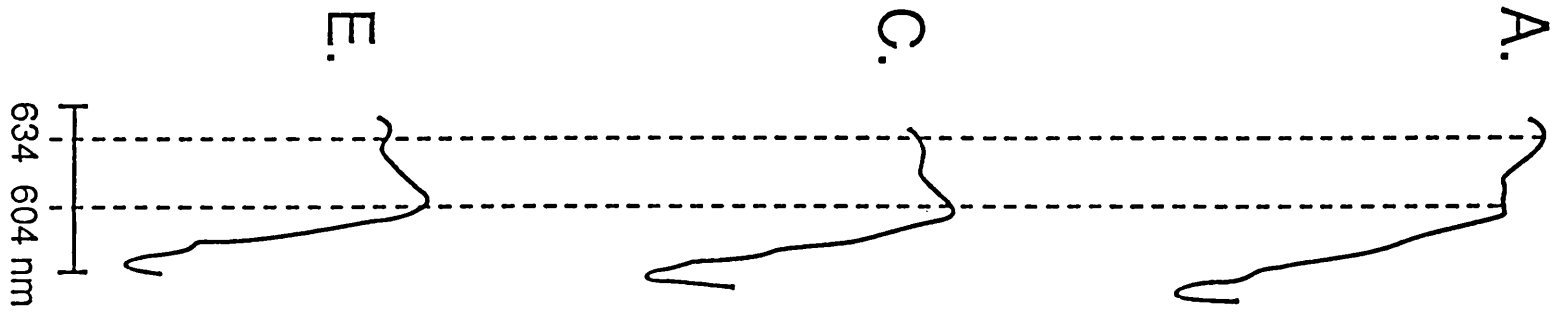
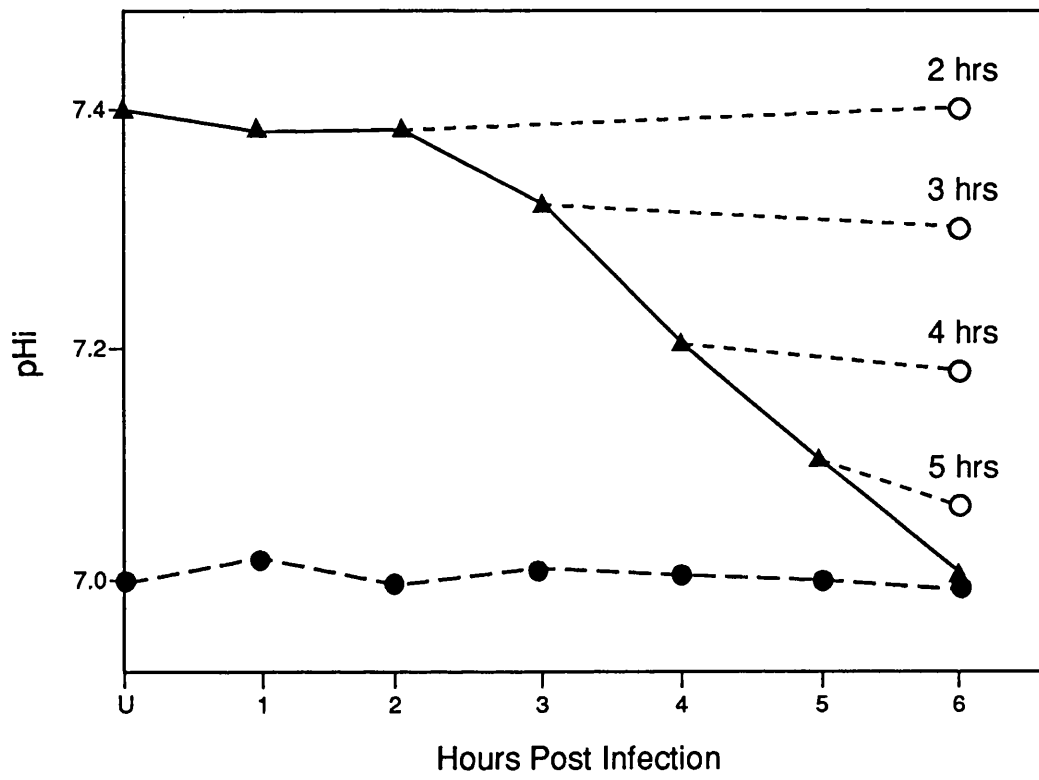


Figure 16: The effect of cycloheximide on the cytoplasmic pH decrease observed in Rostock-infected MDCK cells.

Uninfected (U) and Rostock-infected MDCK cells at hourly intervals p.i. were loaded with SNARF-1-AM for 1 hour (\blacktriangle). 634/604nm emission ratios were used to estimate the cytoplasmic pH of cells by reference to the SNARF-1 calibration curve (figure 11B).

Cycloheximide (100 μ g/ml) was added to the virus-infected cells at 2, 3, 4 and 5 hours p.i. and their cytoplasmic pH determined at 6 hours p.i. (\circ).

Nigericin (10 μ M) was added to the virus-infected cells for 10 minutes (\bullet).



nigericin. Nigericin had no effect on the cytoplasmic pH of infected cells (from 6 hours p.i.) and it appeared that in terms of their effects on the cytoplasmic pH the consequences of infection and nigericin treatment were similar. This suggests that virus-infection abolishes the membrane pH gradient to equilibrate the internal pH with that of the external medium. To confirm that this was a feature of virus infection, cells infected with UV-inactivated virus were studied. The virus was still able to enter cells, but was incapable of replicating. Inactivation by exposure to ultra-violet light (254nm) was assessed by plaque assay (Table 1). Cells infected with UV-inactivated virus (4 joules) had an cytoplasmic pH equivalent to that of uninfected cells suggesting the pH difference was due to virus replication. The addition of the translation inhibitor cycloheximide (100 μ g), to the infected cells at different time intervals p.i., prevented any further significant decrease in the pH (Figure 16), indicating that the reduction in infected cell pH required the synthesis of viral proteins. Cycloheximide permits virus infection and primary transcription but blocks protein synthesis.

Evidence for the involvement of M2 in the cytoplasmic pH reduction

The addition of amantadine (5 μ M) to Rostock-infected cells from 1 hour p.i., produced an emission spectrum resembling that of uninfected cells (Figure 15). This suggested that M2 protein was responsible for the pH

Table 1: The inactivation of Rostock virus by ultraviolet light (254nm), as determined by plaque assay.

<u>Dose of UV</u> (Joules)	<u>Virus Titre*</u> (p.f.u./ml)
control	1.6x10 ⁸
0.1	3.7x10 ⁵
0.2	2.2x10 ⁵
0.3	8.4x10 ⁴
0.4	6.7x10 ⁴
0.5	3.3x10 ⁴
1.0	3.0x10 ³
2.0	1.7x10 ³
4.0	1.0x10 ¹

* assessed by plaque assay in MDCK cells

decrease, as low concentrations of amantadine specifically inhibit M2 activity (Hay et al., 1985; Belshe et al., 1988). Within 15 minutes of the addition of 5 μ M amantadine to the cuvette medium, the pH of the virus-infected cells had increased to that of the uninfected cells (Figure 17). The subsequent washing and incubation of the cells in amantadine-free medium showed consistently that the effect of the drug was irreversible over periods of up to 1½ hours.

As observed in Figure 15 the cytoplasmic pH of uninfected cells and cells infected with the amantadine-resistant mutant virus R41R, remained unchanged in the presence of amantadine (Figure 17). Similarly 5 μ M rimantadine, which reversed the pH decrease in Rostock-infected cells had no effect on the pH of uninfected cells or cells infected with drug resistant mutants (data not shown). The inability of amantadine or rimantadine to block cytoplasmic pH changes within cells infected with a number of drug resistant mutant viruses (R41R, 039 and 08) was consistent with the involvement of M2 (Table 2). Notably, cells infected with R41R and 039 viruses (6 hours p.i.) showed reductions in cytoplasmic pH similar to that observed in wildtype virus-infected cells (approximately 0.3-0.4pH units). In no instances did the reduction in pH exceed that produced by nigericin. The cytoplasmic pH of mutant 08-infected cells (6 hours p.i.) showed a partial reduction of only 0.2pH units. This may reflect the reduced activity of the 08 M2 (as discussed later).

Figure 17: The specific reversal by amantadine of the reduced cytoplasmic pH in Rostock-infected MDCK cells.

Uninfected (\blacktriangle) MDCK cells were loaded with SNARF-1-AM for 1 hour. Cells infected with Rostock virus (\bullet) or an amantadine resistant mutant R41R (\circ) were loaded with SNARF-1-AM, 5-6 hours p.i.. Emission spectra were obtained at 5 minute intervals over a 30 minute period, after the addition of amantadine ($5\mu\text{M}$) to the cuvette medium (ND corresponds to no drug) Cytoplasmic pH was estimated from the 634/604nm emission ratio (534nm excitation), using the SNARF-1 calibration curve (figure 11B).

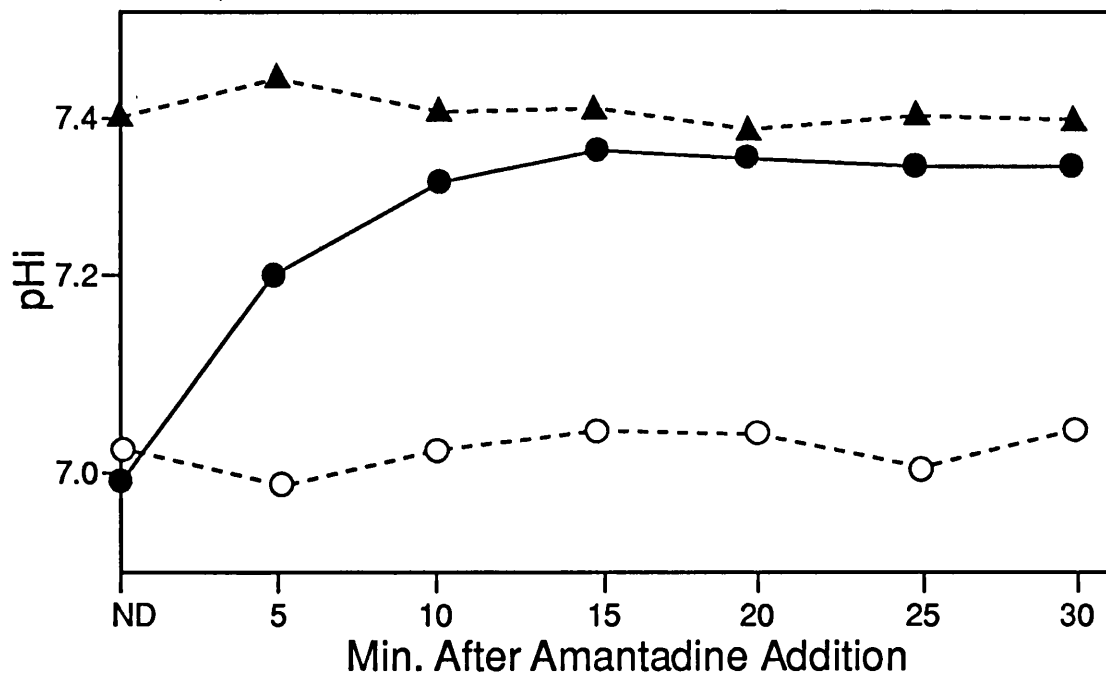


Table 2: The effect of 5 μ M amantadine on the cytoplasmic pH of MDCK cells infected with amantadine-resistant viruses

<u>Cytoplasmic pH</u>		
<u>Virus</u>	<u>No Addition</u>	<u>Amantadine</u>
Uninfected	7.40	7.40
Rostock	7.00 (-0.40)	7.40
R41R	7.05 (-0.35)	7.00 (-0.40)
039	7.05 (-0.35)	7.05 (-0.35)
08	7.20 (-0.20)	7.25 (-0.15)

Uninfected MDCK cells were loaded with 10 μ M SNARF-1-AM for 1 hour. Virus-infected cells were loaded with SNARF-1-AM, 5-6 hours p.i., washed and measured in Gey's+20mM Hepes, pH7.10. Emission ratios (634/604nm) were obtained before and after the addition of 5 μ M amantadine (15 minutes) to the cuvette. These were used to estimate cytoplasmic pH by means of the calibration curve in figure 11B.

The figures in brackets indicate the difference (in pH units) between the intracellular pH of the uninfected and virus-infected cells.

The specific inhibition by anti-M2 antiserum of the decrease in cytoplasmic pH, provided further evidence for the involvement of M2 protein. R53 antiserum recognizes the N-terminus of M2 and R54 antiserum the C-terminus of the protein. Within 45 minutes of the addition of a 1/10 dilution of R53 the reduction in pH of Rostock-infected cells was reversed (Figure 18). The cytoplasmic pH of infected cells treated with pre-immune serum and uninfected cells treated with R53, remained unchanged throughout this period. Similar effects were consistently seen with cells infected with the Weybridge strain, the Weybridge drug-resistant mutant GC16 and the Rostock drug-resistant mutant R41R (Table 3). In contrast however R54 antiserum had no effect on the pH of any of the virus-infected cells (Table 3). Therefore M2 orientated with its N-terminus accessible to antibody appeared to be responsible for the changes in cytoplasmic pH. This suggests that M2 located in the plasma membrane may be involved in the changes in pH.

In immunofluorescence studies discussed earlier brefeldin A was shown to inhibit the transport of M2 protein to the cell surface, without affecting the synthesis of M2 as detected by immunoblotting (data not shown) or its apparent activity within HA-containing vesicles (refer 3.1, pp.78-80). In the presence of 5 μ g/ml BFA, no reduction occurred in the cytoplasmic pH of Rostock-infected cells (6 hours p.i.) and the cells maintained a cytoplasmic pH equivalent to that of uninfected cells (Table 4). Therefore the M2-specific

Figure 18: Reversal of the M2-mediated change in cytoplasmic pH by anti-M2 antiserum.

Uninfected MDCK cells were incubated with SNARF-1-AM for 1 hour. Rostock-infected cells were loaded with SNARF-1-AM, 5-6 hours p.i.. 634/604nm emission ratios were measured at 5 minute intervals over a period of 1 hour, after the addition of a 1/10 dilution of R53 antiserum (against the N-terminus of M2) to uninfected (\blacktriangle) and infected (\bullet) cells. Control infected cells were incubated with a 1/10 dilution of pre-immune rabbit serum (\circ).

Cytoplasmic pH values were determined by reference to the SNARF-1 calibration curve (figure 11B).

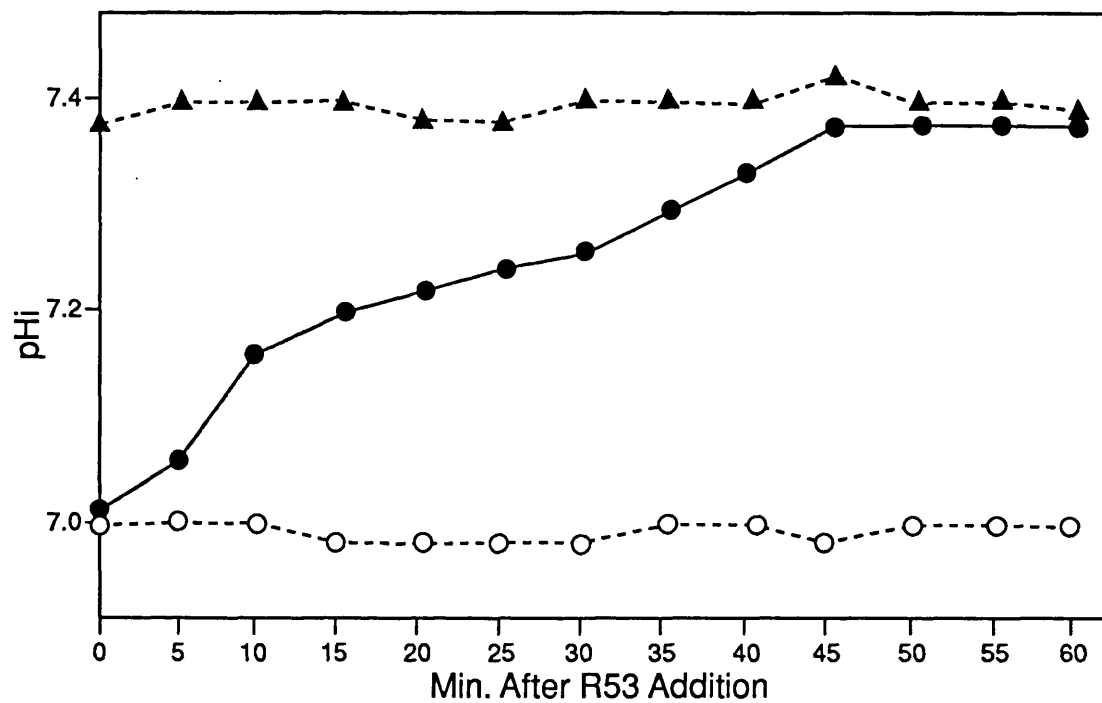


**Table 3: Inhibition of the M2-mediated change
in cytoplasmic pH by anti-M2 antiserum**

<u>Cytoplasmic pH</u>			
<u>Virus</u>	<u>No Addition</u>	<u>R53</u>	<u>R54</u>
Uninfected	7.35	7.40	7.35
Rostock	7.00 (-0.35)	7.35 (-0.05)	7.00 (-0.35)
R41R	7.05 (-0.30)	7.40 (0)	7.05 (-0.30)
Weybridge	7.05 (-0.30)	7.35 (-0.05)	7.10 (-0.25)
GC16	7.00 (-0.35)	7.40 (0)	7.05 (-0.30)

Uninfected MDCK cells were incubated with SNARF-1-AM for 1 hour. Virus-infected cells were loaded with SNARF-1-AM, 5-6 hours p.i.. A 1/10 dilution of R54 or R53 antiserum was added to the cells during the loading period (1 hour). The coverslips were washed and measured in Gey's+20mM HEPES, pH7.10 containing a 1/10 dilution of antiserum.

R53 antiserum recognizes the N-terminus of M2 and R54 the C-terminus of the protein.

634/604nm (534nm excitation) ratios were used to estimate the cytoplasmic pH by reference to figure 11B. The figures in brackets indicate the difference (in pH units) between the cytoplasmic pH of uninfected and virus-infected MDCK cells.

Table 4: The effect of BFA on the cytoplasmic pH of Rostock-infected MDCK cells.

		<u>Cytoplasmic pH</u>	
<u>Cells</u>	<u>BFA</u>	<u>No treatment</u>	<u>Amantadine</u>
Uninfected	+	7.40	7.40
	-	7.40	7.40
Infected	+	7.40	7.40
	-	7.00 (-0.4)	7.40

Uninfected and Rostock-infected cells (1 hour p.i.) were incubated in the presence of 5 μ g/ml BFA for 5 hours. The cells were loaded with 10 μ M SNARF-1-AM from 4 to 5 hours after the addition of BFA and 634/604nm emission ratios were obtained in Gey's+20mM Hepes, pH7.10. 5 μ g/ml BFA was present during the measurements of BFA-treated cells. Estimates of cytoplasmic pH were obtained using the calibration curve shown in figure 11B.

Measurements of amantadine-treated cells were carried out 15 minutes after the addition of 5 μ M amantadine to the cuvette medium.

reduction in cytoplasmic pH was absent from cells where the cell surface expression of M2 protein was reduced by BFA. Together with the effects of R53/R54 antiserum, this data suggests that M2 protein within the plasma membrane is responsible for the change in cytoplasmic pH.

The relationship between M2 and cytoplasmic pH

The relationship between M2 production and cytoplasmic pH is shown in MDCK cells infected with wildtype (Rostock) virus (Figure 19) and two amantadine-resistant mutants 039 and 08 (Figures 20 and 21 respectively). In all three of the virus-infected cells the addition of cycloheximide, inhibited the synthesis of M2 protein and prevented the reduction in cytoplasmic pH, as previously observed in Figure 16. Throughout the 8 hour infection period the addition of amantadine ($5\mu\text{M}$) completely reversed the pH decrease in Rostock-infected cells (Figure 19), but had no effect on cells infected with the resistant mutants 039 or 08 (Figure 20A and 21A respectively), as previously observed (Table 2).

A decrease in cytoplasmic pH was observed from 2 hours p.i. in Rostock-infected MDCK cells (Figure 19A). By 6 hours p.i. the pH had stabilized resulting in an approximate 0.4pH unit difference between uninfected (pH7.4) and virus-infected cells (pH7.0). As previously noted in Figure 16 virus infection produced a similar reduction in pH after 6 hours p.i., as was observed after the addition of nigericin, indicating that the internal and external pHs were equivalent. Similar results were

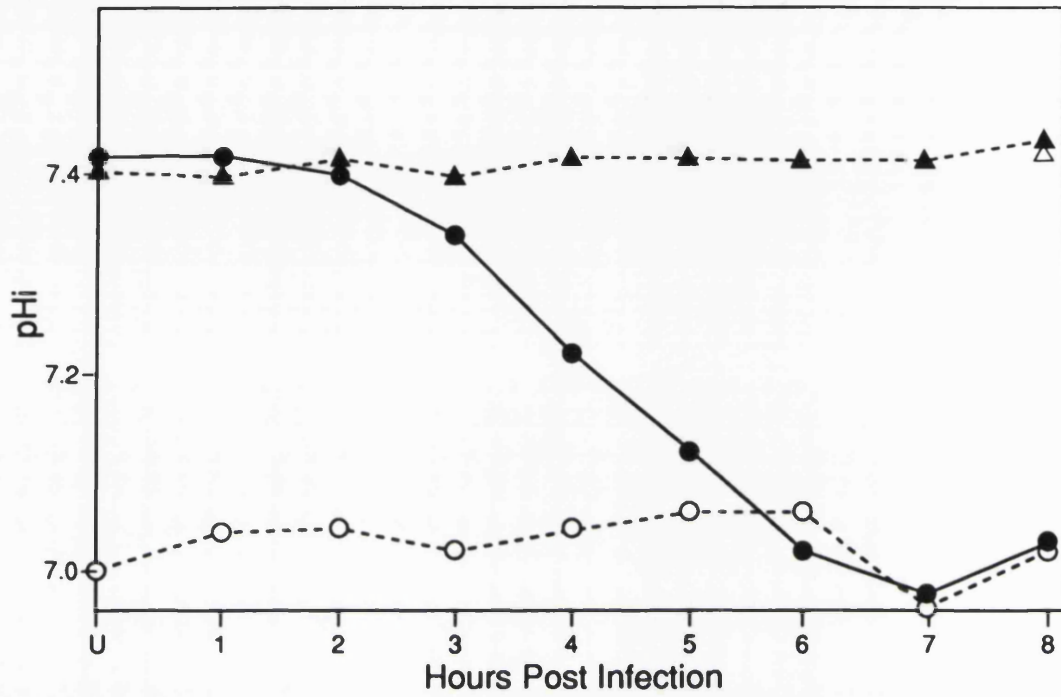
Figure 19: Comparison between the synthesis of M2 protein and the reduction in cytoplasmic pH in Rostock-infected MDCK cells

A. At hourly intervals p.i., Rostock-infected (●) MDCK cells were loaded with SNARF-1-AM for 1 hour. 634/604nm emission ratios (534nm excitation) were measured and used to estimate the cytoplasmic pH by reference to the calibration curve shown in figure 11B.

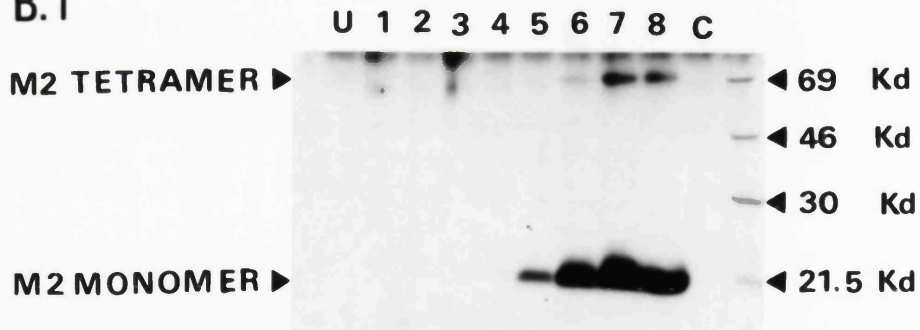
Amantadine (5 μ M) was added to the cuvette for 15 minutes (\blacktriangle) and nigericin (10 μ M) for 10 minutes (\circ). Cells at 1 hour p.i. were incubated with 100 μ g/ml cycloheximide (Δ).

B. Cell lysates were taken at hourly intervals (1-8 hours p.i.) and subjected to polyacrylamide gel electrophoresis. After transferring to Immobilon-P, M2 was detected using anti-M2 polyclonal serum (R54) and secondary antibody conjugated to ¹²⁵I (details in materials and methods). The blot was exposed to film for 10 hours (i) and 24 hours (ii). Left to right the lanes show uninfected cells (U), Rostock-infected cells 1 to 8 hours p.i. (1-8) and infected cells treated with 100 μ g/ml cycloheximide from 1 to 8 hours (C).

A.



B. i



ii



Figure 20: Comparison between the synthesis of M2 and the reduction in cytoplasmic pH in 039-infected MDCK cells

A. At hourly intervals p.i. mutant 039-infected MDCK cells (●) were loaded with SNARF-1-AM for 1 hour. 634/604nm emission ratios (534nm excitation) were used to estimate the cytoplasmic pH by reference to figure 11B.

Amantadine (5 μ M) was added to the cuvette for 15 minutes (▲) and nigericin (10 μ M) for 10 minutes (○). Cycloheximide was added to cells at 1 hour p.i. (Δ).

B. Cell lysates were collected at hourly intervals and treated as outlined in figure 19. The blot was exposed to film for 24 hours. The lanes show (left to right) uninfected cells (U), 039-infected cells 1 to 7 hours p.i. (1-7) and cells treated with 100 μ g/ml cycloheximide from 1 to 8 hours p.i. (C).

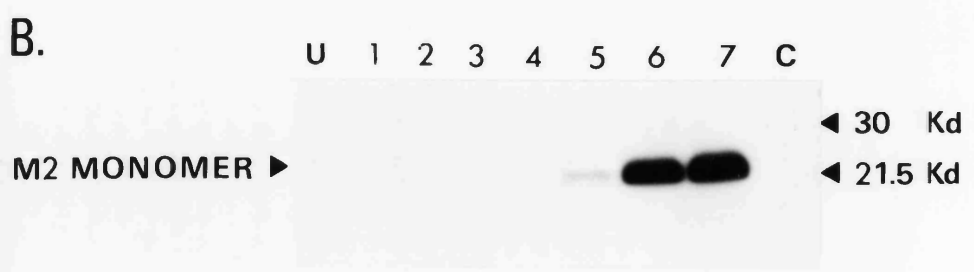
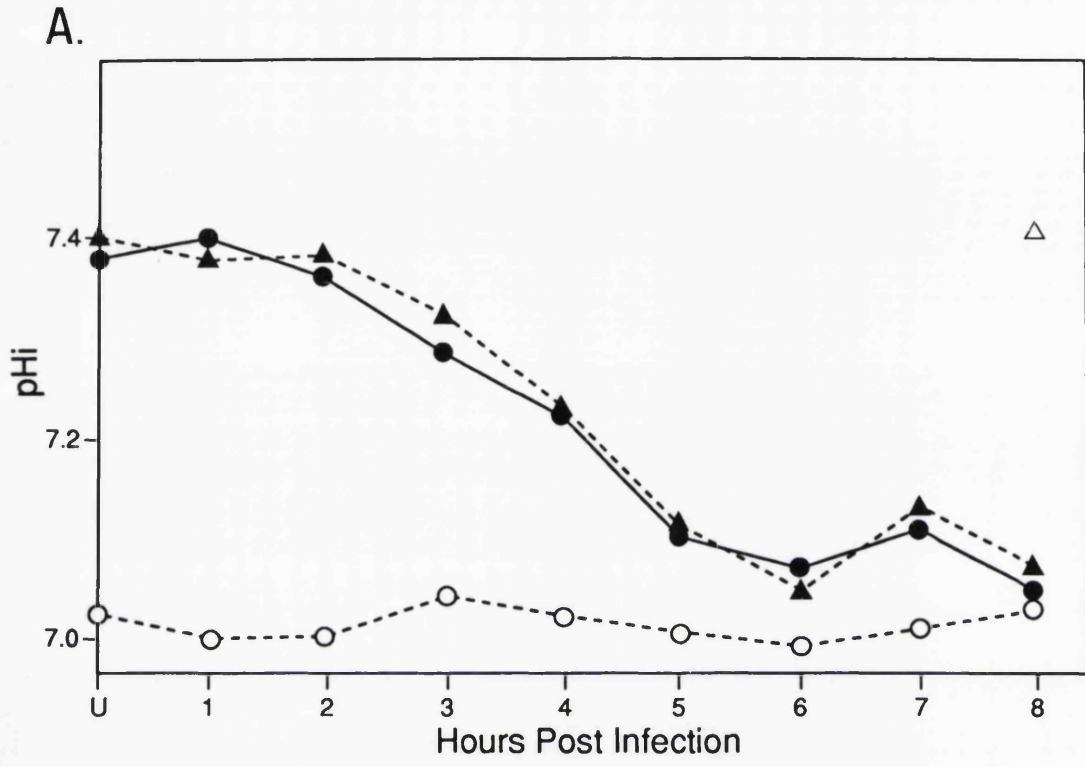


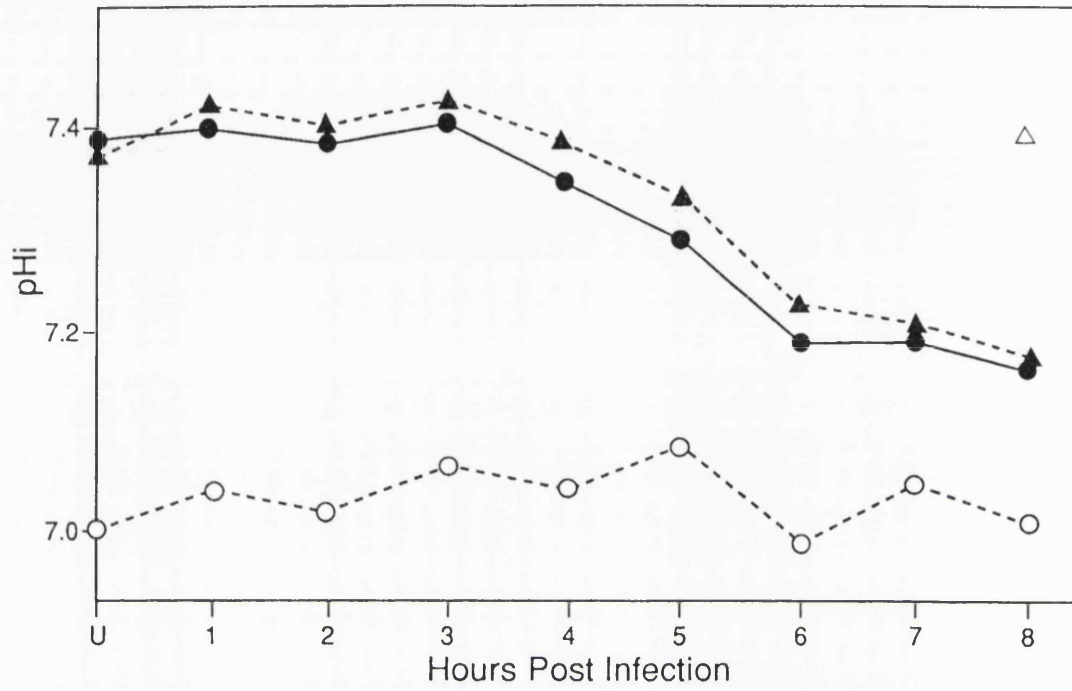
Figure 21: Comparison between the synthesis of M2 and the reduction in cytoplasmic pH in 08-infected MDCK cells

A. Mutant 08-infected MDCK cells (●) were loaded with SNARF-1-AM at hourly intervals p.i. and their emission spectra scanned. Cytoplasmic pH was estimated from the 634/604nm emission (534 excitation) ratios using the SNARF-1 calibration curve (figure 11B).

Amantadine (5 μ M) was added to the cuvette for 15 minutes (\blacktriangle) and nigericin (10 μ M) for 10 minutes (\circ). Cycloheximide (100 μ g/ml) was added from 1 hour p.i. (Δ).

B. Cell lysates collected at hourly intervals from 1 to 8 hours p.i. were treated as outlined in figure 19. The blot was exposed to film for 15 hours (i) and 28 hours (ii). The lanes (from left to right) show uninfected cells (U), 08-infected cells 1 to 8 hours p.i. (1-8) and cells treated with 100 μ g/ml cycloheximide from 1 hour p.i. (C).

A.



B. i



ii



obtained on three separate occasions and in no instance did the pH decrease below this level.

M2 production was detected by immunoblotting in Rostock-infected cells from 4 hours p.i. (Figure 19B). The initial reduction in pH (from 2 hours p.i.) occurred when only small amounts of M2 were detected. From 6 hours p.i., the synthesis of M2 was such that not all of the protein was reduced and the tetrameric form of M2 was detected.

Similar to Rostock-infected cells, a 0.35-0.4pH unit decrease in cytoplasmic pH was observed from 2 to 5 hours p.i. on two separate occasions, in cells infected with 039 virus (Figure 20A). This again corresponded to the decrease in pH observed in the presence of nigericin. The production of M2 protein was detected in the 039-infected cells from 5 hours p.i., by which time the reduction in pH was complete. This may reflect a lack of sensitivity in the detection of M2 when only very low amounts are present. It would be of interest with respect to this point to repeat these experiments and in addition to follow the synthesis of M2 by ³⁵S-labelling.

Cells infected with the resistant mutant 08 showed a smaller reduction in pH (approximately 0.2pH units), failing to reduce the cytoplasmic pH to the level of that associated with nigericin treatment, even after 8 hours p.i. (Figure 21A). Similar results were obtained on two separate occasions and in addition it was consistently observed throughout the pH studies previously described, that 08-infected cells (6 hours p.i.) showed only a 0.2pH

unit decrease in pH. This suggests that the 08 virus M2 protein is less active than that of the Rostock and 039 viruses. The 08 virus contains an A30T mutation in its M2 protein, which has been reported to reduce the pH modification activity of the protein within the trans-Golgi (Grambas et al., 1992). The lack of activity of 08 M2 in reducing the cytoplasmic pH was highlighted by the fact that a 2½-fold increase in the amount of M2 (6 to 7 hours p.i.) had no effect on the pH.

From the study of all three viruses it was obvious that the reduction in pH was not proportional to the amount of M2 protein present. Comparisons of the amount of M2 detected and the corresponding change in the cytoplasmic pH indicated that initially small amounts of M2 were capable of producing considerable changes in pH. The ratios (Δ pH to amount of M2) for all three different virus-infected cells fell dramatically, by 86%, 75% and 82% for cells infected with Rostock (4-5 hours p.i.), 039 (5-6 hours p.i.) and 08 (5-6 hours p.i.) viruses, respectively (Figure 22). After 6 hours p.i. the cytoplasmic pH of each of the three different virus-infected cells remained relatively constant. In MDCK cells infected with Weybridge virus (Figure 23) a decrease in cytoplasmic pH was observed after 3 hours p.i. (Figure 23A) and M2 protein was detected from 5 hours p.i. (not shown). By 6 hours p.i. the cytoplasmic pH of the virus-infected cells had been reduced by approximately 0.35pH units as compared to that of the uninfected cells. Similar results were obtained on two

Figure 22: The ratio of the change in cytoplasmic pH to the change in the amount of M2 protein, with respect to time p.i..

Densitometry scans of the autoradiographs shown in figures 19, 20 and 21 were used to assess the amount of M2 protein present at different times p.i.. The ratio of the change in pH to the amount of M2 protein was calculated and plotted with respect to time p.i. for Rostock (A), 039 (B) and 08 (C) infected cells.

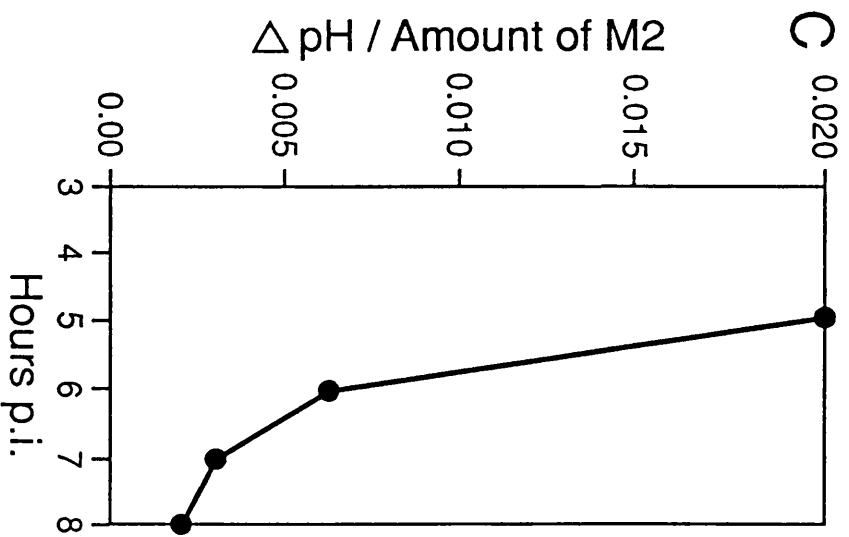
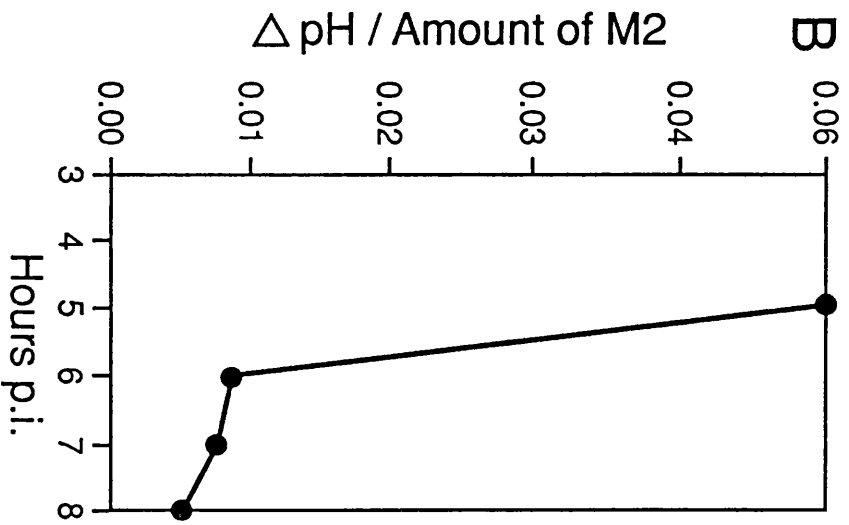
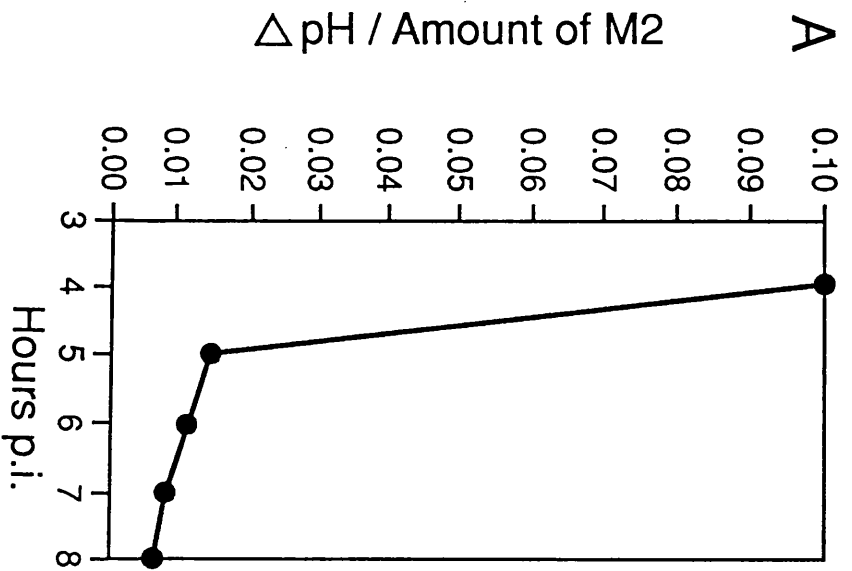
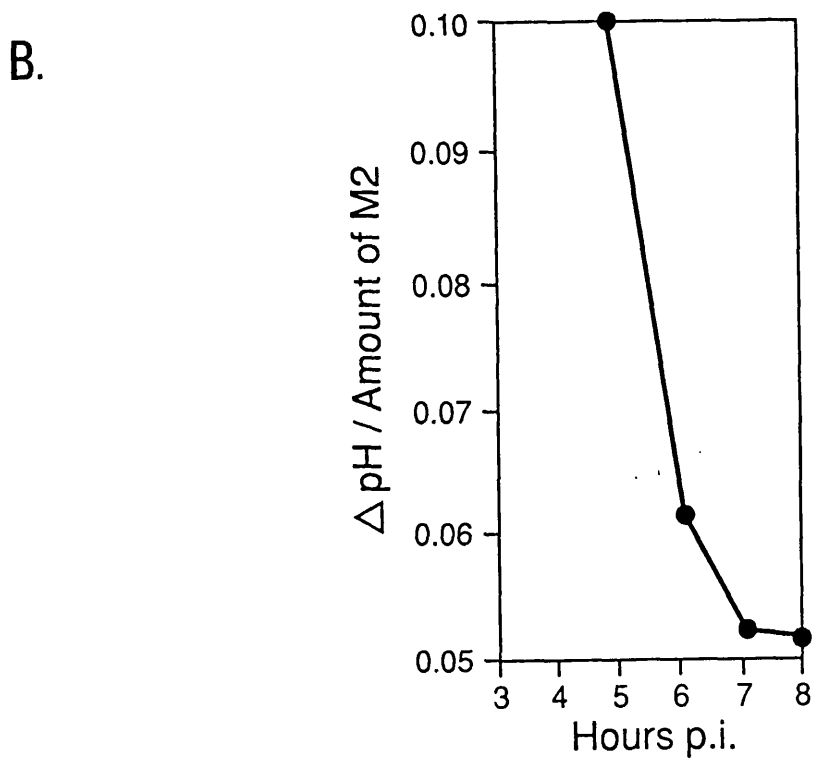
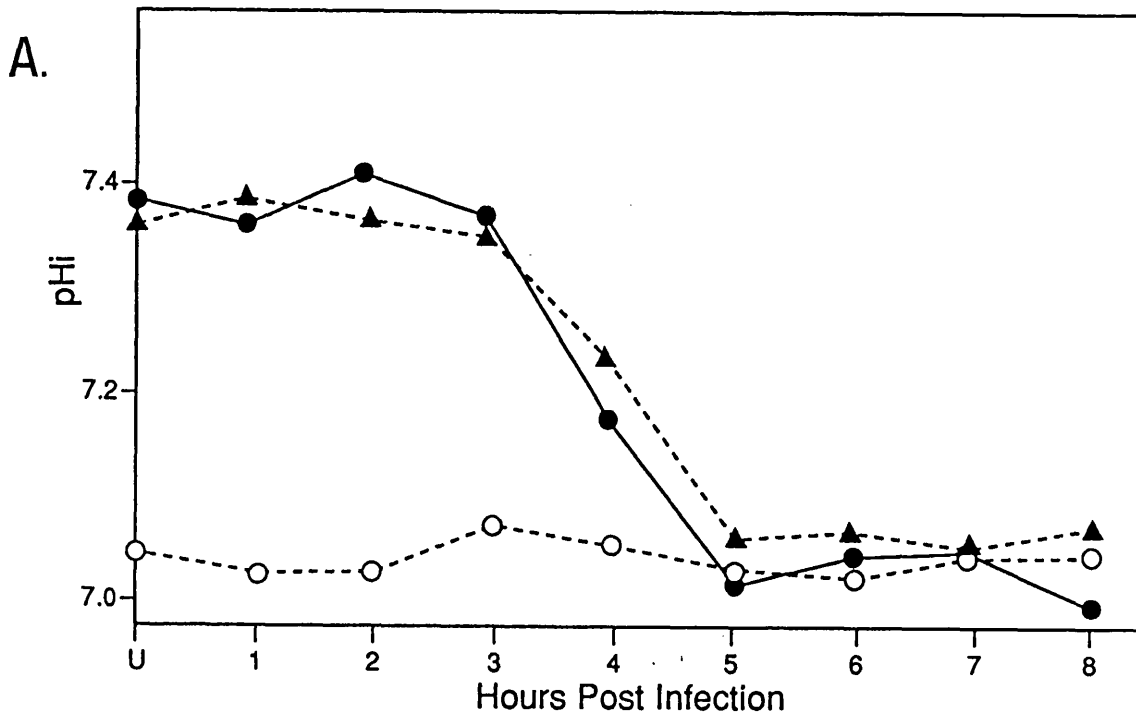


Figure 23: Comparison between the synthesis of M2 and the reduction in cytoplasmic pH in Weybridge-infected cells.

A. Weybridge-infected MDCK cells (●) at hourly intervals p.i. were loaded with SNARF-1-AM (1 hour). The calibration curve shown in figure 11B was used to estimate the cytoplasmic pH from the 634/604nm emission ratio (534nm excitation).

Amantadine (5 μ M) was added to the cuvette for 15 minutes (▲) and nigericin (10 μ M) for 10 minutes (○). Cells were incubated with 100 μ g/ml cycloheximide from 1 hour p.i. (Δ).

B. At hourly intervals (1-8 hours p.i.) after infection, cell lysates were collected and treated as outlined in figure 19. The blot was exposed to film and the autoradiograph subject to densitometry to assess the amount of M2 protein present. The ratio of the change in pH to the amount of M2 protein present was calculated and plotted with respect to time p.i..



separate occasions. Again the production of M2 protein was not proportional to the decrease in pH and correspondingly the ratio of ΔpH to the amount of M2 decreased dramatically 5-7 hours p.i. (Figure 23B). The decrease in pH in Weybridge-infected cells appeared to occur more rapidly than that observed in Rostock-infected and 039-infected cells. This may reflect the relative synthesis of M2 protein as it was not possible using the data shown to compare the relative amounts of M2 produced in each instance. Alternatively Weybridge virus infection has been shown to be far more effective at shutting down host cell protein synthesis, which may decrease the synthesis of cellular ion channels that are capable of buffering the changes in cytoplasmic pH. This may cause the pH decrease in Weybridge-infected cells to occur more rapidly as there would be less resistance from the cellular systems responsible for maintaining the internal pH.

Differences in the drug sensitivity of different M2 proteins

Amantadine ($5\mu\text{M}$) consistently failed to reverse the pH reduction in Weybridge-infected cells. This lack of amantadine sensitivity was observed throughout infection and so was not related to the amount of M2 present (Figure 23). Weybridge virus infection in tissue culture is however sensitive to both amantadine ($5\mu\text{M}$) and rimantadine ($5\mu\text{M}$). In order to investigate the apparent insensitivity of the Weybridge M2 protein, the effects of various concentrations of amantadine and rimantadine on the

cytoplasmic pH of Rostock and Weybridge-infected cells (6 hours p.i.) was investigated. In each instance the effect of drug was complete after 25 minutes and in certain cases after 5 minutes where high concentrations ($>5\mu\text{M}$) of the drugs were used (Figure 24 and 25). However when interpreting the M2 specificity of the effects of high concentrations ($>5\mu\text{M}$) of amantadine and rimantadine, their properties as weak bases must be considered. Similar studies using uninfected MDCK cells showed that the cytoplasmic pH was not significantly effected by either of the drugs over the range of concentrations used (data not shown).

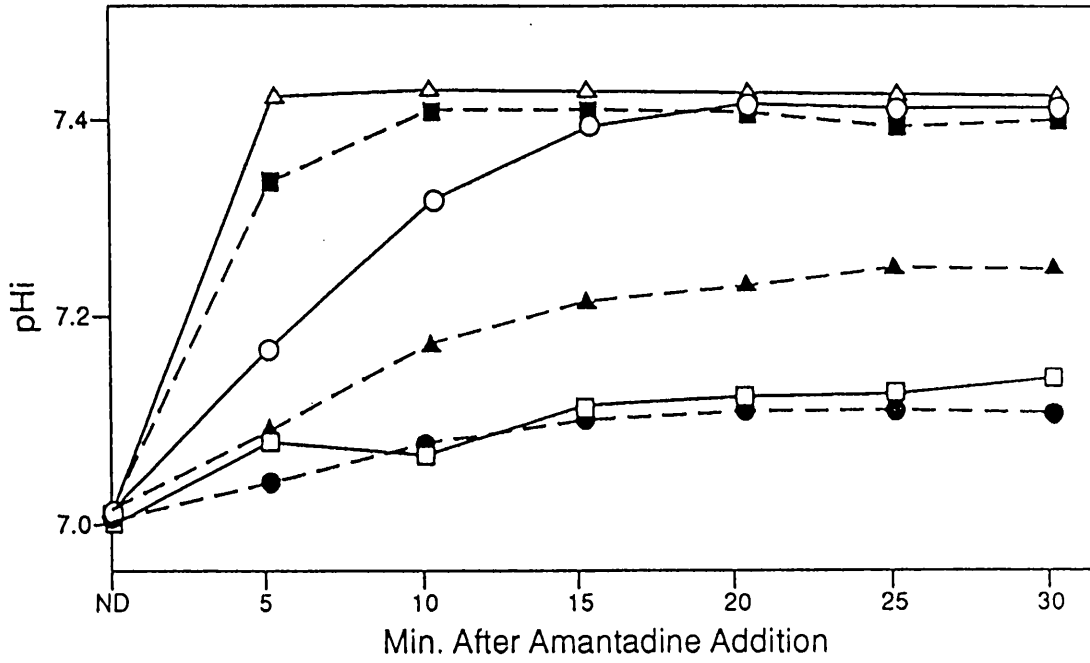
The reduction in the pH of Rostock-infected cells was similarly sensitive to amantadine and rimantadine. $5\mu\text{M}$, $50\mu\text{M}$ and $500\mu\text{M}$ concentrations of both drugs completely abolished the pH difference in Rostock-infected cells after 15, 10 and 5 minutes respectively (Figure 24). A 50% reversal (0.2pH units) was observed in the presence of $0.5\mu\text{M}$ amantadine and rimantadine. $0.05\mu\text{M}$ amantadine and rimantadine produced an approximate 0.1pH unit increase in the Rostock-infected cell pH after 25 minutes. Differences were apparant in the activity of $0.005\mu\text{M}$ concentrations of the drugs. Amantadine ($0.005\mu\text{M}$) produced a similar increase in pH with time to $0.05\mu\text{M}$ amantadine, whilst $0.005\mu\text{M}$ rimantadine had no significant effect on the cytoplasmic pH even after 30 minutes. In summary, in terms of the final pH values attained in the present of drug no obvious differences were observed between amantadine and

Figure 24: The effect of various concentrations of amantadine and rimantadine on the cytoplasmic pH of Rostock-infected MDCK cells.

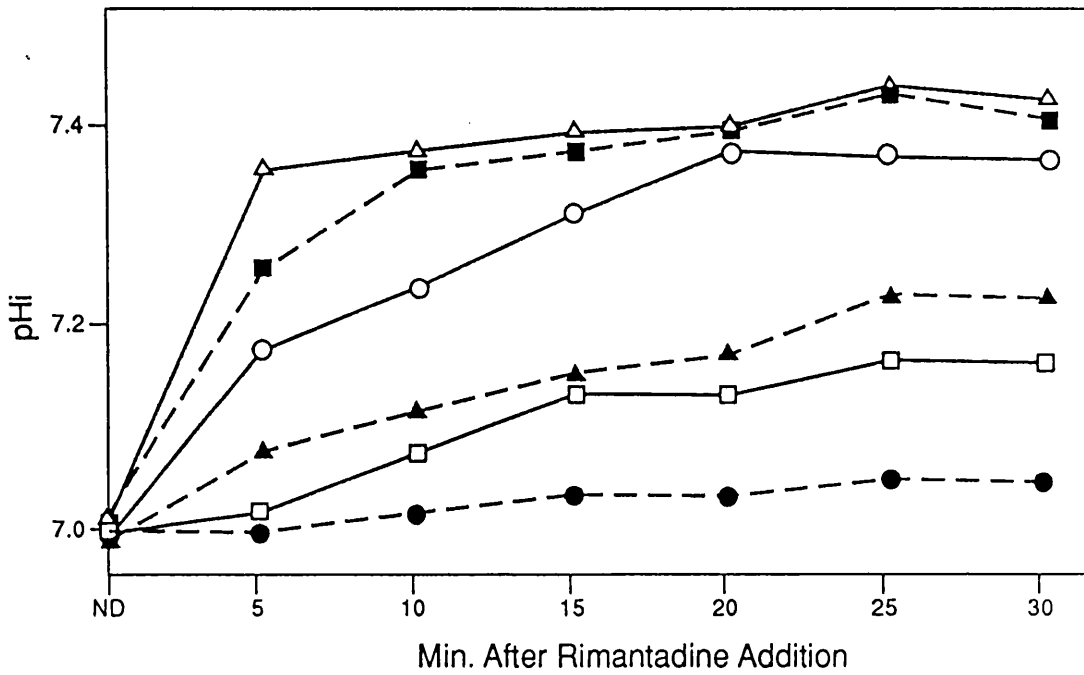
Rostock-infected MDCK cells (5-6 hours p.i.) were loaded with 10 μ M SNARF-1-AM. Emission ratios (634/604nm) were obtained at 5 minute intervals over a period of 30 minutes, before (ND) and after various concentrations of amantadine or rimantadine were added to the cuvette medium. Cytoplasmic pH values were determined using the SNARF-1 calibration curve (figure 11B).

0.005 μ M (\bullet), 0.05 μ M (\square), 0.5 μ M (\blacktriangle), 5 μ M (\circ), 50 μ M (\blacksquare) and 500 μ M (\triangle) concentrations of amantadine (A) and rimantadine (B) were used.

A.



B.



rimantadine at concentrations of 500, 50 and 5 μ M. However at lower concentrations (0.05 and 0.005 μ M), the reduction in the cytoplasmic pH appeared to be more sensitive to amantadine than rimantadine. Similar observations were made on two separate occasions.

Weybridge virus-infected cells in contrast showed a marked difference in their sensitivity to the two drugs (Figure 25). 500 μ M amantadine produced only a partial reversal in pH (approximately 0.2pH units), whereas rimantadine concentrations of greater than 5 μ M completely reversed the 0.4pH unit difference after 15 minutes. At concentrations of 0.005 μ M, 0.05 μ M and 0.5 μ M rimantadine had no effect on the cytoplasmic pH of the Weybridge-infected cells. In contrast 0.5 μ M and 0.05 μ M concentrations of amantadine did produce an approximate 0.05-0.1pH unit difference in the infected cell pH, after 30 minutes. However 0.005 μ M amantadine had no significant effect. Therefore at concentrations of 5 μ M and above rimantadine was more effective than amantadine at reversing the 0.4pH unit difference in cytoplasmic pH. At concentrations below 5 μ M, amantadine appeared to be more effective than rimantadine. Similar responses to both drugs were again observed on two separate occasions.

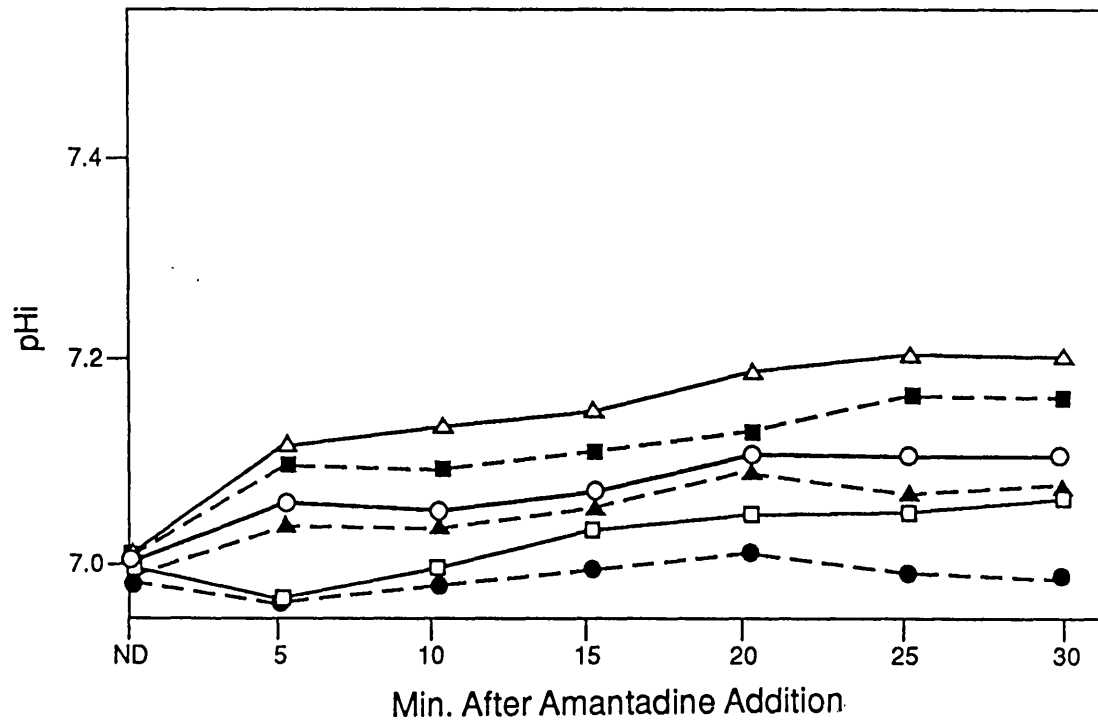
Hay et al. (1985) demonstrated that the specific anti-M2 action of the amantadine and rimantadine was dependent on their large hydrocarbon ring structures. The actions of a range of amines possessing hydrocarbon ring structures of varying sizes (cyclobutylamine, cyclopentylamine,

Figure 25: The effect of various concentrations of amantadine and rimantadine on the cytoplasmic pH of Weybridge-infected MDCK cells.

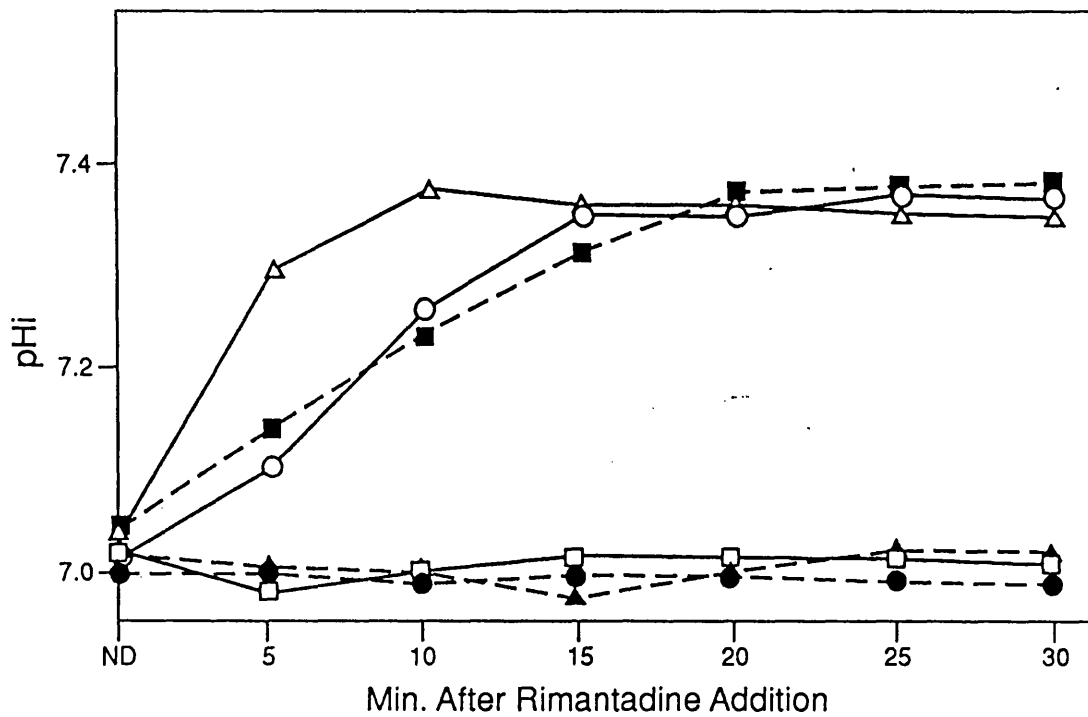
MDCK cells infected with Weybridge virus were loaded with SNARF-1-AM (5-6 hours p.i.). Emission ratios (634/604nm) were obtained at 5 minute intervals over a 30 minute period before (ND) and after the addition of various concentrations of amantadine or rimantadine to the cuvette. Cytoplasmic pH was determined using the SNARF-1 calibration curve (figure 11B).

0.005 μ M (\bullet), 0.05 μ M (\square), 0.5 μ M (\blacktriangle), 5 μ M (\circ), 50 μ M (\blacksquare) and 500 μ M (Δ) concentrations of amantadine (A) and rimantadine (B) were used.

A.



B.



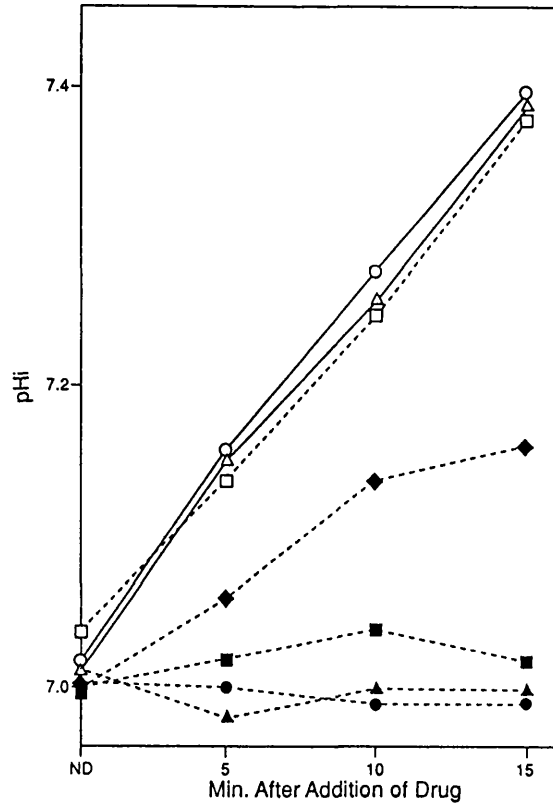
cyclohexylamine, cycloheptylamine and cyclooctylamine), were investigated (Figure 26). The effects were monitored over a 15 minute period, this corresponded to the amount of time required by 5 μ M amantadine and rimantadine to completely reverse the pH reduction in Rostock-infected cells. None of the drugs had any effect on the cytoplasmic pH of uninfected cells. Figure 26A shows that the inhibition of the M2-induced pH change in Rostock-infected cells was dependent on the structure of the amines. At 5 μ M concentrations compounds with ring structures containing less than 7 carbon atoms were incapable of completely reversing the 0.4pH unit difference. Similar to amantadine and rimantadine, 5 μ M cyclooctylamine completely abolished the pH difference. 5 μ M cycloheptylamine exhibited a partial effect, increasing the pH by 0.15pH units. Therefore the pH difference between uninfected and Rostock-infected cells was completely abolished only by those compounds possessing hydrocarbon ring structures with 8 or more carbons.

The reversibility of the pH reduction in Weybridge-infected cells was also dependent on structure of the amine (Figure 26B). Compounds with ring structures containing less than 7 carbon atoms similarly did not completely abolish the pH difference between uninfected and Weybridge-infected cells. In contrast to Rostock-infected cells 5 μ M rimantadine was the only compound capable of completely reversing the reduction in pH of Weybridge-infected cells.

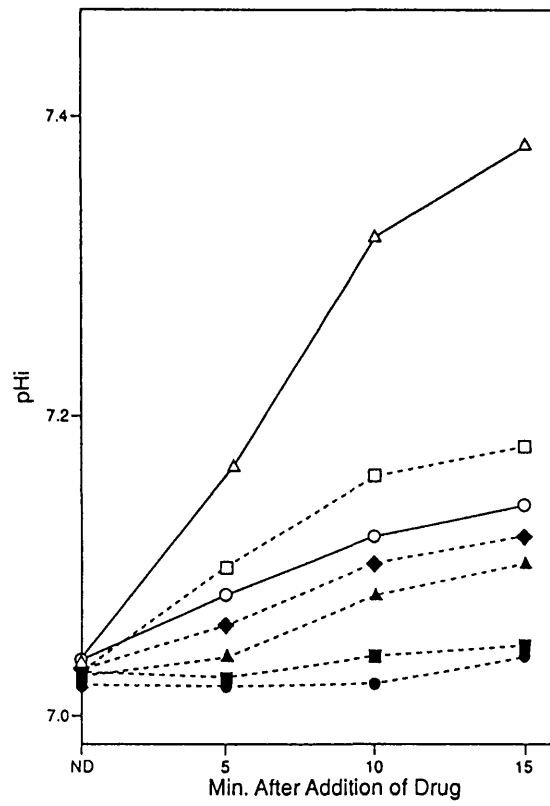
Figure 26: Reversal of the reduced cytoplasmic pH in Rostock and Weybridge-infected MDCK cells, by amantadine, rimantadine and cyclooctylamine.

Rostock (A) and Weybridge (B) infected MDCK cells were loaded with 10 μ M SNARF-1-AM 5-6 hours p.i.. Emission spectra were scanned before (ND) and after the addition to the cuvette medium of 5 μ M amantadine (\circ), 5 μ M rimantadine (Δ), 5 μ M cyclooctylamine (\square), 5 μ M cycloheptylamine (\blacklozenge), 5 μ M cyclohexylamine (\blacktriangle), 5 μ M cyclopentylamine (\blacksquare) or 5 μ M cyclobutylamine (\bullet). 634/604nm emission ratios (534nm excitation) were converted into cytoplasmic pH using the calibration curve shown in figure 11B.

A.



B.



Cyclooctylamine like amantadine consistently caused only a partial reversal of the reduction in pH (between 0.1 and 0.2pH units as observed previously in Figure 25A). Cyclooctylamine was slightly more active than amantadine. These results suggested that the inhibition of Weybridge M2 activity in MDCK cells, was also dependent on the size of the amine hydrocarbon ring. In addition, the relative inactivity of amantadine (5 μ M) and cyclooctylamine (5 μ M) suggested that other structural features of the amines were also important.

The effect of varying ionic conditions on the M2-specific pH change in virus-infected cells.

In view of the observations that M2 is capable of modifying the pH of the cell cytoplasm, attempts were made to investigate further the nature of this M2 activity and to determine the ions involved. For this reason the influence of various different ion concentrations (Na⁺, Cl⁻, K⁺ and H⁺) on the activity of M2 were investigated, using the SNARF-1 assay. Table 5 shows the composition of Gey's medium in comparison to the Na⁺ and Cl⁻ buffers used in this investigation. Cytoplasmic pH measurements were also carried out in the high KCl buffer (115mM KCl, 1mM MgCl₂, 20mM Hepes, pH7.10) used for SNARF-1-AM calibration. The pH of solutions unless otherwise stated was 7.10 and in order to maintain the osmolarity of solutions Cl⁻ was replaced by gluconate and Na⁺ by NMDG (N-methyl-D-glucamine). Alterations in cell size as a result of changes in osmolarity can trigger the activity of cellular

Table 5: The composition of Gey's, 0mM Na⁺, 30mM Na⁺, 0mM Cl⁻ and 30mM Cl⁻ media.

<u>Components</u>	<u>Gey's</u>	<u>Na⁺ buffers</u>		<u>Cl⁻ buffers</u>	
		<u>0mM</u>	<u>30mM</u>	<u>0mM</u>	<u>30mM</u>
NaCl	123mM	-	30mM	-	30mM
Na⁺ gluconate	-	-	-	123mM	90mM
KCl	5mM	5mM	5mM	-	-
K⁺ gluconate	-	-	-	5mM	5mM
NMDG	-	123mM	90mM	-	-
Na₂HPO₄.12H₂O	0.86mM	-	-	0.86mM	0.86mM
K₂HPO₄.12H₂O	-	0.86mM	0.86mM	-	-
KH₂PO₄	0.18mM	0.18mM	0.18mM	0.18mM	0.18mM
Glucose	5.7mM	5.7mM	5.7mM	5.7mM	5.7mM
MgCl₂.6H₂O	1.3mM	1.3mM	1.3mM	-	-
Mg²⁺ gluconate	-	-	-	1.3mM	1.3mM
CaCl₂.2H₂O	1.46mM	1.46mM	1.46mM	-	-
Ca²⁺ gluconate	-	-	-	1.46mM	1.46mM
Hepes	20mM	20mM	20mM	20mM	20mM
pH*	7.10	7.10	7.10	7.10	7.10

* adjusted using 1M HCl for Gey's and Na⁺ solutions and 1M citric acid for Cl⁻ solutions.

NMDG (N-methyl-D-glucamine) was used as a substitute for Na⁺ and gluconate as a substitute for Cl⁻.

ion channels (Ritter et al., 1991).

When incubated in media containing 0mM Na⁺ the pH of uninfected cells was reduced by 0.45pH units as compared to the pH in Gey's. The removal of Cl⁻ correspondingly decreased the pH of the uninfected cells by 0.35pH units. In both instances the decrease in pH corresponded to the removal of the plasma membrane pH gradient in the uninfected cells. The removal of Na⁺ and Cl⁻ had little significant effect on the pH of the Rostock-infected cells. A 0.15 and 0.05pH unit decrease (respectively) was observed, in comparison with the cytoplasmic pH of Rostock-infected cells in Gey's medium (Table 6). The net effect of these alterations was to reduce the M2-specific pH difference observed in the absence of Na⁺ and Cl⁻ to 0.1pH units. The apparent reduction in M2 activity is not unexpected if M2 acts to abolish the plasma membrane pH gradient, as no gradient was present in the uninfected cells under these conditions. The removal of Cl⁻ and Na⁺ from the system may not be complete, however this appeared to be of little significance as similar results were obtained in solutions containing 30mM concentrations of the ions. Altering the concentration of K⁺ had no discernable effect on either uninfected or virus-infected cells.

To try to further investigate the influence of Na⁺ on the M2 channel activity experiments were carried out to monitor changes in the levels of Na⁺ within the cells. This involved the use of a fluorescent probe SBFI-AM (Molecular Probes Inc., USA), which upon binding Na⁺ undergoes a shift

Table 6: The cytoplasmic pH of MDCK cells incubated under different ionic conditions.

<u>Cytoplasmic pH of cells</u>				
<u>Conditions</u>	<u>Uninfected</u>		<u>Infected</u>	
	<u>Untreated</u>	<u>Amantadine</u>	<u>Untreated</u>	<u>Amantadine</u>
Control (Gey's)	7.35	7.40	6.95	7.40
0mM Cl ⁻	7.00	7.00	6.90	7.05
30mM Cl ⁻	7.15	7.15	7.00	7.15
0mM Na ⁺	6.90	6.90	6.80	6.90
30mM Na ⁺	6.95	7.00	6.85	7.00
115mM K ⁺ *	7.40	7.40	6.90	7.40

* 115mM KCl, 1mM MgCl₂, 20mM Hepes, pH7.10

Uninfected MDCK cells were loaded with 10 μ M SNARF-1-AM for 1 hour. Rostock-infected cells were labelled with SNARF-1-AM, 5-6 hours p.i.. Cells were washed and incubated in various media as noted above and described in table 5. After allowing an equilibration period of 15 minutes 634/604nm emission ratios were obtained before and 15 minutes after the addition of 5 μ M amantadine to the cuvette medium. Using the calibration curve in figure 11B estimates of the cytoplasmic pH were obtained.

in its excitation spectrum. Similarly to the fluorescent pH probes used, the concentration of Na^+ can be determined from a ratio of the fluorescence intensities at two excitation wavelengths. However difficulties in loading sufficient quantities of the probe into the cells and problems with its accumulation in cytoplasmic vesicles prevented its use in this system.

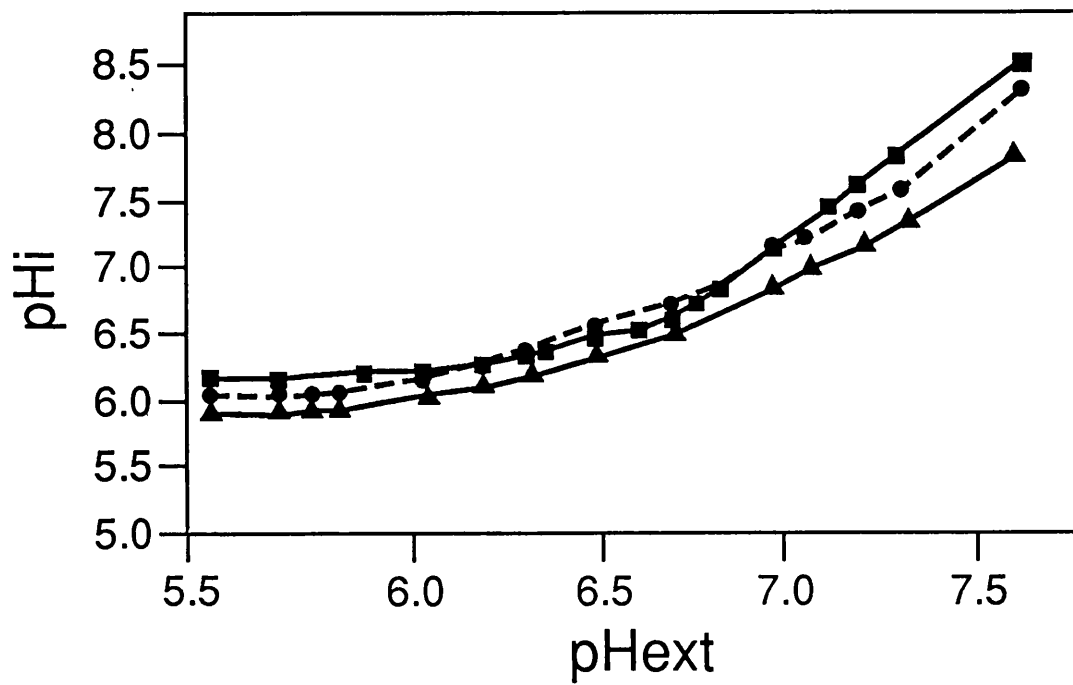
In order to determine the effect of external pH on the M2-specific changes in cytoplasmic pH, the pH virus-infected cells was determined in Gey's+20mM Hepes adjusted to various pHs (Figure 27). The cytoplasmic pH of Rostock-infected MDCK cells (6 hours p.i.) remained below that of uninfected cells over a range of pH values from pH5.5 to pH7.6. The difference between the two cells was however more pronounced above pH7. Amantadine ($5\mu\text{M}$) completely reversed the pH difference between pH6.2 and pH7.2, beyond these pH values small differences were apparent between the uninfected cell pH and that of virus-infected cells treated with amantadine ($5\mu\text{M}$). Therefore the M2-specific pH decrease in virus-infected MDCK cells was at its maximum in the Gey's+20mM Hepes, pH7.10 used throughout these experiments.

With respect to the ability of M2 to modify the cytoplasmic pH of cells, the relationship between ΔpH and the amount of M2 synthesized appears to be disproportional. This could be due to changes in the activity of the M2 or its ability to influence the activity of other cellular ion channels. Cellular ion channels may also act to buffer the

Figure 27: The cytoplasmic pH of uninfected and Rostock-infected MDCK cells incubated in Gey's, adjusted to various pHs

Uninfected (●) MDCK cells were loaded with 10 μ M SNARF-1-AM for 1 hour. Rostock-infected cells (▲) were loaded with SNARF-1-AM, 5-6 hours p.i.. The cells were washed and incubated in Gey's+20mM Hepes adjusted to various pHs (pH_{ext}). The cytoplasmic pHs (pH_i) were determined from the 634/604nm emission ratios (at 534nm excitation), using the SNARF-1 calibration curve shown in figure 11B.

5 μ M amantadine was added to the cuvette medium for 15 minutes (■)



M2-specific changes in pH. In MDCK cells the Na^+/H^+ antiporter and the $\text{HCO}_3^-/\text{Cl}^-$ exchanger are believed to play important roles in the regulation of intracellular pH (Borle and Bender, 1991; Kurtz and Golchini, 1987). For this reason drugs capable of blocking such channels were added to the uninfected and virus-infected cells, to determine if they had any influence on the ability of M2 to modify the cytoplasmic pH (results not shown). Amiloride selectively inhibits the Na^+/H^+ antiporter and DIDS (4, 4'-diisothiocyanatostilbene-2,2'-disulfonic acid) the $\text{Cl}^-/\text{HCO}_3^-$ exchanger. Neither 1mM amiloride or 500 μM DIDS exhibited any significant effect on the cytoplasmic pH of uninfected or Rostock-infected cells. For this reason it would be of interest to try using higher concentrations of the drugs or to use alternative ion channel blockers. In respect to the latter point a number of amiloride derivatives are available and these may be more effective at blocking the Na^+/H^+ antiporter.

M2 specific pH changes within other influenza virus-infected cell systems

M2 specific alterations in cytoplasmic pH (as judged by their sensitivity to amantadine) were also consistently observed in other cell types simultaneously infected with Rostock virus (Table 7). Decreases in cytoplasmic pH of 0.40, 0.30, 0.25, 0.05 and 0.20pH units were observed after 6 hours p.i. in CEF, Hela, VERO, MDCK and an alternative line of MDCK cells respectively. The MDCK cells used throughout these studies showed the greatest reduction in

Table 7: The cytoplasmic pH of various cell types infected with Rostock virus (6 hours p.i.).

<u>Cell Type</u>	<u>Infection</u>	<u>Amount of M2</u>	<u>Cytoplasmic pH</u>		
			<u>No Addition</u>	<u>Nigericin</u>	<u>Amantadine</u>
MDCK	-	-	7.40	7.00	7.40
	+	48.0	7.00 (-0.40)	-	7.40
MDCK *	-	-	7.40	7.05	7.35
	+	42.5	7.10 (-0.30)	-	7.35
VERO	-	-	7.30	7.05	7.30
	+	2.6	7.15 (-0.25)	-	7.30
Hela	-	-	7.25	7.10	7.25
	+	30.0	7.20 (-0.05)	-	7.25
CEF	-	-	7.25	7.05	7.25
	+	40.0	7.05 (-0.20)	-	7.25

* Alternative MDCK cell line

Uninfected (-) MDCK cells were incubated with 10 μ M SNARF-1-AM for 1 hour. Rostock-infected cells (+) were loaded with SNARF-1-AM, 5-6 hours p.i.. Emission spectra were measured in Gey's+20mM Hepes, pH7.10 before and after the addition of 10 μ M nigericin (10 minutes) or 5 μ M amantadine (15 minutes) to the cuvette. Cytoplasmic pH was estimated from the 634/604nm emission ratio using SNARF-1 calibration curves.

The relative amount of M2 was assessed by densitometry using the autoradiograph shown in figure 29.

The figures in brackets indicate the pH difference (in pH units) between the Rostock-infected cells and the uninfected cells.

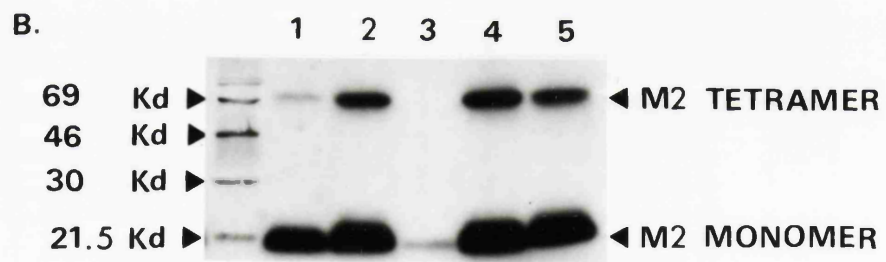
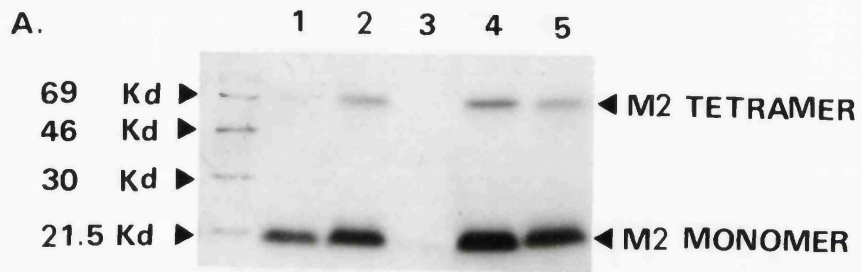
cytoplasmic pH. Amantadine ($5\mu\text{M}$) completely reversed the pH change in each infected cell type confirming that the effect was due to M2 protein. In only two of the cell types studied, control MDCK cells and CEF cells, did the Rostock virus infection (6 hours p.i.) succeed in abolishing the transmembrane pH gradient as judged by the addition of $10\mu\text{M}$ nigericin.

The differences in the apparent effectiveness of the Rostock M2 at (6 hours p.i.) to reduce the cytoplasmic pH, could be due to differences in the synthesis of M2 in the various cell types. Indeed differences were observed in the amount of M2 detected in the cells by immunoblotting (Figure 28). This was particularly pronounced in the case of VERO cells where very little M2 was detected in comparison to the other cell types (Table 7). The M2 specific decrease in these cells was only approximately 0.25pH units. However this was not a satisfactory explanation for the low pH difference (0.05pH units) observed in Hela cells, where quite a substantial amount of M2 protein was synthesized (Table 7). This may be due to ability of the virus to shut down host cell protein synthesis in Hela cells. The virus may be less effective in Hela cells at shutting down the synthesis of host ion channels, which may be responsible for buffering the cytoplasmic pH and resisting the M2-specific decrease in pH. Alternatively the M2 produced in Hela cells may not be in a form which is as active as in other cell types i.e. the M2 may be in a slightly different conformation or it

Figure 28: The production of M2 protein in various Rostock-infected cell types, as detected by immunoblotting.

Lysates of Rostock-infected MDCK cells (6 hours p.i.) were collected and subject to polyacrylamide gel electrophoresis (as detailed in materials and methods). After transferring to Immobilon-P M2 protein was detected using anti-M2 antiserum (R54) and an ¹²⁵I-labelled secondary antibody. The blot was exposed to film for 8 hours (A) and 14 hours (B).

The lanes show (left to right): Rostock-infected Hela (1), CEF (2), VERO (3), MDCK (4) and MDCK * (5) cells.



may have been processed differently.

Reductions in cytoplasmic pH which were reversed by amantadine (5 μ M) and rimantadine (5 μ M) were also observed in MDCK cells infected with three different influenza A subtypes (Table 8). Cells infected with A/Singapore/1/57 (H2N2), A/Victoria/36/88 (H1N1) or A/Beijing/32/92 (H3N2) showed a respective 0.25, 0.30 or 0.25pH unit decrease in cytoplasmic pH. These virus-infected cells consistently showed a pH change that was less than that produced in Rostock-infected MDCK cells, (0.4pH units). Similar amounts of M2 protein were detected in cells infected with A/Victoria/36/88 and Rostock virus (Figure 29 and Table 8), however the pH difference in Rostock-infected cells was twice that of the cells infected with A/Victoria/36/88. Similarly a relatively large amount of M2 was synthesized in A/Beijing/32/92-infected cells, almost twice that detected in Rostock-infected cells (Figure 29 and Table 8), but a pH difference of only 0.2pH units was recorded. This is probably due to differences in the activities of the various M2 proteins. However the sensitivity of the detection assay is also a consideration, as differences in the amino acid sequences of the various M2 proteins may affect the binding affinity of the R53 antiserum used in the immunoblotting procedure. Indeed R53 was incapable of recognizing the A/Singapore/1/57 M2 protein which has four amino acids within its N-terminal domain which differ from those found in Rostock. It is necessary therefore to repeat the immunoblot analysis using alternative anti-M2

Table 8: The effects of amantadine and rimantadine on cytoplasmic pH changes within MDCK cells infected with different influenza viruses.

<u>Virus</u>	<u>Cytoplasmic pH</u>			
	<u>No Addition</u>	<u>Amount of M2</u>	<u>Amantadine</u>	<u>Rimantadine</u>
Uninfected	7.40	-	7.40	7.35
Rostock (H7N1)	7.00 (-0.40)	6.0	7.40	7.40
A/Singapore/1/57 (H2N2)	7.15 (-0.25)	ND	7.40	7.35
A/Victoria/36/88 (H1N1)	7.10 (-0.30)	6.4	7.40	7.40
A/Beijing/32/92 (H3N2)	7.20 (-0.20)	42.5	7.40	7.35
B/Panama/45/90	7.20 (-0.20)	ND	7.20	7.25

Uninfected MDCK cells were loaded with 10 μ M SNARF-1-AM for 1 hour. Virus-infected cells were loaded with SNARF-1-AM, 5-6 hours p.i. and 634/604nm emission ratios obtained in Gey's+20mM Hepes, pH 7.10. Cytoplasmic pH was estimated by reference to the standard curve (figure 11B). Measurements were obtained before and after the addition of 10 μ M nigericin (10 minutes), 5 μ M amantadine (15 minutes) and 5 μ M rimantadine to the cuvette medium.

The relative amounts of M2 protein were assessed by densitometry using the autoradiographs shown in figure 30. ND indicates that the M2 protein could not be detected using R53.

The figures shown in brackets indicate the difference (in pH units) between the cytoplasmic pH of uninfected and virus-infected cells.

Figure 29: M2 production in MDCK cells infected with different influenza A viruses as detected by immunoblotting.

Lysates of MDCK cells infected with various influenza viruses were collected 6 hours p.i. and subject to polyacrylamide gel electrophoresis (as detailed in materials and methods). After transferring to Immobilon-P M2 protein was detected by anti-M2 antiserum (R54) and a secondary antibody conjugated to ^{125}I . The blot was exposed to film for 24 hours.

Left to right the lanes show uninfected cells (1) and cells infected with the following viruses: Rostock (2), A/Singapore/1/57 (3), A/Victoria/36/88 (4), A/Beijing/32/92 (5) and B/Panama/45/90 (6) (included as a negative control).



antiserum.

Interestingly MDCK cells infected with an influenza B strain (B/Panama/45/90) were also shown to have a lower cytoplasmic pH than uninfected cells (Table 8). Influenza B viruses do not possess an M2 protein and consequently amantadine and rimantadine have no activity '*in vitro*' or '*in vivo*', against type B infections. Thus the pH change observed in the influenza B-infected cells was not reversed by the presence of 5 μ M amantadine or rimantadine (Table 8). It has been suggested however that the NB protein, a small transmembrane protein encoded by segment 6 of the type B RNA, may perform a similar function to M2.

3.3 CYTOPLASMIC pH CHANGES WITHIN M2-EXPRESSING CELLS

The study of M2-expressing cell systems provides more definitive evidence that the pH change is due to M2. SNARF-1-AM was used to monitor the cytoplasmic pH of M2-expressing MEL (murine erythroleukaemia) cells and cells infected with a recombinant M2-expressing baculovirus. Both cell types were effectively loaded with the fluorescent probe using similar conditions to those used for MDCK cells.

M2-expressing baculovirus-infected cells

A recombinant baculovirus expressing the Weybridge M2 protein was used to infect Sf9 spodoptera cells which were subsequently loaded with SNARF-1-AM. The maintenance requirements of the spodoptera cells in culture deemed that

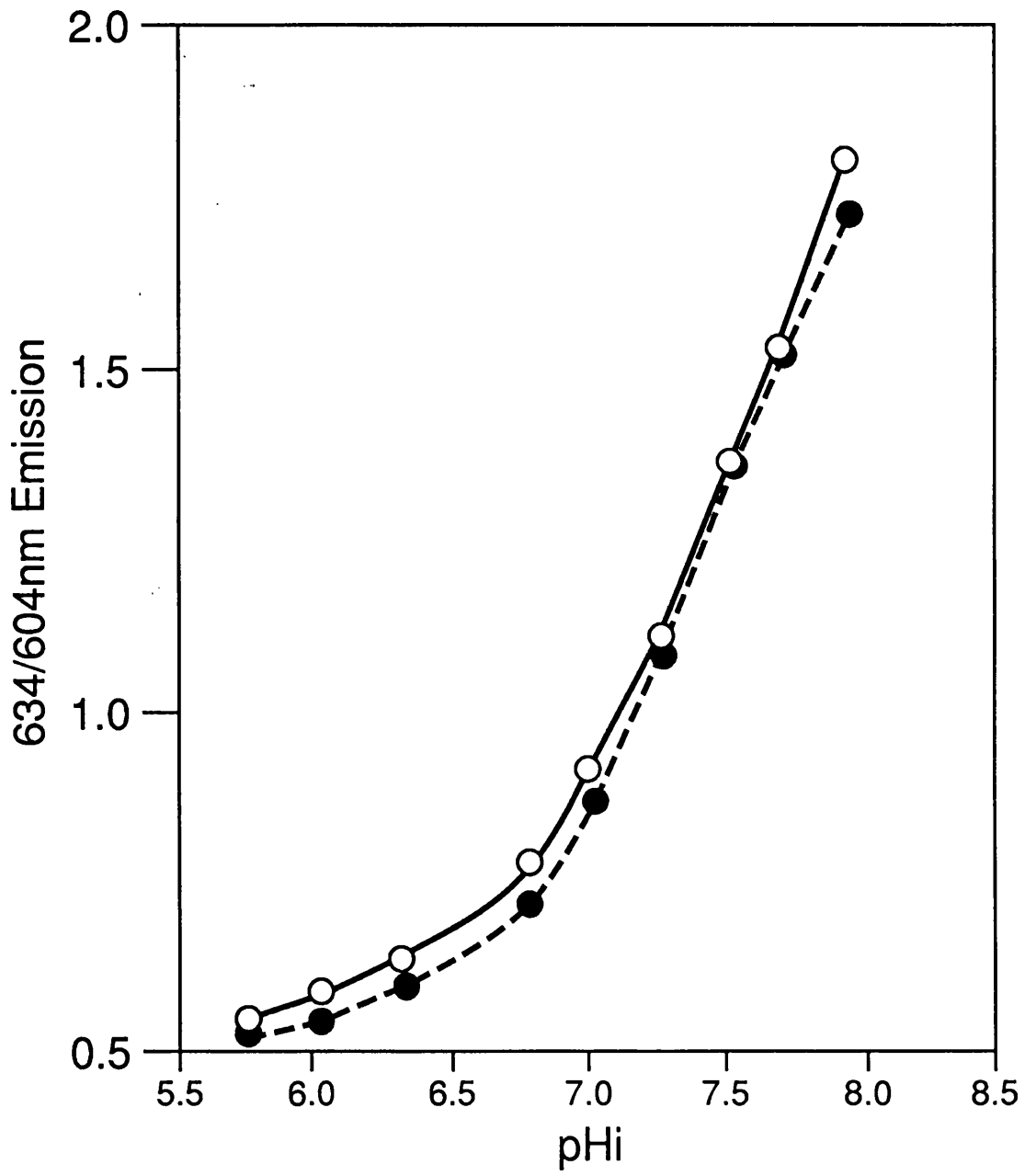
the temperature condition used in previous studies on MDCK cells was not appropriate. Consequently measurements were carried out at 27°C as well as 37°C. Ratio measurements were converted into pH values using the calibration curve shown in Figure 30. The addition of nigericin identified a relatively small difference in pH between the interior and exterior of the cells in media below pH7.50 and no significant difference above pH7.50. Possibly as a consequence of this, no reproducible differences in cytoplasmic pH were apparent between uninfected control cells and recombinant virus-infected cells (data not shown). This was despite the use of a range of different media (Gey's+20mM Hepes, TC100), temperature (27°C and 37°C) and pH (pH6.45 and pH7.10) conditions, in an attempt to mimic closely the conditions required for spodoptera cell maintenance in cell culture (i.e. TC100, pH6.45, 27°C).

M2-expressing MEL cells

MEL cells are erythroid progenitor cells whose development has been arrested at the pro-erythroid stage of development as a result of their transformation by Friend virus (Marks and Rifkind, 1978). Upon treatment with various chemical agents including dimethyl sulphoxide (DMSO) the cells are induced to undergo terminal erythroid differentiation (Friend et al., 1978; Marks and Rifkind, 1978). This is accompanied by significant changes in cell morphology and alterations in a number of cellular processes (Muller et al., 1980; Volloch and Housman, 1982), highlighted by high levels of β -globin expression (Kabat et

**Figure 30: Calibration curve for SNARF-1 in Sf9
spodoptera cells.**

Uninfected Sf9 Spodoptera cells were loaded with 10 μ M SNARF-1-AM for 1 hour at 27°C and placed in a cuvette with different pH solutions of 115mM KCl, 1mM MgCl₂ and 20mM Hepes buffer. The 634/604nm emission ratio (534nm excitation) was obtained at each pH before (○) and after 10 μ M nigericin (10 minutes) (●) was added to the cuvette.



al., 1975). A high-level MEL cell expression system has been developed using a vector containing the β -globin gene and promoter region (Needham et al., 1992). This system was used to produce a cell clone C39, expressing the Weybridge virus M2 protein.

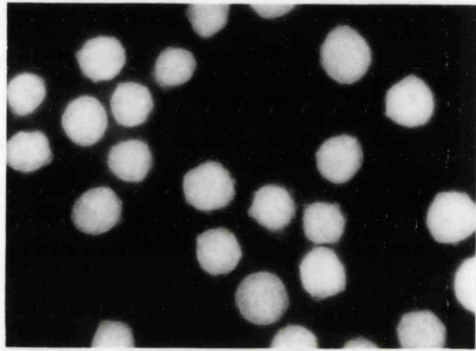
The SNARF-1 probe was distributed evenly throughout the cytoplasm of both the non-M2-expressing C88 control cells and the M2-expressing C39 cells (Figure 31). Figure 32 shows the calibration of the probe within C88 cells. Nigericin caused a significant decrease in the cytoplasmic pH of the cells when incubated at pH7.4 and below, indicating that similarly to MDCK cells the interior of the cells was buffered to maintain a pH above that of the external medium. The membrane pH gradient was reversed when the cells were incubated at a pH above pH7.4.

The cytoplasmic pH of the DMSO-induced C39 cells was monitored over a 5 day period. A decrease in the cytoplasmic pH occurred between 1 and 4 days post-induction (Figure 33A). This was accompanied by an increase in the amount of M2 protein synthesized, as detected by immunoblotting (Figure 33B). In a similar manner to Weybridge-infected MDCK cells small amounts of M2 appeared to be capable of producing a disproportionate decrease in the cytoplasmic pH (data not shown). By 4 days post induction a difference of 0.30pH units was apparent between the uninduced (pH7.30) and induced (pH7.0) cells. This was equivalent to the dissipation of the pH gradient across the plasma membrane, as indicated by the treatment of cells

Figure 31: The distribution of SNARF-1 in control and M2-expressing MEL cells, as observed by fluorescence microscopy.

C88 (A) and 4 day-induced M2-expressing C39 (B) MEL cells were loaded with 10 μ M SNARF-1-AM for 1 hour. After washing in Gey's+20mM Hepes, pH7.10, the coverslips were placed cell surface down onto microscope slides and observed using a fluorescence microscope (FITC filter).

A.



B.

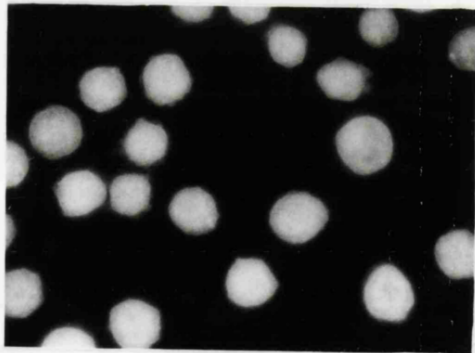
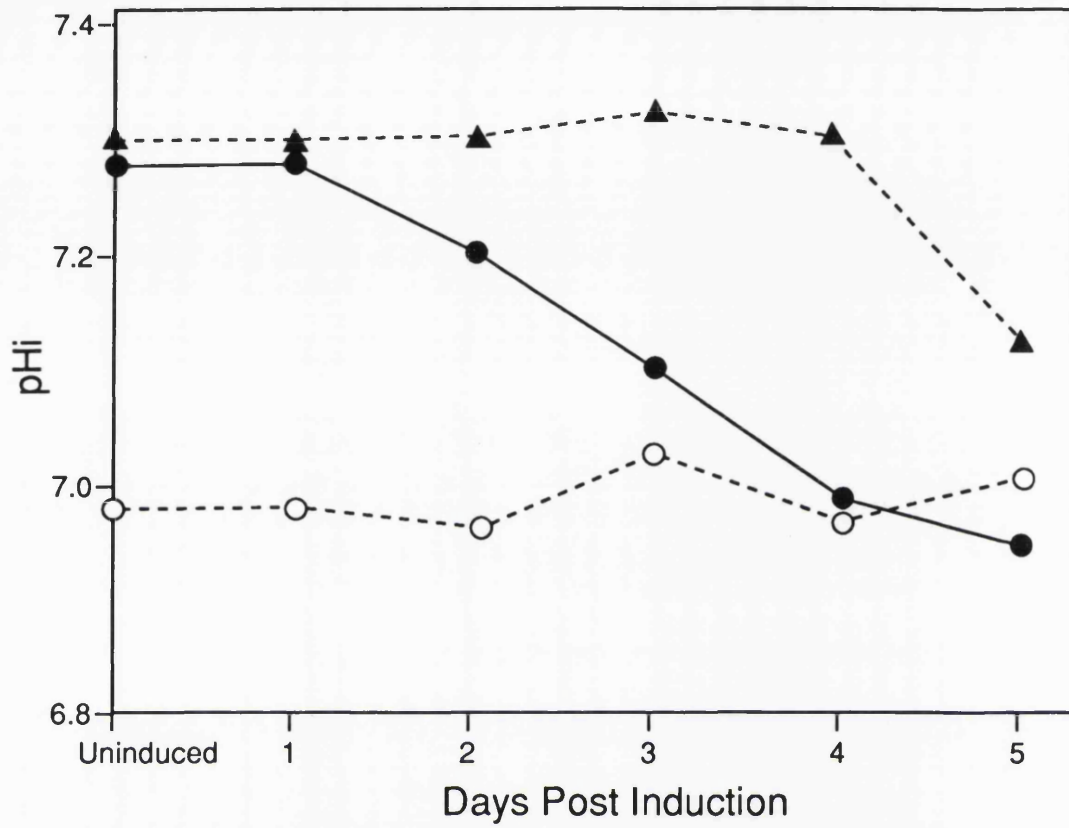


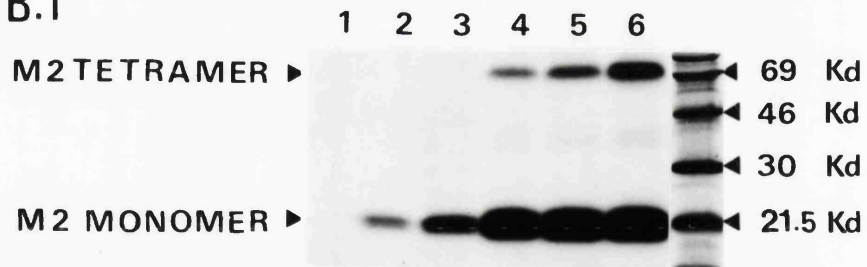
Figure 32: Calibration curve for SNARF-1 in MEL cells.

C88 MEL cells were incubated with $10\mu\text{M}$ SNARF-1-AM for 1 hour (37°C) and placed in a cuvette with solutions of 115mM KCl, 1mM MgCl_2 and 20mM Hepes adjusted to various pHs. Emission ratios (634/604nm) were obtained at each pH before (\circ) and after (\bullet) the addition of $10\mu\text{M}$ nigericin (10 minutes).

A.



B.i



ii

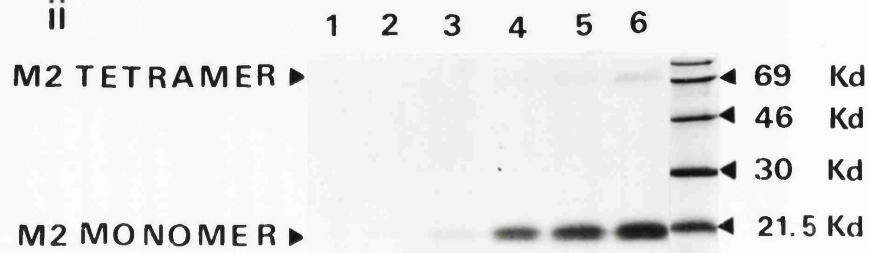
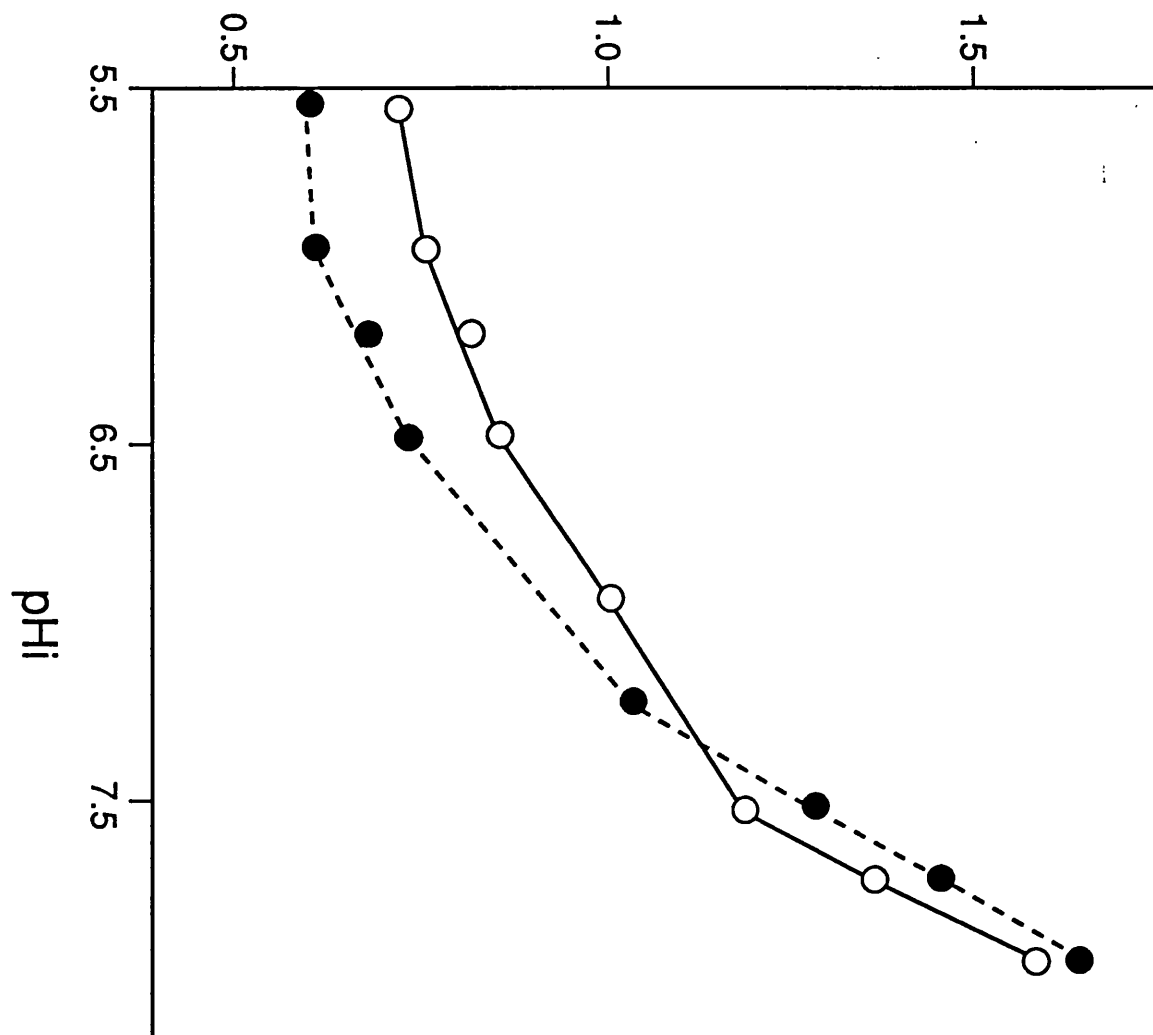


Figure 33: M2 production in DMSO-induced C39 MEL cells in relation to the reduction in cytoplasmic pH.

A. C39 MEL cells expressing Weybridge M2 protein (1, 2, 3, 4 and 5 days post induction with DMSO) were loaded with 10 μ M SNARF-1-AM for 1 hour. Emission ratios (634/604nm) were obtained before (\bullet) and after the addition of 5 μ M rimantadine (15 minutes) (\blacktriangle) or 10 μ M nigericin (10 minutes) (\circ). The cytoplasmic pH was determined using the SNARF-1 calibration curve shown in figure 32.

B. Cell lysates were subjected to polyacrylamide gel electrophoresis and transferred to Immobilon-P. M2 protein was detected using anti-M2 antiserum (R54) and an 125 I-labelled secondary antibody. The blot was exposed to film for 20 hours (i) and 10 hours (ii). From right to left the lanes show uninduced cells (1) and cells induced with DMSO for 1 day (2), 2 days (3), 3 days (4), 4 days (5) and 5 days (6).

634/604 nm Emission



with nigericin. Removal of the pH difference upon the addition of $5\mu\text{M}$ rimantadine confirmed that this was specifically due to the presence of M2 protein. The apparent inability of rimantadine to completely reverse the M2 effect in cells 5 days post induction may be due to the large amount of protein present or possibly a deterioration in cell viability. Cells beyond 5 days post induction were not used as their viability was impaired. This may have been due to the presence of DMSO or large amounts of the M2 protein. Both of these may have deleterious effects on the integrity of the cell membrane.

The M2-specificity of the pH reduction in 4 day-induced C39 cells was further confirmed by its specific reversal by R53 antiserum (Table 9). R53 had no effect on the cytoplasmic pH of C88 control cells or uninduced C39 cells. G34E cells expressing a M2 protein resistant to rimantadine, produced a 0.35pH unit reduction in the cytoplasmic pH by 4 days post induction. This was equivalent to that observed in 4 day-induced C39 cells. The pH difference was reversed by the addition of R53 antiserum, but not by R54 antiserum (data not shown) or $5\mu\text{M}$ rimantadine (Table 9). In summary all these observations are consistent with a M2-specified effect and add support to the proposed pH modification activity of M2 in virus-infected cells.

Table 9: The effects of nigericin, rimantadine and R53 antiserum on the cytoplasmic pH of MEL cells.

<u>Cells</u>	<u>Cytoplasmic pH</u>			
	<u>No Addition</u>	<u>Rimantadine</u>	<u>R53</u>	<u>Nigericin</u>
Control C88	7.30	7.30	7.30	6.90
Control C88-induced	7.30	7.30	7.30	6.95
C39	7.30	7.30	7.30	6.95
C39-induced	6.95 (-0.35)	7.30	7.30	6.95
G34E	7.10 (-0.20)	7.10 (-0.20)	7.30	6.95
G34E-induced	6.95 (-0.35)	6.95 (-0.35)	7.30	6.95

Uninduced and 4 day DMSO-induced C88, C39 and G34E MEL cells, were loaded with SNARF-1-AM for 1 hour and incubated in Gey's+20mM Hepes, pH7.10. Cytoplasmic pH measurements were estimated from 634/604nm emission ratios by means of the calibration curve shown in figure 32. Measurements were taken before and after the addition of 5 μ M rimantadine (15 minutes) or 10 μ M nigericin (10 minutes) to the cuvette. A 1/10 dilution of anti-M2 antiserum (R53) was added for 1 hour (37°C).

The figures in brackets indicate the difference (in pH units) between the cytoplasmic pH of the control C88 cells and the M2-expressing cells.

The inhibition of Weybridge M2 protein expressed in MEL cells

To compare in more detail the activity of the Weybridge M2 protein expressed in the MEL system with its activity in the virus-infected cell, the inhibitory effects of amantadine, rimantadine and a number of other amines (cyclobutylamine, cyclopentylamine, cyclohexylamine, cycloheptylamine and cyclooctylamine) were investigated more closely.

The activity of Weybridge M2 expressed in C39 cells was completely inhibited by 500 μ M amantadine after 15 minutes (Figure 34A). In contrast to Weybridge-infected MDCK cells where the same concentration of amantadine only produced a partial reversal in the cytoplasmic pH even after 30 minutes (Figure 25). Similar to Weybridge-infected MDCK cells 0.005, 0.05 and 0.5 μ M concentrations of amantadine had no significant effect on the pH of the induced C39 cells. 5 and 50 μ M concentrations caused an increase in pH of 0.2 and 0.25pH units respectively.

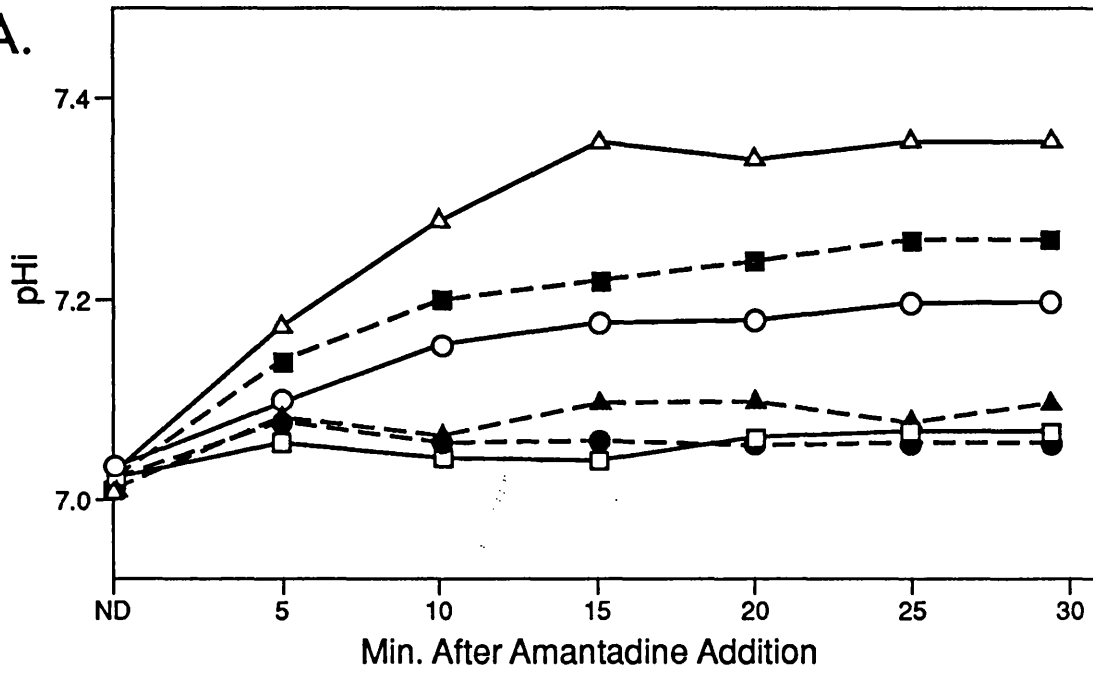
0.5 and 5 μ M rimantadine completely abolished the 0.3pH unit difference in pH between the control induced C88 cells and the M2-expressing C39 cells, after 15 minutes (Figure 34B). 500 and 50 μ M concentrations of rimantadine produced a 0.4pH unit difference after 15 minutes. This was 0.1pH units above the pH of the control non-M2-expressing cells and suggested that the basic properties of rimantadine may also be influencing the increase in pH. In contrast to the observations made in Weybridge-infected cells where 0.05

Figure 34: The effect of various concentrations of amantadine and rimantadine on the cytoplasmic pH of M2-expressing C39 MEL cells.

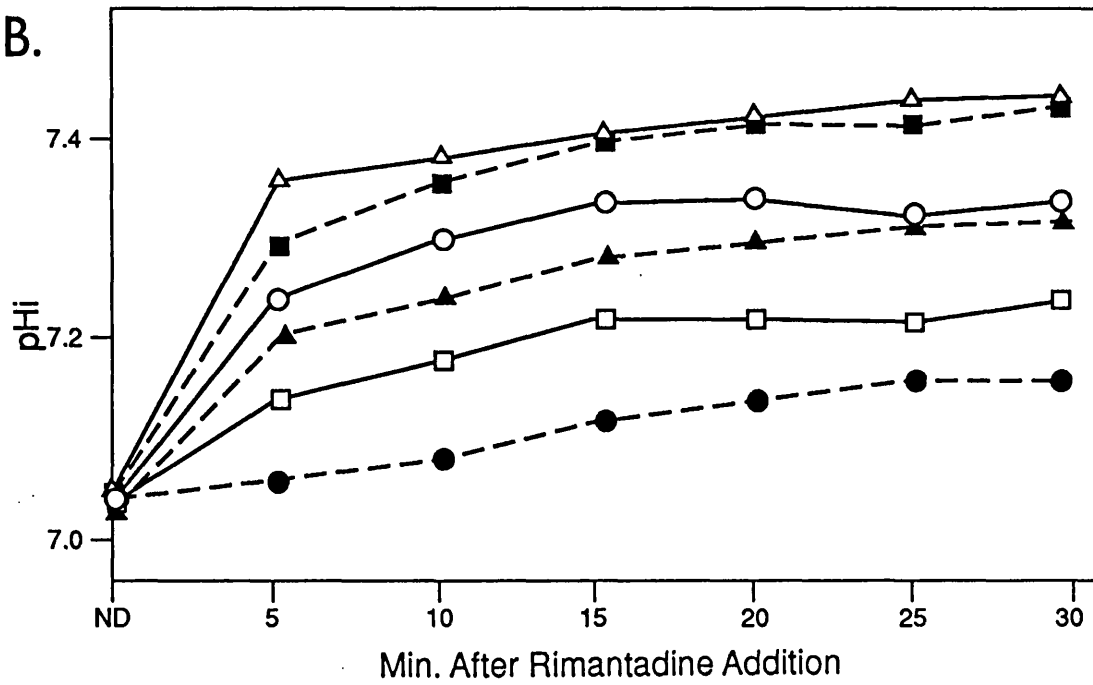
C39 MEL cells (4 days post induction with DMSO) were loaded with 10 μ M SNARF-1-AM for 1 hour. Emission ratios (634/604nm) were obtained before (ND) and after the addition of various concentrations of amantadine or rimantadine. Cytoplasmic pH values were estimated using the SNARF-1 calibration curve shown in figure 32.

0.005 μ M (\bullet), 0.05 μ M (\square), 0.5 μ M (\blacktriangle), 5 μ M (\circ), 50 μ M (\blacksquare) and 500 μ M (\triangle) concentrations of amantadine (A) and rimantadine (B) were used.

A.



B.

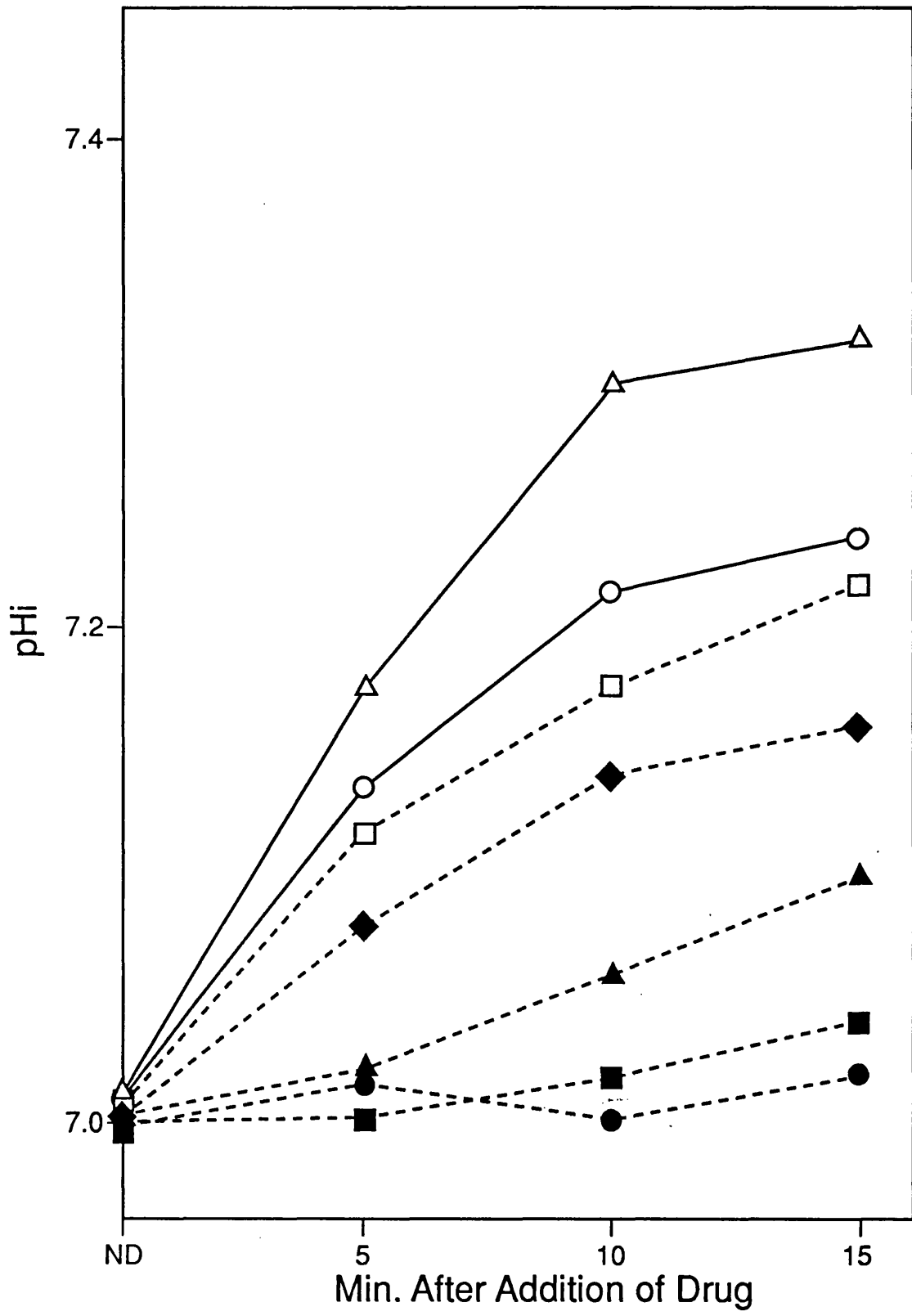


and 0.5 μ M concentrations of rimantadine had no effect on the M2 activity, they produced 0.15 and 0.20pH unit increases respectively in the pH of the induced-C39 cells. In summary the amantadine and rimantadine sensitivity of Weybridge M2 expressed in the MEL cell system appears to be similar to that in Weybridge-infected cells, with the exception of a slight increase in the susceptibility of the C39 M2 to 500 μ M amantadine and lower concentrations of rimantadine (0.005, 0.05 and 0.5 μ M).

Figure 35 shows the relative activities of the amines used in previous studies on the infected cell system. 5 μ M rimantadine was the only compound capable of completely abolishing the 0.3pH unit difference observed in induced-C39 cells. 5 μ M cyclobutylamine and 5 μ M cyclopentylamine had no significant effect on the cytoplasmic pH of the cells and thus in this respect the relative activities of the compounds in the infected cell and MEL cell systems were similar. However amantadine, cyclooctylamine, cycloheptylamine and cyclohexylamine appeared more active in terms of reversing the pH reduction in induced-C39 cells, than in Weybridge-infected MDCK cells. Respectively they increased the pH of the induced-C39 cells by 0.21, 0.22, 0.15 and 0.1pH units. Overall these results suggest that the specific inhibition of the MEL cell-expressed M2 protein exhibits a similar dependence on large hydrocarbon ring structures, as does the M2 in

Figure 35: Inhibition of the M2-specific decrease in the cytoplasmic pH of C39 MEL cells, by amantadine, rimantadine and cyclooctylamine.

4-day DMSO-induced C39 cells expressing 'Weybridge' M2 protein were loaded with 10 μ M SNARF-1-AM for 1 hour. Emission ratios (634/604nm) were obtained before (ND) and after the addition of 5 μ M amantadine (\circ), 5 μ M rimantadine (Δ), 5 μ M cyclooctylamine (\square), 5 μ M cycloheptylamine (\blacklozenge), 5 μ M cyclohexylamine (\blacktriangle), 5 μ M cyclopentylamine (\blacksquare) or 5 μ M cyclobutylamine (\bullet). Cytoplasmic pH was determined using the SNARF-1 calibration curve shown in figure 32.



infected MDCK cells.

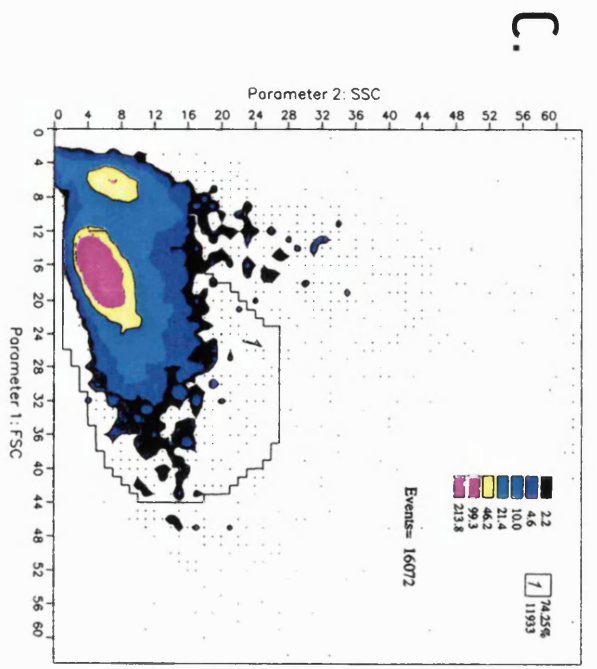
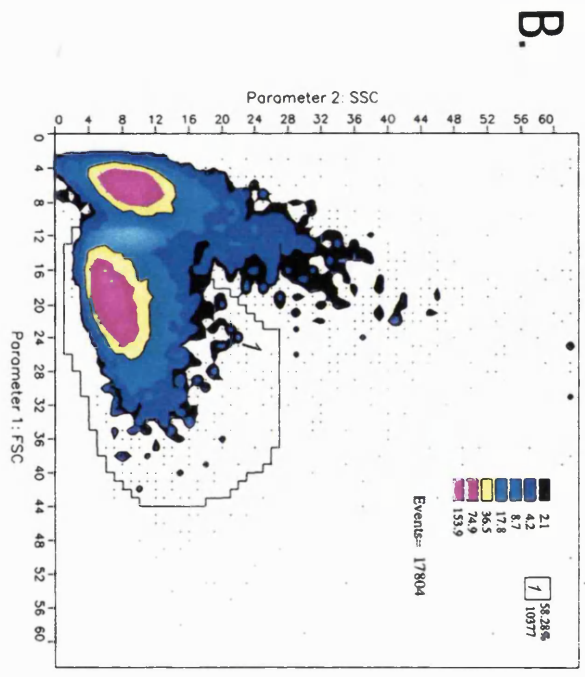
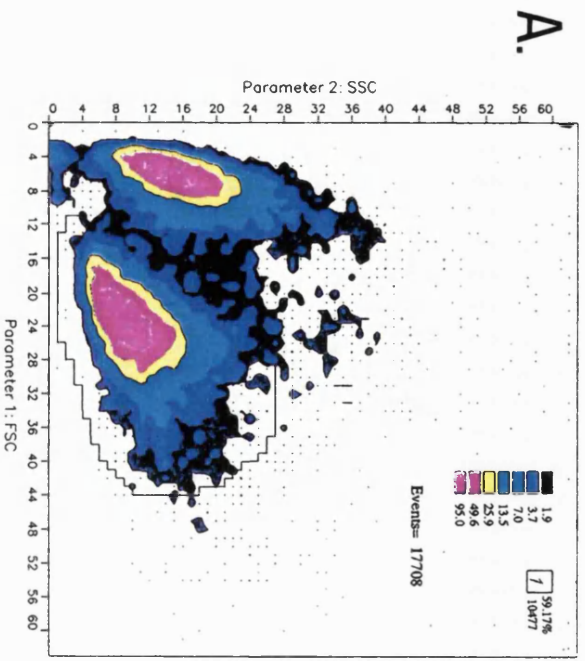
Flow cytometric analysis of the pH changes within M2-expressing MEL cells

In an attempt to try to develop a more routine assay based on the SNARF-1 system, two alternative approaches were investigated. The first involved the analysis of SNARF-1-loaded cells in microtitre plates using a plate reader attached to the fluorescence spectrophotometer. The equipment however was not sensitive enough to monitor changes in SNARF-1 fluorescence. The second approach involved the analysis of SNARF-1-loaded MEL cells by flow cytometry. MEL cells are grown in suspension and so are more suitable for this form of analysis than MDCK cells. SNARF-1 can be excited using either of the 488 or 514nm lines produced by the argon laser, making the pH probe suitable for flow cytometric analysis (Blank *et al.*, 1992; van Erp *et al.*, 1991). Consequently SNARF-1-AM-loaded C88 and 4 day-induced C39 MEL cells were analysed by flow cytometry.

Using flow cytometry the viability of cells can be easily assessed by the degree of light scattering. Dead cells can subsequently be omitted from the analysis. Figure 36 (A-C) shows the relative degree of forward light scatter (FSC) against the relative degree of side scatter (SSC) for C88 and 4 day-induced C39 cells. The latter provides information concerning the granularity of the cell. Dead cells show a low level of forward light scatter and/or an increase in granularity. Typically the

Figure 36: The viability of SNARF-1 loaded MEL cells as determined by flow cytometry.

Samples of C88 control cells and 4 day-induced M2-expressing C39 cells were washed and loaded for 1 hour at 37°C with 10 μ M SNARF-1-AM. After washing twice in Gey's+20mM Hepes, pH7.10 the cells were resuspended for flow cytometric analysis. The degree of forward (FSC) and side (SSC) angle light scatter was used to determine the percentage of viable cells (box 1). C88 control cells (A) and 4 day DMSO-induced C39 cells before (B) and after (C) the addition of 5 μ M rimantadine (15 minutes) were used.



percentage of live cells in each of the samples varied between 55% and 80% (Figure 36A-C). The remaining dead cells were omitted from the analysis. The centrifugation and washing stages required before the measurement of the cells may contribute to the rather large numbers of dead cells present. Changes in the cell membrane during DMSO induction may also contribute to the fragility of the cells.

During the determination of the changes in SNARF-1 fluorescence both the 488nm and 514nm lines of the argon laser were used. Initial experiments suggested that the 488nm emission was more suitable for the observation of changes in the SNARF-1-loaded MEL cells. Accordingly pH-induced changes in probe fluorescence were monitored using a ratio of emission intensities at 640 and 580nm. It was not possible using the data analysis program available, to obtain 640/580nm emission ratio values for the individual cells. Figure 37 shows the ratio data expressed as histograms where the logarithm of each ratio value has been assigned to a channel number. The histograms are divided into 3 zones and alterations in the emission ratio are indicated by changes in the mean channel number of zone B. On this basis slight shifts in the 640/580nm emission ratio (488nm excitation) were observed in 4 day-induced C39 cells as compared to the control C88 cells (Figure 37). When incubated in the presence of 5 μ M rimantadine the ratio resembled that of the control cells. However it was not possible without the actual ratio values, to determine how

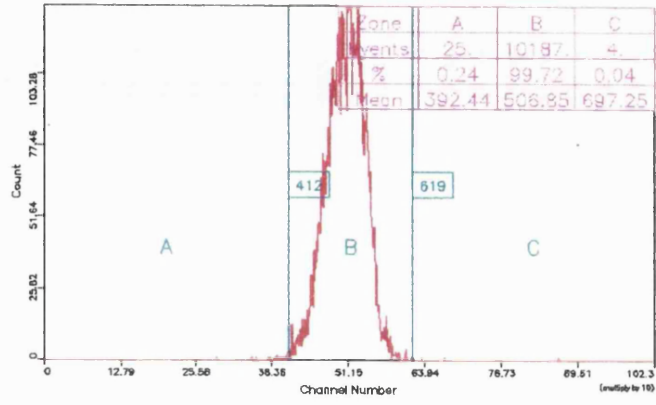
significant the changes in mean channel number were in terms of 640/580nm emission ratios. Cells examined in parallel in the usual manner, using the fluorescence spectrophotometer showed typical shifts in cytoplasmic pH as indicated by changes in their 634/604nm emission ratios. Over a series of 5 separate experiments, the apparent changes in emission ratio observed using the flow cytometer were not as reproducible as those observed using the conventional method. This suggests that flow cytometric analysis may offer some potential for the measurement of pH changes within SNARF-1 loaded cells, however further study is required to try to optimize the sensitivity of the system.

Figure 37: Comparison of the 640/580nm emission ratios of SNARF-1-loaded MEL cells, as determined by flow cytometry

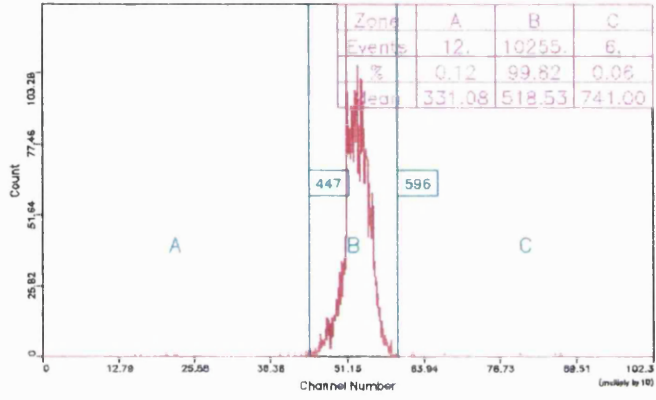
The 640/580nm emission (488nm excitation) ratios of viable C88 control cells (A), untreated C39 cells (B) and C39 cells treated with 5 μ M rimantadine (C), were determined and represented in the form of histograms. The channel number represents the logarithm of the 640/580nm emission ratio and the count represents the number of cells that have been assigned to each individual channel number. The histograms are divided into 3 zones (A, B and C), zone B containing >99% of the cells studied. The maximum and minimum channel numbers within zone B are highlighted in boxes. The number of events (cells), the % of the total number of events and the mean channel number within each section are shown in the top righthand corner of each histogram.

Histogram D. shows the histograms of the C88 control cells (red), C39 untreated cells (blue) and C39 cells treated with 5 μ M rimantadine (black) in comparison to each other.

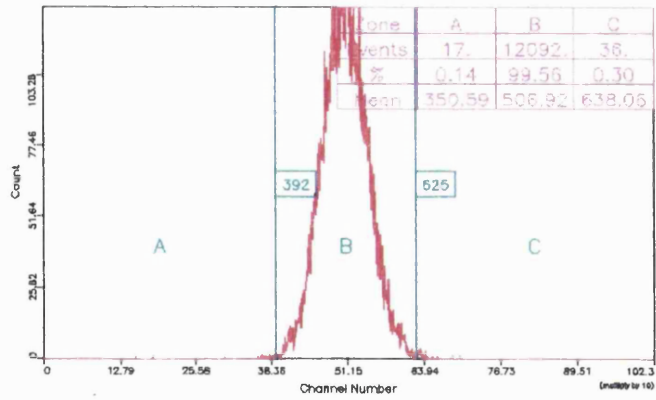
A.



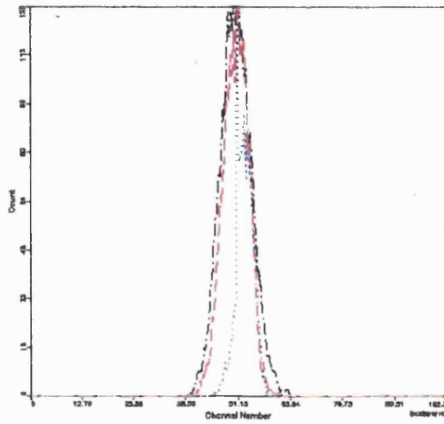
B.



C.



D.



DISCUSSION

DISCUSSION

4.1 M2-specific pH changes within the transport pathway

Amantadine and rimantadine are currently the only antiviral drugs licensed for use against influenza A. They specifically inhibit the M2 protein of the virus which although only a minor component of the envelope, is abundantly expressed in virus-infected cells. With a view to developing further more effective therapies for influenza, it is of great interest to determine the role of this protein in the virus replication cycle. The specific inhibition of M2 by amantadine has identified two roles of the protein, in virus uncoating and in virus maturation. Sugrue et al., (1990a) showed that the inhibition of virus maturation by amantadine was due to pH-induced conformational changes in HA, converting the protein into its low pH form prior to its insertion into the plasma membrane. Only the cleaved form of HA is susceptible to the effects of low pH and consequently only the H5 and H7 viruses which have HAs that are cleaved intracellularly are susceptible to the effects of amantadine at this late stage in the replication cycle. Cleavage occurs within the trans-Golgi compartment of the cell, suggesting that the pH-induced conformational changes in HA occur late in the transport pathway, in the trans-Golgi or TGN which are known to be acidic. The work reported here and published in Ciampor et al., (1992b) was initially based on

observations made by F. Ciampor concerning the effect of M2 inhibition on HA maturation. The immunofluorescence studies carried out confirmed the appearance of large, low pH HA-containing vesicles within virus-infected cells treated with amantadine. These structures were labelled by WGA, indicating more precisely that amantadine exerts its effects on HA maturation within the trans-Golgi or TGN. Native HA was found within the trans-Golgi of both untreated and amantadine-treated cells, which is consistent with HA only becoming susceptible to the effects of amantadine late in the transport pathway after it has undergone post-translational cleavage into HA1 and HA2 (Sugrue et al., 1990a). No conformational changes in HA were observed within cells infected with an amantadine-resistant virus containing a mutation within its M2 protein. This confirms the M2 specificity of the amantadine effect.

Consistent with the role of M2 in the modification of vesicular pH and the amantadine-induced changes in the conformation of HA, M2 was shown to be colocalized with both native and low pH HA. In a similar manner to HA, M2 was distributed throughout the virus-infected cell, within the Golgi apparatus, cytoplasmic vesicles and on the cell surface. M2 was evenly distributed across the cell surface and was found to extend into the junctions between the cells effectively outlining the individual cells. Confocal microscopy would be required however to determine whether the distribution of the protein extended to the basolateral

surface of the cells. The distribution of M2 was unaffected by the addition of amantadine which suggests that in agreement with Sugrue et al., (1990a), the drug has no gross effects on the synthesis or transport of M2 to the cell surface. Hughey et al., (1992) have reported a similar distribution of M2 in untreated MDCK cells. In addition they confirm the predominantly apical expression of M2, more precisely identifying its presence on the microvilli of the cell and its association with budding virions. The budding process occurs rapidly upon the association of the viral M1 protein and nucleoprotein capsids with the plasma membrane (Hay, et al., 1974; Patterson et al., 1985). The association between M1 and the lipid envelope is sensitive to pH and other ionic conditions (Zhirnov, 1990). It may be possible that M2 is important in creating the ionic conditions required for the association of the virion components during the budding process. This still remains to be determined, as does the role of M2 within the mature virion where only small amounts of the protein are found. It has been suggested that during virus uncoating in endocytic vesicles, M2 within the virion envelope permits the entry of protons into the virion interior to create the acidic conditions required for the dissociation of the M1 protein from the RNP core. To investigate this activity of the M2 protein in the virion, preliminary attempts were made to monitor the pH of the virions using the SNARF-1 fluorescent pH probe. Problems were encountered however in loading the

virions with sufficient amounts of the probe to obtain a measurable fluorescent signal.

Using DAMP, it has been observed that the inhibition of M2 by amantadine results in the appearance of large acidic vesicles within the infected cell (Ciampor et al., 1991a). These correspond to the vesicles containing low pH HA. This is consistent with the direct involvement of M2 in the regulation of pH within HA-containing transport vesicles. The vesicles were apparent only after prolonged exposure to amantadine (Ciampor et al., 1991a), which suggests that they are probably the result of the accumulation of low pH HA, which has a tendency to form aggregates. Alterations in pH may affect the morphology of the Golgi apparatus and so it was of interest to investigate which events were involved in the enlargement of the low pH vesicles. Unfortunately attempts using DAMP to follow pH changes in vesicular compartments over shorter periods of time were unsuccessful.

The relationship between M2 and HA in H7 virus-infected cells has been investigated using HA as a probe for the pH encountered within the transport pathway (Grambas and Hay, 1992). Mutations in HA can affect the pH at which the conformational changes occur (Daniels et al., 1985; Skehel et al., 1982; Steinhauer et al., 1991) and thus the conversion of HA from its native to its low pH form provides an estimation of the pH encountered within the transport pathway. The importance of the relationship between the activity of M2 and the pH stability of HA, was

emphasized by the correlation between the low pH stability of the Rostock HA and the greater activity of its M2 protein in reducing the pH encountered within the transport pathway. The Rostock M2 protein appeared to be capable of increasing the pH of the transport pathway in MDCK cells, by as much as 0.8pH units as compared to the 0.2pH unit increase produced by the Weybridge M2 protein (Grambas and Hay, 1992). This correlates with the difference in pH at which their HA's undergo conformational changes (pH5.3 and 5.9 respectively). Amino acid changes within the transmembrane domain of the protein were shown to affect the ability of M2 to modify the vesicular pH and to protect the structural integrity of the HA molecule (Grambas et al., 1992). A decrease in the activity of M2 may be compensated for by an increase in the stability of HA at low pH and a decrease in the stability of HA at low pH by an increase in the activity of M2.

The relevance of this activity of the M2 protein in situations where the HA is not cleaved intracellularly and therefore is not susceptible to the major conformational changes induced by low pH, remains uncertain. Although uncleaved HA (HA0) is sensitive to pH (Boulay et al., 1987), the changes involved seem to be of little significance in terms of the transport and maturation of HA (Sugrue, unpublished observations). It may be possible however that M2 is important in creating a suitable ionic environment for the maturation of the viral glycoproteins, within the transport pathway. When expressed in oocytes M2

has been shown to exhibit a Na⁺ conductance (Pinto et al., 1992). Ionophores such as monensin and nigericin which disrupt Na⁺ and K⁺ gradients respectively, have been shown to interfere with the processing and transport of HA, indicating that ionic conditions within the transport pathway are important in the maturation of the virus (Daniels and Edwardson, 1988). In addition studies have shown that virus infection appears to cause a general increase in the acidity of MDCK cells (Ciampor et al., 1991a). Acidification of the trans-Golgi has been shown to slow down the transport in MDCK cells, of the endogenous gp80 protein (Pilarsky and Koch-Brandt, 1992) and the vesicular stomatitis virus G protein (Cosson et al., 1989). Thus M2 may also influence the transport of the viral glycoproteins by counteracting the increase in acidity associated with virus infection.

One approach which was considered in order to investigate further the activity of M2 within the trans-Golgi, was the study of isolated M2-containing transport vesicles. Exocytic transport vesicles have been isolated from MDCK cells using a technique which 'strips' away the apical plasma membrane, to allow vesicles to escape from the cell (Bennett et al., 1988; Bennett et al., 1989; Bennett et al., 1990). Vesicles loaded with DAMP or a fluorescent pH probe, such as was used to study the pH of the cell cytoplasm, could be used to directly study the influence of M2 on the luminal pH. A number of fluorescent probes are available, to monitor changes in the

concentration of Na^+ , K^+ , Ca^{2+} and Cl^- ions (Tsien, 1989). These could be used to investigate other possible effects of M2 on the ionic environment within the vesicles. Unfortunately due to the constraints of time such studies did not proceed beyond a preliminary stage. Hopefully the future use of such techniques will provide a greater insight into the origin of the low pH vesicles and the activity of M2 within this cellular compartment.

4.2 The role of M2 in modifying the pH of the infected cell cytoplasm

In view of the observations made by F. Ciampor concerning the increased acidity of virus-infected cells, changes in the pH of the cell cytoplasm were investigated. The fluorescent pH probes BCECF and SNARF-1 have been used successfully by a number of other workers to investigate intracellular pH changes within various cells (Bassnett et al., 1990; Seksek et al., 1991). In the work presented here SNARF-1 was found to be more suitable for monitoring the intracellular pH of MDCK cells. After infection with Rostock virus a decrease in cytoplasmic pH was observed in MDCK cells and a number of other cell types. The cytoplasm of the MDCK cells (pH7.4) was found to be slightly alkaline (by approximately 0.4pH units) in comparison to the external pH, in agreement with previously reported pH values under similar conditions (Selvaggio et al., 1986). Virus infection (6 hours p.i.) caused the pH of the

cytoplasm to decrease by 0.4pH units to pH7.0, which was equivalent to the pH observed when the plasma membrane pH gradient in uninfected cells was abolished by the ionophore nigericin.

The fact that virus infection caused an alteration in the pH of the cell cytoplasm was not unexpected. The permeability of cell membranes with respect to a variety of ions including protons, is known to be affected by virus infection (Carrasco et al., 1989; Carrasco et al., 1993). Increases in membrane permeability are associated with both the early and late phases of infection and are believed to be important in a number of stages in the viral replication cycle. This includes the 'shut off' of host protein synthesis and the development of cytopathic effects within the cell. Notably two animal viruses are known to cause alterations in the cytoplasmic pH of the cells they infect. Poliovirus infection of Hela cells activates cellular ATPases, causing an alkalinization of the cell interior which promotes the replication of the virus genome (Holsey and Nair, 1993). The precise mechanism by which this occurs is unknown, however it requires both the expression and translation of the input genome. It has also been reported that the infection of baby hamster kidney (BHK) cells by sindbis virus, produces a 0.5pH unit decrease in the cytoplasmic pH of the cells (Moore et al., 1988). Sindbis virus production was found to be inhibited if the pH of the cell cytoplasm was increased. Again the exact mechanism involved is unknown, however expression of the

viral genome is required.

As in other systems the reduction in the cytoplasmic pH of Rostock-infected cells was found to be dependent on the expression of the viral genome and the synthesis of viral protein. In this instance the decrease in cytoplasmic pH was specifically due to the production of one viral protein:- M2. M2 is abundantly expressed in infected cells and has been shown to affect the pH of the transport pathway. In view of these observations it is not unreasonable to suggest that its activity may influence the pH of other cell compartments. Anti-M2 antiserum and concentrations of amantadine which have been shown to specifically inhibit the M2 protein, reversed the pH change in Rostock-infected cells. In addition similar M2-induced changes in pH were evident in cells infected with various influenza A strains and in M2-expressing MEL cells. The latter indicated that the changes in cytoplasmic pH were not dependent on any other factors of virus infection except the production of M2.

The amantadine inhibition of the cytoplasmic pH changes was irreversible, in agreement with previous studies which have reported that the amantadine inhibition of both viral replication and HA maturation is irreversible (Kato and Eggers, 1969; Hay and Zambon, 1984). Measurements of M2 channel activity in oocytes also suggest that amantadine irreversibly inhibits M2 (Wang et al., 1993). Both amantadine and rimantadine were capable of inhibiting the decrease in cytoplasmic pH in Rostock-infected MDCK cells.

In contrast rimantadine was more effective than amantadine at reversing the pH decrease in Weybridge-infected cells. Cytoplasmic pH changes in C39 MEL cells expressing Weybridge M2 however appeared to be similarly sensitive to both amantadine and rimantadine. With respect to the latter observation Grambas and Hay, (1992) also noted that the influence of amantadine and rimantadine on the activity of M2 in the trans-Golgi was dependent on the cell type used. Studies of virus replication in tissue culture have also shown that different influenza A strains vary in their sensitivity to amantadine (Hay et al., 1985; Hay and Zambon, 1984). In particular the replication of Weybridge virus has been shown to be more sensitive than Rostock to low concentrations of amantadine (Hay et al., 1985, Hay et al., 1986). The apparent discrepancy between the drug sensitivity of Rostock and Weybridge reported here and that previously reported, could be due a number of reasons. Most significantly it should be noted that the work reported here refers to M2 activity in a different area of the cell to that previously studied. The distribution of both drugs is influenced by pH as they have been shown to accumulate in acidic compartments such as lysosomes (Richman et al., 1981). The drug concentration therefore varies between different cells and different cell compartments. The inhibition of M2 is dependent on the concentration of drug and so the location of M2 and the concentration of amantadine or rimantadine within that cell compartment will influence the degree of inhibition

observed. The studies of cytoplasmic pH were carried out at pH7.10 whereas previous studies were carried out at pH7.50, this may also influence the apparent drug sensitivity observed. Differences in the concentrations of drug may indeed account for the apparent increased ability of amantadine to inhibit the Weybridge M2-specific effect in MEL cells. Differences in the permeability of the MDCK and MEL cell membranes may influence the effective concentrations of the drugs within the cytosol. As previously mentioned the virus infection of cells produces alterations in the permeability of the cell membrane to various compounds (Carrasco, 1978; Carrasco et al., 1993; Pasternak and Micklem, 1981). This could influence the concentration of drug within the virus-infected MDCK cells, as opposed to the M2-expressing MEL cells.

Similarly to amantadine the amine cyclooctylamine was shown to inhibit the changes in cytoplasmic pH. Previous studies have shown that cyclooctylamine and amines with hydrocarbon ring structures containing more than 7 carbon atoms are capable of inhibiting both viral replication and HA maturation in a manner similar to amantadine (Hay et al., 1985). Thus the inhibition of M2-specific changes in cytoplasmic pH shows a similar dependance on amine structure to that previously reported.

It is not known how amantadine and rimantadine interact with the M2 channel in order to block its activity. The location of mutations which abolish M2 sensitivity to amantadine, are consistent with the drug directly

interacting with the transmembrane domain of the M2 channel (Hay et al., 1991; Hay et al., 1985). This is analogous to the interaction of amantadine with the ion channel of the nicotinic acetylcholine receptor (Warnick et al., 1982). In addition ion channel studies of a M2 transmembrane peptide in lipid bilayers indicate that amantadine is capable of interacting with the transmembrane domain to block its proton conductance properties (Duff and Ashley, 1992). These observations suggest that amantadine directly interacts with and blocks the M2 channel. However ion channel measurements of M2 expressed in oocytes, were not consistent with this model (Wang et al., 1993). These studies suggested that amantadine may interact outside the transmembrane domain to block the activity of the protein by inducing conformational changes within the M2 channel. These studies also suggested that one amantadine molecule is sufficient to block the activity of a single M2 channel and that the drug has a greater affinity for the channel in its inactive state. Single ion channel measurements however are required in order to provide a more definitive insight into the nature of the M2 channel and its inhibition by amantadine.

In view of the evidence supporting the role of M2 in the modification of cytoplasmic pH, the relationship between the production of M2 and the reduction in pH was investigated. Small amounts of the M2 protein were associated with a disproportional decrease in the pH and this applied to both wildtype and amantadine-resistant

viruses. The regulation of intracellular pH is very important for a number of cell functions and as a result, the pH of the cell interior is accurately controlled with respect to the external pH by the activities of various channels and pumps. One possible explanation for the relationship between M2 and the decrease in pH is that as the pH decreases with the increased production of M2, cellular ion channels/pumps are activated in order to buffer the changes in pH. The effects of inhibiting two of the channels important in the pH regulation of MDCK cells, the Na^+/H^+ antiporter and $\text{Cl}^-/\text{HCO}_3^-$ exchanger, using amiloride and DIDS respectively, were inconclusive. Neither of the drugs appeared to have any effect on the pH of uninfected nor infected cells. The lack of activity of amiloride may be due to the presence of physiological concentrations of Na^+ , as it has been reported that under such conditions amiloride may not be able to effectively block the antiporter (Borle and Bender, 1991). Another possible explanation for the disproportional relationship between the amount of M2 and the pH change is the formation at high concentrations of M2 of inactive M2 multimers on the cell surface. The active form of the M2 channel is believed to be a tetramer, however higher orders of M2 structure have been observed by a number of workers (Holsinger and Lamb, 1991; Sugrue and Hay, 1991). The relevance of these structures in terms of ion channel activity is not understood; they may perhaps have a different activity to the tetramer in terms of their ion selectivity. This could

explain the observation that M2 expressed in large amounts in oocytes shows a Na⁺ conductance.

The studies reported here also suggest that differences in activity exist between M2 proteins in different viruses. In cells infected with the resistant mutant 039 the pH decrease was almost complete before any M2 was detected by immunoblotting. The amantadine resistant mutant 08 which possesses the mutation A30T in the transmembrane domain of its M2 protein, was incapable of completely abolishing the transmembrane pH gradient, even after 8 hours p.i.. This suggests that the protein is less active than the corresponding wildtype Rostock virus, which is consistent with previous reports on the activity of the protein within the trans-Golgi (Grambas et al., 1992). Grambas et al., (1992), reported that amino acid substitutions at positions 26, 30, 31 and 34 in the transmembrane domain of the Rostock M2 protein decreased the ability of the protein to modify trans-Golgi pH. In contrast changes at position 27 appeared to increase the activity of M2. Ion channel studies of oocytes expressing a mutant A/Udorn/72 M2 protein S31N, have also suggested that mutations within the transmembrane domain can influence the channel activity of the protein (Pinto et al., 1992). It is not possible without single channel measurements however to determine if this was due to any differences in the ion flux through the channel. Cells infected with the mutant I27T showed a reduction in cytoplasmic pH equivalent to that observed with the wildtype Rostock virus. Weybridge-infected cells

showed a similar reduction in pH to that of Rostock-infected cells. It has been suggested that the Rostock M2 protein is more active than that of the Weybridge virus (Grambas and Hay, 1992). It was not possible using the data shown here however to compare the relative activities of the two M2 proteins.

The SNARF-1 studies directly measure an M2-specific pH change which indicates that M2 directly or indirectly results in the transport of H⁺ ions. Preliminary studies were carried out to investigate the nature of the ion flow involved in the M2 modification of cytoplasmic pH. These studies showed that the activity of M2 was not significantly affected by changes in the concentration of K⁺ ions. Lowering the concentrations of Na⁺ and Cl⁻ ions removed the transmembrane pH gradient of the uninfected cells and resulted in the production of M2 having no significant effect on the cytoplasmic pH. This is consistent with M2 acting in situations where a transmembrane pH gradient is present and causing that gradient to be abolished. Similar observations have been made in C39 MEL cells (E. Chizhnikov, personal communication). The MDCK cell system however appears too complex to obtain any further information regarding the ion selectivity of M2, using the SNARF-1 assay. Studies by other workers however do suggest that M2 is capable of directly transferring H⁺. An inward proton current (i.e. in a N to C terminal direction with respect to the orientation of M2), has been directly measured by whole

cell patch clamping in C39 M2-expressing MEL cells (E. Chizhnikov, personal communication). This shows similar kinetics of inhibition by rimantadine, to those reported here. In addition a rimantadine-inhibitable decrease in pH has been measured in lipid vesicles containing purified M2, using the fluorescent pH probe pyranine (Schroeder et al., submitted). This effect is directly attributable to an inward flux of protons. The transmembrane domain of M2 in lipid bilayers has also been shown to be capable of transporting H⁺ ions in an amantadine-inhibitable manner. The concentrations of drug required to inhibit the ion channel activity however were greater than those used to inhibit cytoplasmic pH changes (Duff and Ashley, 1992). Evidence obtained from whole cell patch clamp studies of M2 expressed in oocytes however suggest that M2 exhibits an inward Na⁺ conductance (Pinto et al., 1992). This activity was inhibited by amantadine and rimantadine though again at greater concentrations than those required to inhibit the reduction in cytoplasmic pH.

The physiological significance of the ability of M2 to modify cytoplasmic pH remains unclear as the studies were carried out in bicarbonate-free Gey's+20mM HEPES, pH7.10. With the equipment available it was not possible to carry out measurements in media requiring CO₂ buffering as would occur under physiological conditions. Large numbers of M2 molecules (in the order of 10⁶-10⁷) accumulate at the surface of cells infected with influenza A virus (Zebedee et al., 1985). If the M2 ion channel was active under

physiological conditions it could presumably lead to major changes in the ionic composition of the cell, which would be deleterious. It has been suggested for this reason that the M2 channel is only activated under conditions such as those found within endosomes and the vesicles of the trans-Golgi. Both of these cell compartments are acidic and so the effect of altering the external pH on the cytoplasmic pH changes was investigated. Over the pH range 6.0-7.7 infected cells were shown to be more acidic than the uninfected cells. The pH reduction in the infected cells was specifically reversed by amantadine and consequently attributable to M2. Therefore using the SNARF-1 assay, an M2-specific decrease in pH was observed over a range of external pHs. There was no obvious enhancement of this activity at low pH. Ion channel measurements in M2-expressing oocytes showed that the activity of the A/Udorn/72 M2 channel was increased 8 fold upon lowering the external pH from pH7.5 to pH5.8 (Pinto et al., 1992). It may not be possible however using the SNARF-1 assay to detect any such increase in M2 activity at pHs below pH6.3, as the sensitivity of the SNARF-1 probe is reduced. With respect to this point, it would be of interest to investigate the use of alternative fluorescent probes which have lower pH ranges. The results reported here show that using the SNARF-1 assay, M2 is active over a range of external pH values (pH6.0-pH7.7) and acts to remove the pH gradient across the cell membrane.

The ability of M2 to remove the pH gradient across the

plasma membrane suggests that M2 located within the plasma membrane may be responsible for the changes in cytoplasmic pH. However the M2 protein is expressed in a number of other locations throughout the virus-infected cell and it is necessary to consider the involvement of M2 located in other regions of the cell. Studies of M2 activity within the transport pathway and in C39 MEL cells (E. Chizhnikov, personal communication) suggest that M2 allows H⁺ ions to flow in a N to C-terminal direction. Studies of M2-specific changes in the trans-Golgi and the cytoplasm show that in both circumstances the protein produces an effect similar to that seen with the ionophore nigericin, which abolishes the plasma membrane pH gradient. On the basis of these two observations, there would appear to be three possible locations for the M2 responsible for cytoplasmic pH changes :- 1) the trans-Golgi/TGN, 2) the plasma membrane and 3) the endocytic pathway. In all three instances a proton flow through M2 in a N to C terminal direction would lead to an decrease in the cytoplasmic pH of the cell.

Antibody against the N-terminus of the M2 protein blocked the decrease in cytoplasmic pH. This suggests more specifically the involvement of M2 orientated with its N-terminus accessible to antibody. It seems unlikely that the N-terminus of M2 located in the trans-Golgi/TGN would be accessible to antibody as it faces into the lumen of the compartment. The extent to which antibody is capable of binding to M2 within the transport pathway, could be

assessed by monitoring the uptake of fluorescently-tagged antibody by fluorescence microscopy.

M2 protein located within the plasma membrane of the infected cell is orientated with its N-terminus accessible to antibody and so could be responsible for the cytoplasmic pH changes (Lamb et al., 1985; Zebedee et al., 1985). However it is possible that the antibody may be internalized into endocytic vesicles containing M2 and that M2 protein located within this cell compartment may also be involved. It has been observed that anti-M2 antibody can indeed be found in association with M2 within coated pits (Hughey et al., 1992). However the question remains as to whether the M2 protein is normally associated with endocytic vesicles or if its uptake is dependent on the presence of antibody (i.e. by antibody-mediated endocytosis).

A further observation which is consistent with the involvement of cell surface or endosomal M2 protein is the absence of the M2-mediated reduction in cytoplasmic pH in the presence of brefeldin A. Brefeldin A was shown to interfere with and inhibit the transport of M2 to the cell surface. M2 synthesis was not affected by brefeldin A and the absence of low pH HA in amantadine-treated cells incubated in the presence of BFA suggested that M2 was still active within the transport pathway. This again suggests that M2 within the trans-Golgi/TGN is not involved in the M2-specific changes in cytoplasmic pH. In addition if M2 in the transport pathway was responsible for the

cytoplasmic pH changes then blocking the synthesis of M2 using cycloheximide and chasing the remaining protein to the cell surface, would be expected to remove the pH decrease. In fact such a study showed that the pH decrease was not affected, suggesting that M2 that has reached the plasma membrane is responsible for the cytoplasmic pH changes. The amantadine and rimantadine sensitivity of the cytoplasmic pH changes also did not correspond to that observed for M2 within the trans-Golgi/TGN.

To determine whether M2 protein located within endosomal membranes exhibited any activity in terms of the modification of pH, preliminary experiments were carried out to monitor pH changes within endosomes, using the fluorescent pH probe DM-NERF conjugated to dextran (Dunn et al., 1991; Whitaker et al., 1991). DM-NERF is capable of measuring pH changes within the range of pH4.5-6.0 and is therefore suitable for studying the acidic pHs encountered within endosomes. By studying the effects of amantadine and anti-M2 antiserum (R53) on the pH within endosomes the intention was to determine whether M2 was responsible for any changes in endosomal pH which could account for the M2-specific decrease in cytoplasmic pH. Unfortunately due to the lack of time these studies did not proceed beyond a preliminary stage, however it would be of interest to pursue these studies further in order to determine whether M2 within the endosome is capable of modifying pH. It seems more likely however that M2 within the plasma membrane is involved in the pH changes within the cell

cytoplasm. Patch clamping studies of C39 MEL cells are consistent with this model.

Cytoplasmic pH changes within other virus-infected cells

M2-specific cytoplasmic pH changes were detected in a number of other influenza A viruses. Of particular interest however was the observation that MDCK cells infected with the influenza B virus B/Panama/45/90 also showed a reduction in pH. Influenza B viruses do not possess a M2 protein and are therefore not inhibited by low ($5\mu\text{M}$) concentrations of amantadine or rimantadine. It has been suggested however that the small, integral protein NB which is encoded by segment 6 of the influenza B virus (Williams and Lamb, 1986), may perform a similar function to M2. The detection of an apparent virus specific decrease in the cytoplasmic pH of influenza B infected cells is therefore of great interest. As yet no compound has been shown to specifically inhibit the NB protein and so unlike M2 there is no assay for NB activity. It would be interesting to determine whether the apparent activity was dependent on the synthesis of NB protein and if it could be specifically blocked by the addition of anti-NB antibody. A number of other viruses are known to possess small integral proteins which have structural similarities to M2. Their functions are as yet undetermined, however in view of the activity of M2 it has suggested that they may play a similar roles in infection. Such proteins include the SH protein of the paramyxoviruses simian virus 5 (Hiebert et al., 1985) and respiratory syncytial virus

(RSV) (Olmsted and Collins, 1989; Collins et al., 1990), the 1A protein of RSV, the 6K and E1 proteins of Semliki Forest virus (Schlegel et al., 1991), the D3 protein of infectious bronchitis virus (Smith et al., 1990), and the vpu protein of HIV-1 (Klimkait et al., 1990; Maldarelli et al., 1993). Vpu is an 81 amino acid type I integral membrane protein which is structurally similar to M2 and is involved in the maturation and release of HIV-1 virus. More precisely vpu appears to affect the processing of the HIV-1 envelope precursor glycoprotein gp160. The precise mechanism by which this occurs is unknown, however vpu appears to destabilize the interaction between gp160 and CD4, the cell receptor for HIV-1 (Willey et al., 1992). If vpu does possess ion channel activity then it may influence the ionic environment of the transport pathway and cause the destabilization of the gp160/CD4 complex. In view of the specific anti-influenza action of amantadine, the possibility that vpu may display a similar activity to M2 would be of interest with respect to the development of anti-HIV compounds.

It has previously been shown that M2 modifies the pH within the trans-Golgi in order to protect the structural integrity of the HA glycoprotein. By directly monitoring the pH of virus-infected cells the work reported here shows that M2, is also capable of modifying the pH of the cell cytoplasm in order to abolish the plasma membrane pH gradient, over a range of external pHs. Further evidence

suggests that M2 in the plasma membrane is responsible for the changes in cytoplasmic pH and that the changes are consistent with the transport of H⁺. The relevance of this activity of M2 under physiological conditions still remains to be determined, however it provides further evidence to support the ion channel activity of M2 and its role in the modification of pH within the virus-infected cells. The use of SNARF-1 to monitor M2-specific changes in pH is also of interest in terms of the development of a routine assay for M2 activity and for the screening of potential anti-influenza agents.

REFERENCES

REFERENCES

- AIR, G.M., Laver, W.G.** (1989). The neuraminidase of influenza virus. *Proteins: Structure, Function and Genetics* 6, 341-356.
- ALMOND, J.W., Felsenreich, V.** (1982). Phosphorylation of the nucleoprotein of an avian influenza virus. *Journal of General Virology* 60, 295-305.
- ALONSO-CAPLEN, F.V., Nemeroff, M.E., Qiu, Y., Krug, R.M.** (1992). Nucleocytoplasmic transport: the influenza NS1 protein regulates the transport of spliced NS2 mRNA and its precursor NS1 mRNA. *Genes and Development* 6, 255-267.
- AMANO, H., Uemoto, H., Kuroda, K., Hosaka, Y.** (1992). Immunoelectron microscopy of influenza A virus neuraminidase glycoprotein topography. *Journal of General Virology* 73, 1969-1975.
- ANDERSON, R.G.W., Falck, J.R., Goldstein, J.L., Brown, M.S.** (1984). Visualisation of acidic organelles in intact cells by electron microscopy. *Proceedings of the National Academy of Sciences* 81, 4838-4842.
- ANDERSON, R.G.W., Pathak, R.K.** (1985). Vesicles and cisternal in the trans-Golgi apparatus of human fibroblasts are acidic compartments. *Cell* 40, 635-643.
- APOSTOLOV, K., Flewett, T.H.** (1969). Further observations on the structure of influenza viruses A and C. *Journal of General Virology* 4, 365-370.
- APPLEYARD, G.** (1977). Amantadine-resistance as a genetic marker for influenza viruses. *Journal of General Virology* 36, 249-255.
- ATKINSON, W.L., Arden, N.H., Patriarca, P.A., Leslie, N., Liu, K-J, Gogd, R.** (1986). Amantadine prophylaxis during an institutional outbreak of type A (H1N1) influenza. *Archives of Internal Medicine* 146, 1751-1756.
- BASAK, S., Tomana, M., Compans, R.W.** (1985). Sialic acid is incorporated into influenza hemagglutinin glycoproteins in the absence of viral neuraminidase. *Virus Research* 2, 61-68.
- BASSNETT, S., Ranisch, L., Beebe, D.C.** (1990). Intracellular pH measurement using single excitation-dual emission fluorescence ratios. *American Journal of Physiology* 258, C171-178.
- BEAN, W.J., Threlkeld, S.C., Webster, R.G.** (1989). Biologic potential of amantadine-resistant influenza virus

in an avian model. *Journal of Infectious Diseases* 159, 1050-1056.

BEAN, W.J., Schell, M., Katz, J., Kawaoka, Y., Naeve, C., Gorman, O., Webster, R.G. (1992). Evolution of the H3 influenza virus hemagglutinin from human and non-human hosts. *Journal of Virology* 66, 1129-1138.

BEARD, C.W., Brugh, M., Webster, R.G. (1987). Emergency of amantadine-resistant H5N2 avian influenza virus during a stimulated layer flock treatment program. *Avian Diseases* 31, 533-537.

BEARLE, A.S., Webster, R.G. (1991). Replication of avian viruses in humans. *Archives of Virology* 119, 37-42.

BEATON, A.R., Krug, R.M. (1986). Transcription antitermination during influenza viral template RNA synthesis requires the nucleocapsid protein and the absence of a 5' capped end. *Proceedings of the National Academy of Sciences* 83, 6282-6286.

BEKTIMIROV, T.A., Douglas, R.G., Dolin, R., Galasso, G.J., Krylov, V.F., Oxford, J. (1985). Current status of amantadine and rimantadine as anti-influenza A agents: memorandum from a WHO meeting. *Bulletins of the World Health Organisation* 63, 51-56.

BELSHE, R.B., Hall-Smith, M., Hall, C.B., Betts, R., Hay, A.J. (1988). Genetic basis of resistance to rimantadine emerging during treatment of influenza virus infection. *Journal of Virology* 62, 1508-1512.

BENNETT, M.K., Wandinger-Ness, A., Brändli, A.W., Simons, K. (1990). *In vitro* recovery of exocytic transport vesicles from polarized MDCK cells. In 'Methods in Enzymology, Volume 191', pp.813-825. Edited by S. Fleischer and B. Fleischer, Academic Press, London.

BENNETT, M.K., Wandinger-Ness, A., de Curtis, I., Antony, C., Simons, K. (1989). Perforated cells for studying intracellular membrane transport. In 'Methods in Cell Biology, Volume 31', pp.103-126. Edited by A.M. Tartakoff, Academic Press Inc..

BENNETT, M.K., Wandinger-Ness, A., Simons, K. (1988). Release of putative exocytic transport vesicles from perforated MDCK cells. *EMBO Journal* 7, 4075-4085.

BEYER, W.E.P., Palache, A.M., Baljet, M., Masurel, N. (1989). Antibody induction by influenza vaccines in the elderly a review of the literature. *Vaccine* 7, 385-394.

BLANK, P.S., Silverman, H.S., Chung, O.Y., Hogue, B.A., Stern, M.D., Hansford, R.G., Lakatta, E.G., Capogrossi, M.C. (1992). Cytosolic pH measurements in single cardiac

myocytes using carboxy-seminaphthorhodafluor-1. American Journal of Physiology 263, H276-284.

BLASS, D., Patzelt, R., Keuchler, E. (1982). Identification of cap binding protein of influenza virus. Nucleic Acids Research 10, 4803-4812.

BLOK, J., Air, G.M., Laver, W.G., Ward, C.W., Lilley, G.G., Woods, E.F., Roxburgh, C.M., Inglis, A.S. (1982). Studies on the size, chemical composition and partial sequence of the neuraminidase (NA) from type A influenza viruses show that the N-terminal region of the NA is not processed and serves to anchor the NA in the viral membrane. Virology 119, 109-121.

BODIAN, D.L., Yamasaki, R.B., Buswell, R.L., Stearns, J.F., White, J.M., Kuntz, I.D. (1993). Inhibition of the fusion-inducing conformational change of influenza hemagglutinin by benzoquinones and hydroquinones. Biochemistry 32, 2967-2978.

BORLE, A.B., Bender, C. (1991). Effects of pH on Ca_{i2+} , Na_{i+} and pH_i of MDCK cells: Na^+-Ca^{2+} and Na^+-H^+ antiporter interactions. American Journal of Physiology 261, C482-C489.

BOS, K., Wraight, C., Stanley, K.K. (1993). TGN is maintained in the trans-Golgi network by a tyrosine-containing motif in the cytoplasmic domain. EMBO Journal 12, 2219-2228.

BOULAY, F., Doms, R.W., Wilson, I., Helenius, A. (1987). The influenza haemagglutinin precursor an acid-sensitive probe of the biosynthetic pathway. EMBO Journal 6, 2643-2650.

BRAAKMAN, I., Hoover-Litty, H., Wagner, K.R., Helenius, A. (1991). Folding of influenza hemagglutinin in the endoplasmic reticulum. Journal of Cell Biology 114, 401-411.

BRAAM, J. Ulmanen, I., Krug, R.M. (1983). Molecular model of a eukaryotic transcription complex: functions and movements of influenza P proteins during capped RNA-primed transcription. Cell 34, 609-618.

BRON, R., Kendal, A.P., Klenk, H-D, Wilschut, J. (1993). Role of the M2 protein in influenza virus membrane fusion: effects of amantadine and monensin on fusion kinetics. Virology 195, 808-811.

BUKRINSKAYA, A.G., Vorkunova, N.K., Kornilayeva, G.V., Narmanbetova, R.A., Vorkunova, G.K. (1982a). Influenza virus uncoating in infected cells and effect of rimantadine. Journal of General Virology 60, 49-59.

BUKRINSKAYA, A.G., Vorkunova, N.K., Pushkarskaya, N.L. (1982b). Uncoating of a rimantadine-resistant variant of influenza virus in the presence of rimantadine. *Journal of General Virology* 60, 61-66.

BUONAGURIO, D.A., Krystal, M., Palese, P., DeBorde, D.C., Maassab, H.F. (1984). Analysis of an influenza A virus mutant with a deletion in the NS segment. *Journal of Virology* 49, 418-425.

CARR, C.M., Kim, P.S. (1993). A spring-loaded mechanism for the conformational change of influenza hemagglutinin. *Cell* 73, 823-832.

CARRASCO, L. (1978). Membrane leakiness after viral infection and a new approach to the development of antiviral agents. *Nature* 272, 807-809.

CARRASCO, L., Otero, M.J., Castrillo, J.L. (1989). Modification of membrane permeability by animal viruses. *Pharmacology and Therapeutics* 40, 171-212.

CARRASCO, L., Pérez, L., Irurzun, A., Lama, J., Martinez-Abaroa, F., Rodriguez, P., Guinea, R., Castrillo, J.L., Sanz, M.A., Ayala, J. (1993). Modification of membrane permeability by animal viruses. In 'Regulation of Gene Expression in Animal Viruses', pp.283-303. Edited by L. Carrasco, N. Sonenberg and E. Wimmer, Plenum Press, New York and London.

CASTRUCCI, M.R., Donatelli, I., Sidoli, L., Barigazzi, G., Kawaoka, Y., Webster, R.G. (1993). Genetic reassortment between avian and human influenza A viruses in Italian pigs. *Virology* 193, 503-506.

CASTRUCCI, M.R., Kawaoka, Y. (1993). Biologic importance of neuraminidase stalk length in influenza A virus. *Journal of Virology* 67, 759-764.

CHOPPIN, B.W., Compans, R. (1975). The structure of influenza viruses. In 'The Influenza Virus and Influenza', pp.15-47. Edited by E.D. Kilbourne, Academic Press, New York.

CHOPPIN, P.W., Richardson, C.D., Scheid, A. (1983). Analogues of viral polypeptides which specifically inhibit viral replication. In 'Problems of Antiviral Therapy', pp.13-25. Edited by C.H. Stuart-Harris and J.S. Oxford, Academic Press, London.

CIAMPOR, F., Bayley, P.M., Nermut, M.V., Hirst, E.M.A., Sugrue, R.J., Hay, A.J. (1992a). Evidence that the amantadine-induced, M2-mediated conversion of influenza A hemagglutinin to the low pH conformation occurs in an acidic trans Golgi compartment. *Virology* 188, 14-24.

CIAMPOR, F., Thompson, C.A., Grambas, S., Hay, A.J. (1992b). Regulation of pH by the M2 protein of influenza A viruses. *Virus Research* 22, 247-258.

CLEMENTS, M.L., Snyder, M.H., Sears, S.D., Maassab, H.F., Murphy, B.R. (1990). Evaluation of the infectivity and efficacy of live cold-adapted influenza B/Ann Arbor/1/86 reassortant virus vaccine in adult volunteers. *Journal of Infectious Diseases* 161, 869-877.

CLOAD, P.A., Hutchinson, D.W. (1983). The inhibition of the RNA polymerase activity of influenza virus A by pyrophosphate analogues. *Nucleic Acids Research* 11, 5621-5628.

COLLINS, P.L., Olmsted, R.A., Johnson, P.R. (1990). The small hydrophobic protein of human respiratory syncytial virus: comparison between antigenic subgroups A and B. *Journal of Virology* 71, 1571-1576.

COLLIER, N.C., Knox, K., Schlesinger, M.J. (1991). Inhibition of influenza virus formation by a peptide that corresponds to sequences in the cytoplasmic domain of the hemagglutinin. *Virology* 183, 769-772.

COLMAN, P.M., Laver, W.G., Varghese, J.N., Baker, A.T., Tulloch, P.A., Air, G.M., Webster, R.G. (1987). Three-dimensional structure of a complex of antibody with influenza virus neuraminidase. *Nature* 326, 358-363.

COLMAN, P.M., Varghese, J.N., Laver, W.G. (1983). Structure of the catalytic and antigenic sites in influenza virus neuraminidase. *Nature* 303, 41-44.

COLMAN, P.M., Ward, C.W. (1985). Structure and diversity of influenza virus neuraminidase. *Current Topics in Microbiology and Immunology* 114, 177-255.

COMPANS, R.W., Klenk, H-D. (1979). Viral membranes. In 'Comprehensive Virology, volume 13', pp. 293-385. Edited by H.Fraenkel-Conrat and R.G. Wagner, Plenum Publishing, New York.

COPELAND, C.S., Doms, R.W., Bolzau, E.M., Webster, R.G., Helenius, A. (1986). Assembly of influenza hemagglutinin trimers and its role in intracellular transport. *Journal of Cell Biology* 103, 1179-1191.

COPELAND, C.S., Zimmer, K-P., Wagner, K.R., Healey, G.A., Mellman, I., Helenius, A. (1988). Folding, trimerization and transport are sequential events in the biogenesis of influenza hemagglutinin. *Cell* 53, 197-209.

COSSON, P., de Curtis, I., Pouysségur, J., Griffiths, G., Davoust, J. (1989). Low cytoplasmic pH inhibits endocytosis and transport from the trans-Golgi network to

the cell surface. *Journal of Cell Biology* 108, 377-387.

COX, N.J., Bai, Z.S., Kendal, A.P. (1983). Laboratory-based surveillance of influenza A (H1N1) and A (H3N2) viruses in 1980-81: antigenic and genomic analyses. *Bulletin of the World Health Organisation* 61, 143-152.

DANIELS, R.S., Douglas, A.R., Skehel, J.J., Waterfield, M.D., Wilson, I.A., Wiley, D.C. (1983a). Studies of the influenza virus hemagglutinin in the pH5 conformation. In 'The Origin of Pandemic Influenza Viruses', pp.1-7. Edited by W.G. Laver, Elsevier, New York.

DANIELS, R.S., Douglas, A.R., Skehel, J.J., Wiley, D.C. (1983b). Analyses of the antigenicity of influenza haemagglutinin at the pH optimum for virus-mediated fusion. *Journal of General Virology* 64, 1657-1661.

DANIELS, R.S., Downie, J.C., Knossow, M., Skehel, J.J., Wang, M-L., Wiley, D.C. (1985). Fusion mutants of influenza virus haemagglutinin glycoprotein. *Cell* 40, 431-439.

DANIELS, P.U., Edwardson, J.M. (1988). Intracellular processing and transport of influenza-virus envelope proteins in Madin-Darby canine kidney cells. Effects of the carboxylic ionophores nomenclin and nigericin. *Biochemical Journal* 252, 693-700.

DAVEY, J., Dimmock, N.J., Colman, A. (1985). Identification of the sequence responsible for the nuclear accumulation of the influenza virus nucleoprotein in *Xenopus* oocytes. *Cell* 40, 667-675.

DEGRADO, W.F., Wasserman, Z.R., Lear, J.D. (1989). Protein design, a minimalist approach. *Science* 243, 622-628.

DOLIN, R., Reichman, R.C., Madore, H.P., Maynard, R., Linton, P.N., Webber-Jones, J. (1982). A controlled trial of amantadine and rimantadine in the prophylaxis of influenza A infection. *New England Journal of Medicine* 307, 580-584.

DOMS, R.W., Helenius, A., White, J.M. (1985). Membrane fusion activity of the influenza virus hemagglutinin. *Journal of Biological Chemistry* 260, 2973-2981.

DOMS, R.W., Russ, G., Yewdell, J.W. (1989). Brefeldin A redistributes resident and itinerant Golgi proteins to the endoplasmic reticulum. *Journal of Cell Biology* 109, 61-72.

DOUGLAS, R.G. (1990). Prophylaxis and treatment of influenza. *New England Journal of Medicine* 322, 443-450.

DUFF, K.C., Ashley, R.H. (1992). The transmembrane domain

of influenza A M2 protein forms amantadine-sensitive proton channels in planar lipid bilayers. *Virology* 190, 485-489.

DUFF, K.C., Kelly, S.M., Price, N.C., Bradshaw, J.P. (1992). The secondary structure of influenza A M2 transmembrane domain. A circular dichroism study. *FEBS Letters* 311, 256-258.

DUNN, K.W., Maxfield, F.R., Whitaker, J.E., Haugland, R.P., Haugland, R.P. (1991). Fluorescence excitation ratio pH measurements of lysosomal pH using laser scanning confocal microscopy. *Biophysical Journal* 59, 345a (abstract).

ENAMI, K., Qiao, Y., Fukuda, R., Enami, M. (1993). An influenza virus temperature-sensitive mutant defective in the nuclear-cytoplasmic transport of the negative-sense viral RNAs. *Virology* 194, 822-827.

ERIKSSON, B., Helgstrand, E., Johnsson, N.G., Larsson, A., Misiorny, A., Noren, J.O., Philipson, L., Stenberg, K., Stening, G., Stridh, S., Oberg, B. (1977). Inhibition of influenza virus ribonucleic acid polymerase by ribavirin triphosphate. *Antimicrobial Agents and Chemotherapy* 11, 946-951.

ETKIND, P.R., Krug, R.M. (1975). Purification of influenza viral complementary RNA: its genetic content and activity in wheatgerm extracts. *Journal of Virology* 16, 1464-1475.

FIELDS, S., Winter, G. (1981). Structure of the neuraminidase gene in human influenza virus A/PR/8/34. *Nature* 290, 213-217.

FODOR, E., Soeng, B.L., Brownlee, G.G. (1993). Photochemical crosslinking of influenza A polymerase to its virion RNA promoter defines a polymerase binding site at residues 9 to 12 of the promoter. *Journal of General Virology* 74, 1327-1333.

FRIEND, C., Scher, W., Holland, J.G., Sato, T. (1978). *Proceedings of the National Academy of Sciences* 68, 378-382.

FUJIWARA, T., Oda, K., Yokota, S., Takatsuki, A., Ikehara, Y. (1988). Brefeldin A causes disassembly of the Golgi complex and accumulation of secretory proteins in the endoplasmic reticulum. *Journal of Biological Chemistry* 263, 18545-18552.

GALLAGHER, P.J., Henneberry, J.M., Sambrook, J.F., Gething, M-J.H. (1992). Glycosylation requirements for intracellular transport and function of the hemagglutinin of influenza virus. *Journal of Virology* 66, 7136-7145.

GARTEN, W., Will, C., Buckard, K., Kuroda, K., Ortmann, D.,

Munk, K., Scholtissek, C., Schnittler, H., Drenckhahn, D., Klenk, H-D. (1992). Structure and assembly of hemagglutinin mutants of fowl plague virus with impaired surface transport. *Journal of Virology* 66, 1495-1505.

GETHING, M.J., McCammon, K., Sambrook, J. (1986). Expression of wild-type and mutant forms of influenza hemagglutinin: the role of folding in intracellular transport. *Cell* 46, 939-950.

GETHING, M.J., Sambrook, J. (1989). Protein folding and intracellular transport: studies on influenza virus haemagglutinin. *Biochemistry Society Symposium* 55, 155-166.

GILBERT, B.E., Knight, V. (1986). Biochemistry and clinical applications of ribavirin. *Antimicrobial Agents and Chemotherapy* 30, 201-205.

GILBERT, B.E., Wilson, S.Z., Knight, V., Couch, R.B., Quarles, J.M., Dure, I., Hayes, N., Willis, G. (1985). ribavirin small-particle aerosol treatment of infections caused by influenza virus strains A/Victoria/7/83 (H1N1) and B/Texas/1/84. *Antimicrobial Agents and Chemotherapy* 27, 309-313.

GOSWAMI, B.B., Borek, E., Sharma, O.K., Fujikaki, J., Smith, R.A. (1979). The broad spectrum antiviral agent ribavirin inhibits capping of m RNA. *Biochemical and Biophysical Research Communications* 89, 830-836.

GOTTSCHALK, A. (1957). Neuraminidase: the specific enzyme of influenza virus and *Vibrio cholerae*. *Biochimica et Biophysica Acta* 23, 645-646.

GOTTSCHALK, A. (1966). The Glycoproteins. Their Composition, Structure and Function. Edited by A. Gottschalk, Elsevier, Amsterdam.

GRAMBAS, S., Bennett, M.S., Hay, A.J. (1992). Influence of amantadine resistance mutations on the pH regulatory function of the M2 protein of influenza A viruses. *Virology* 191, 541-549.

GRAMBAS, S., Hay, A.J. (1992). Maturation of influenza A virus hemagglutinin - estimates of the pH encountered during transport and its regulation by the M2 protein. *Virology* 190, 11-18.

GRAVES, P.N., Schulman, J.L., Young, J.F., Palese, P. (1983). Preparation of influenza subviral particles lacking the HA1 subunit of hemagglutinin: unmasking of cross-reactive HA2 determinants. *Virology* 126, 106-116.

GREENSPAN, D., Krystal, M., Nakada, S., Amheiter, H., Lyles, P.S., Palese, P. (1985). Expression of influenza

virus NS2 nonstructural protein in bacteria and localization of NS2 in infected eukaryotic cells. *Journal of Virology* 54, 833-834.

GREENSPAN, D., Palese, P., Krystal, M. (1988). Two nuclear location signals in the influenza virus NS1 nonstructural protein. *Journal of Virology* 62, 3020-3026.

GREGORIADES, A. (1973). The membrane protein of influenza virus: extraction from virus and infected cells with acidic chloroform-methanol. *Virology* 54, 369-383.

GREGORIADES, A., Christie, T., Markarian, K. (1984). The membrane (M1) protein of influenza virus occurs in two forms and is a phosphoprotein. *Journal of Virology* 49, 229-235.

GREGORIADES, A., Guzman, G.G., Paoletti, E. (1990). The phosphorylation of the integral membrane (M1) protein of influenza virus. *Virus Research* 16, 27-42.

GRIFFIN, J.A., Basak, S., Compans, R.W. (1983). Effects of hexose starvation and the role of sialic acid in influenza virus release. *Virology* 125, 324-334.

GRIFFIN, J.A., Compans, R.W. (1979). Effect of cytochalasin B on the maturation of enveloped viruses. *Journal of Experimental Medicine* 150, 379-391.

GUO, Y.J., Jin, F.G., Wang, P., Wang, M., Zhu, J. (1983). Isolation of influenza C virus from pigs and experimental infection of pigs with influenza C virus. *Journal of General Virology* 64, 177-182.

HAMAGUCHI, M., Maeno, K., Yoshida, T., Nagai, Y., Iinuma, M., Matsumoto, T. (1985). Analysis of nuclear accumulation of influenza nucleoprotein antigen using a temperature-sensitive mutant. *Microbiology and Immunology* 29, 1131-1137.

HANKINS, R.W., Nagata, K., Kato, A., Ishihama, A. (1990). Mechanism of influenza virus transcription inhibition by matrix (M1) protein. *Research in Virology* 141, 305-314.

HATADA, E., Hasegawa, M., Shimizu, K., Hatanska, M., Fukuda, R. (1990). Analysis of influenza A virus temperature sensitive mutants with mutations in RNA segment 8. *Journal of General Virology* 71, 1283-1292.

HATADA, E., Takizawa, T., Fukuda, R. (1992). Specific binding of influenza A virus NS1 protein to the virus minus-sense RNA *in vitro*. *Journal of General Virology* 73, 17-25.

HAY, A.J., Abraham, G., Skehel, J.J., Smith, J.J., Smith, J., Fellner, P. (1977a). Influenza messenger RNAs are

incomplete transcripts of genome RNAs. *Nucleic Acids Research* 4, 4197-4209.

HAY, A.J., Grambas, S., Bennett, M. (1991). Resistance of influenza A viruses to amantine and rimantadine. In 'Advances in Molecular Biology and Targeted Treatment for AIDS', pp.345-353. Edited by A. Kumar, Plenum Press, New York.

HAY, A.J., Kennedy, N.T.C., Skehel, J.J., Appleyard, G. (1979). The matrix protein gene determines amantadine-sensitivity of influenza viruses. *Journal of General Virology* 42, 189-191.

HAY, A.J., Lomnizi, B., Bellamy, A., Skehel, J.J. (1977b). Transcription of the influenza virus genome. *Virology* 83, 337-355.

HAY, A.J., Skehel, J.J., McCauley, J. (1980). Structure and synthesis of complementary RNAs. *Philosophical Transactions of the Royal Society of London Biological Sciences, Series B* 288, 341-348.

HAY, A.J., Skehel, J.J., McCauley, J. (1982). Characterisation of influenza virus complete transcripts. *Virology* 116, 517-522.

HAY, A.J., Wolstenholme, A.J., Skehel, J.J., Smith, M.H. (1985). The molecular basis of the specific anti-influenza action of amantadine. *EMBO Journal* 4, 3021-3024.

HAY, A.J., Zambon, M.C. (1984). Multiple actions of amantadine against influenza viruses. In 'Antiviral Drugs and Interferon: The Molecular Basis of their Activity', pp.301-315. Edited by Y. Becker, Martinus Nijhoff Publishing, Boston, U.S.A..

HAY, A.J., Zambon, M.C., Wolstenholme, A.J., Skehel, J.J., Smith, M.H. (1986). Molecular basis of resistance of influenza A viruses to amantadine. *Journal of Antimicrobial Chemotherapy* 18 (suppl. B), 19-29.

HAYDEN, F.G., Belshe, R.B., Clover, R.D., Hay, A.J., Oakes, M.G., Soo, W. (1989). Emergence and apparent transmission of rimantadine-resistant influenza A virus in families. *New England Journal of Medicine*, 321, 1696-1702.

HIEBERT, S.W., Paterson, R.G., Lamb, R.A. (1985). Identification and predicted sequence of a previously unrecognized small hydrophobic protein, SH, of the paramyxovirus simian virus 5. *Journal of Virology* 55, 744-751.

HOLLAND, J., Spindler, K., Horodyski, F., Grabau, E., Nichol, S., VandePol, S. (1982). Rapid evolution of RNA genomes. *Science* 215, 1577-1585.

HOLSEY, C., Nair, C.N. (1993). Poliovirus-induced intracellular alkalinization involves a proton ATPase and protein phosphorylation. *Journal of Physiology* 155, 606-614.

HOLSINGER, L.J., Lamb, R.A. (1991). Influenza virus M2 integral membrane protein is a homotetramer stabilized by the formation of disulfide bonds. *Virology* 183, 32-43.

HONDA, A., Ueda, K., Nagata, K., Ishihama, A. (1988). RNA polymerase from influenza viruses: role of NP in RNA chain elongation. *Journal of Biochemistry* 104, 1021-1026.

HORISBERGER, M.A. (1980). The large P proteins of influenza A viruses are composed of one acidic and two basic polypeptides. *Virology* 107.302-305.

HOYLE, L., Davies, S.P. (1961). Amino acid composition of the protein components of influenza virus A. *Virology* 13, 53-57.

HUGHEY, P.G., Compans, R.W., Zebedee, S.L., Lamb, R.A. (1992). Expression of the influenza A virus M2 protein is restricted to the apical surfaces of polarized epithelial cells. *Journal of Virology* 66, 5542-5552.

HULL, J.D., Gilmore, R., Lamb, R.A. (1988). Integration of a small integral membrane protein, M2, of influenza virus into the endoplasmic reticulum: analysis of the internal signal-anchor domain of a protein with an ectoplasmic NH₂ terminus. *Journal of Cell Biology* 106, 1489-1498.

HUNZIKER, W., Witney, J.A., Mellman, I. (1991). Selective inhibition of transcytosis by brefeldin A in MDCK cells. *Cell* 67, 617-627.

HUNZIKER, W., Witney, J.A., Mellman, I. (1992). Brefeldin A and the endocytic pathway. Possible implications for membrane traffic and sorting. *FEBS letter.* 307, 93-96.

INGLIS, S.C., Carroll, A.R., Lamb, R.A., Mahy, B.W.J. (1976). Polypeptides specified by the influenza virus genome. 1. Evidence for eight distinct gene products specified by fowl plague virus. *Virology* 74, 489-503.

INGLIS, S.C., Mahy, B.J.W. (1979). Polypeptide specified by the influenza genome. III. Control of synthesis in infected cells. *Virology* 95, 154-164.

ITO, T., Gorman, O.T., Kawaoka, Y., Bean, W.J., Webster, R.G. (1991). Evolutionary analysis of the influenza A virus M gene with comparison of the M1 and M2 proteins. *Journal of Virology* 65, 5491-5498.

JACKSON, D.C., Tang, X-L, Murti, G.K., Webster, R.G.,

Tregear, G.W., Bean, W.J. (1991). Electron microscopic evidence for the association of M2 protein with the influenza virion. *Archives of Virology* 118, 199-207.

KABANOV, A.V., Vinogradov, S.C., Ovcharenko, A.V., Krivonos, A.V., Melik-Nubarov, N.S., Kiselev, V.I., Severin, E.S. (1990). A new class of antivirals: antisense oligonucleotides combined with a hydrophobic substituent effectively inhibit influenza virus reproduction and synthesis of virus-specific proteins in MDCK cells. *FEBS Letters* 259, 327-330.

KABAT, D., Sherton, C.C., Evans, L.H., Bigley, R., Koler, R.D. (1975). Synthesis of erythrocyte-specific proteins in cultured Friend leukemia cells. *Cell* 5, 331-338.

KATES, M., Allison, A.C., Tyrrell, D.A.J., James, A.T. (1961). Lipids of influenza virus and their relation to those of the host cell. *Biochimica et Biophysica Acta* 52, 455-466.

KAWAKAMI, K., Ishihama, A. (1983). RNA polymerase of influenza virus. III. Isolation of RNA polymerase-RNA complexes from influenza virus PR8. *Journal of Biochemistry* 93, 989-996.

KAWAOKA, Y. Krouss, S., Webster, R.G. (1989). Avian-to-human transmission of the PB1 gene of influenza A viruses in 1957 and 1968 pandemics. *Journal of Virology* 63, 4603-4608.

KELSEY, D.R., Flanagan, T.D., Young, J., Yeagle, P.L. (1990). Peptide inhibitors of enveloped virus infection inhibit phospholipid vesicle fusion and sendai virus fusion with phospholipid vesicles. *Journal of Biological Chemistry* 265, 12178-12183.

KENDAL, P., Goldfield, M., Noble, G.R., Dowdle, W.R. (1977). Identification and preliminary antigenic analysis of swine influenza-like virus isolated during an influenza outbreak at Fort Dix, New Jersey. *Journal of Infectious Diseases* 136, 381-385.

KLAUSNER, R.D., Donaldson, J.G., Lippincott-Schwartz, J. (1992). Brefeldin A. Insights into the control of membrane traffic and organelle structure. *Journal of Cell Biology* 116, 1071-1080.

KLENK, H-D, Compans, R.W., Choppin, W.P. (1970). An electron microscopic study of the presence or absence of neuraminic acid in enveloped viruses. *Virology* 42, 1158-1162.

KLENK, E., Faillard, H., Lempfrid, H. (1955). Über die enzymatische wirkung von influenzavirus. *Hoppe-Seylers Zeitschrift für Physiol Chemie* 301, 235-246.

KLENK, H-D., Rott, R. (1988). The molecular biology of influenza virus pathogenicity. *Advances in Virus Research* 34, 247-281.

KLENK, H-D., Rott, R., Orlich, M., Blödorn, J. (1975). Activation of influenza A viruses by trypsin treatment. *Virology* 68, 426-439.

KLIMKAIT, T., Strebelt, K., Hoggan, M.D., Martin, M.A., Orenstein, J.M. (1990). The human immunodeficiency virus type I-specific protein vpu is required for efficient virus maturation and release. *Journal of Virology* 64, 621-629.

KNIGHT, V., McClung, H.W., Wilson, S.Z., Waters, B.K., Quarles, J.M., Cameron, R.W., Greggs, S.E., Zerwas, J.M., Couch, R.B. (1981). Ribavirin small-particle aerosol treatment of influenza. *Lancet* ii, 945-949.

KOBYASHI, M., Tuchuja, K., Nagata, K., Ishihama, A. (1992). Reconstitution of influenza virus RNA polymerase from three subunits expressed using recombinant baculovirus system. *Virus Research* 22, 235-245.

KRUG, R.M., Alonso-Caplen, F.V., Julkunen, I., Katze, M.G. (1989). Expression and replication of the influenza genome. In 'The Influenza Viruses', pp.89-152. Edited by R.M. Krug, Plenum Publishing, New York.

KRUG, R.M., Morgan, M.A., Shatkin, A.J. (1976). Influenza viral mRNA contains internal N6-methyl-adenosine and 5' terminal 7-methyl-guanosine in cap structures. *Journal of Virology* 20, 45-53.

KRUG, R.M., Ueda, M., Palese, P. (1975). Temperature-sensitive mutants of influenza WSN virus defective in virus-specific RNA synthesis. *Journal of Virology* 16, 790-796.

KURTZ, I., Golchini, K. (1987). Na⁺-independent Cl⁻-HCO₃ exchange in Madin-Darby canine kidney cells. *Journal of Biological Chemistry* 262, 4516-4520.

LADINSKY, M.S., Howell, K.E. (1992). The trans-Golgi network can be dissected structurally and functionally from the cisternae of the Golgi complex by brefeldin A. *European Journal of Cell Biology* 59, 92-105.

LAMB, R.A., Choppin, P.W. (1983). Gene structure and replication of influenza virus. *Annual Reviews in Biochemistry* 52, 467-506.

LAMB, R.A., Lai, C-J., Choppin, P.W. (1981). Sequences of mRNAs derived from genome RNA segment 7 of influenza virus: colinear and interrupted mRNA's code for overlapping proteins. *Proceedings of the National Academy of Sciences* 78, 4170-4174.

LAMB, R.A., Zebedee, S.L., Richardson, R.D. (1985). Influenza virus M2 protein is an integral membrane protein expressed on the infected-cell surface. *Cell* 40, 627-633.

LAVER, W.G. (1978). Crystallization and peptide maps of neuraminidase 'heads' from H2N2 and H3N2 influenza virus strains. *Virology* 86, 78-87.

LAVER, W.G., Valentine, R.C. (1969). Morphology of the isolated hemagglutinin and neuraminidase subunits of influenza viruses. *Virology* 38, 105-119.

LAVER, W.G., Webster, R.G. (1973). Studies on the origin of pandemic influenza. III. Evidence implicating duck and equine viruses as possible progenitors of the Hong Kong strain of human influenza. *Virology* 51, 383-391.

LAZAROWITZ, S.G., Compans, R.W., Choppin, P.W. (1973). Proteolytic cleavage of the hemagglutinin polypeptide of influenza virus. Function of the uncleaved polypeptide HA. *Virology* 52, 199-212.

LEAR, J.D., DeGrado, W.F. (1987). Membrane binding and conformational properties of peptides representing the NH₂ terminus of influenza HA2. *Journal of Biological Chemistry* 262, 6500-6505.

LEAR, J.C., Wasserman, Z.R., DeGrado, W.F. (1988). Synthetic amphiphilic peptide models for protein ion channels. *Science* 240, 1177-1181.

LEITER, J.M.E., Agrawal, S., Palese, P., Zamecnik, P.C. (1990). Inhibition of influenza virus replication by phosphorothiate oligodeoxynucleotides. *Proceedings of the National Academy of Sciences* 87, 3430-3434.

LIPPINCOTT-SCHWARTZ, J., Yuan, L.C., Bonifacino, J.S., Klausner, R.D. (1989). Rapid redistribution of Golgi proteins into ER in cells treated with brefeldin A: evidence for membrane cycling from Golgi to ER. *Cell* 56, 801-813.

LIPSKY, N.G., Pagano, R.E. (1985). A vital stain for the Golgi apparatus. *Science* 228, 745-747.

LOW, S.H., Tang, B.L., Wong, S.H., Hong, W. (1992). Selective inhibition of protein targeting to the apical domain of MDCK cells by brefeldin A. *Journal of Cell Biology* 118, 51-62.

LOW, S.H., Wong, S.H., Tang, B.L., Subramaniam, V.N., Hong, W. (1991). Inhibition by brefeldin A of protein secretion from the apical cell surface of Madin-Darby canine kidney cells. *Journal of Biological Chemistry* 266, 17729-17732.

LUBECK, M.D., Schulman, J.L., Palese, P. (1978).

Susceptibility of influenza A viruses to amantadine is influenced by the gene coding for M protein. *Journal of Virology* 28, 710-716.

LUO, G., Luytjes, W., Enami, M., Palese, P. (1991). The polyadenylation signal of influenza virus RNA involves a stretch of uridines followed by the RNA duplex of the panhandle structure. *Journal of Virology* 65, 2861-2867.

LUZIO, J.P., Brake, B., Banting, G., Howell, K.E., Braghetta, P., Stanley, K.K. (1990). Identification, sequencing and expression of an integral membrane protein of the trans-Golgi network (TGN38). *Biochemical Journal* 270, 97-102.

MAHY, B.W.J., Barrett, T., Nichol, S.T., Penn, C.R., Wolstenholme, A.J. (1981). Analysis of the functions of influenza virus genome RNA segments by use of temperature-sensitive mutants of fowl plague virus. In 'The Replication of Negative Strand Viruses', pp. 379-394. Edited by D.H.L. Bishop and R.W. Compans, Elsevier, New York.

MALDARELLI, F., Chen, M-Y., Willey, R.L., Strebel, K. (1993). Human immunodeficiency virus type 1 vpu protein is an oligomeric type I integral membrane protein. *Journal of Virology* 67, 5056-5061.

MANUGUERRA, J.C., Hannoun, C. (1992). Natural infection of dogs by influenza C virus. *Research in Virology* 143, 199-204.

MARKS, P.A., Rifkind, R.A. (1978). Erythroleukemic differentiation. *Annual Reviews in Biochemistry* 47, 419-448.

MARSH, M., Helenius, A. (1989). Virus entry into animal cells. *Advances in Virus Research* 36, 107-151.

MARTIN, K., Helenius, A. (1991a). Transport of incoming influenza virus nucleocapsids into the nucleus. *Journal of Virology* 65, 232-244.

MARTIN, K., Helenius, A. (1991b). Nuclear transport of influenza virus ribonucleoproteins: the viral matrix protein (M1) promotes export and inhibits import. *Cell* 67, 117-130.

MAST, E.E., Harmon, M.W., Gravenstein, S., Ping Wu, S., Arden, N.H., Circo, R., Tyszka, G., Kendal, A.P., Davis, J.P. (1991). Emergence and possible transmission of amantadine resistant viruses during nursing home outbreaks of influenza A (H3N2). *American Journal of Epidemiology* 134, 988-997.

MATLIN, K.S., Reggio, H., Helenius, A., Simons, K. (1981).

Infectious entry pathway of influenza virus in a canine kidney cell line. *Journal of Cell Biology* 91, 601-613.

MATLIN, K.S., Simons, K. (1983). Reduced temperature prevents the transfer of a membrane glycoprotein to the cell surface but does not prevent terminal glycosylation. *Cell* 34, 233-243.

MATROSOVICH, M.N., Mochalova, L.V., Marinina, V.P., Byramova, N.E., Bovin, N.V. (1990). Synthetic polymeric sialoside inhibitors of influenza virus receptor-binding activity. *FEBS Letters* 272, 209-212.

McCLUNG, H.W., Knight, V., Gilbert, B.E., Wilson, S.Z., Quarles, J.M., Divine, G.W. (1983). Ribavirin aerosol treatment of influenza B virus infection. *Journal of American Medical Association* 249, 2671-2674.

MEYER, H.M., Hepps, H.E., Parkman, P.D., Ennis, F.A. (1978). A review of existing vaccines for influenza. *American Journal of Clinical Pathology* 70, 146-152.

MEIKLEJOHN, G., Eickhoff, T.C., Graves, P., Josephine, I. (1978). Antigenic drift and efficacy of influenza virus vaccines, 1976-1977. *Journal of Infectious Diseases* 138, 618-624.

MUKAIGAWA, J., Nayak, D.P. (1991). Two signals mediate nuclear localization of influenza virus (A/WSN/33) polymerase basic protein 2. *Journal of Virology*, 65, 245-253.

MULLER, C.P., Volloch, Z., Shinitzky, M. (1982). Correlation between cell density, membrane fluidity and the availability of transferrin receptors in Friend erythroleukaemia cells. *Cell Biophysics* 2, 233-240.

MURATA, M., Sugahara, Y., Takahashi, S., Ohnishi, S. (1987). pH-dependent membrane fusion activity of a synthetic twenty amino acid peptide with the same sequence as that of the hydrophobic segment of influenza virus hemagglutinin. *Journal of Biochemistry* 102, 957-962.

MURPHY, B.R., Channock, R.M., Clements, M.L., Anthony, W.C., Sear, A.J., Cisneras, L.A., Rennels, M.B., Miller, E.H., Black, R.E., Levine, M.M., Betts R.F., Douglas, R.G., Maassab, H.F., Cox, N.J., Kendal, A.P. (1981). Evaluation of A/Alaska/6/77 (H3N2) cold-adapted recombinant viruses derived from A/Ann Arbor/6/60 cold-adapted donor virus in adult volunteers. *Infection and Immunity* 32, 693-697.

MURPHY, B.R., Holley, H.P., Berquist, E.J., Levine, M.M., Spring, S.B., Maassab, H.F., Kendal, A.P., Channock, R.M. (1979). Cold-adapted variants of influenza A virus: evaluation in adult seronegative volunteers of A/Scotland/840/74 and A/Victoria/3/75 cold-adapted

recombinants derived from the cold-adapted A/Ann Arbor/6/60 strain. *Infection and Immunity* 23, 253-259.

MURTI, K.G., Bean, W.J., Webster, R.G. (1980). Helical ribonucleoproteins of influenza virus: an electron microscopic analysis. *Virology* 104, 224-229.

MURTI, K.G., Brown, P.S., Bean, W.J., Webster, R.G. (1992). Composition of the helical internal components of influenza virus as revealed by immunogold labeling/electron microscopy. *Virology* 186, 294-299.

MURTI, K.G., Webster, R.G. (1986). Distribution of hemagglutinin and neuraminidase on influenza virions as revealed by immunoelectron microscopy. *Virology* 149, 36-43.

MURTI, K.G., Webster, R.G., Jones, I.M. (1988). Localization of RNA polymerases on influenza viral ribonucleoproteins by immunogold labelling. *Virology* 164, 562-566.

NAEVE, C.W., Williams, D. (1990). Fatty acids on the A/Japan/305/57 influenza virus hemagglutinin have a role in membrane fusion. *EMBO Journal* 9, 3857-3866.

NAGAI, T., Miyaichi, Y., Tominori, T., Suzuki, Y., Yamada, H. (1990). Inhibition of influenza virus sialidase and anti-influenza virus activity by plant flavonoids. *Chemical Pharmacology Bulletin* 38, 1329-1332.

NAGAI, T., Miyaichi, Y., Tomimori, T., Suzuki, Y., Yamada, H. (1992). *In vivo* anti-influenza virus activity of plant flavonoids possessing inhibitory activity for influenza virus sialidase. *Antiviral Research* 19, 207-217.

NAGATA, K., Sakagami, H., Harada, H., Nonoyama, M., Ishihama, A., Konno, K. (1990). Inhibition of influenza virus infection by pine cone antitumor substances. *Antiviral Research* 13, 11-22.

NAIM, H.Y., Amarneh, B., Ktistakis, N.T., Roth, M.G. (1992). Effects of altering palmitoylation sites on biosynthesis and function of the influenza virus hemagglutinin. *Journal of Virology* 66, 7585-7588.

NAKAMURA, K., Compans, R.W. (1979). Host cell- and virus strain-dependent differences in oligosaccharides of hemagglutinin glycoproteins of influenza A viruses. *Virology* 95, 8-23.

NATH, S.T., Nayak, D.P. (1990). Function of two discrete regions is required for nuclear localization of polymerase basic protein I of A/WSN/33 influenza virus (H1N1). *Molecular and Cellular Biology* 10, 4139-4145.

NEEDHAM, M., Gooding, C., Hudson, K., Antoniou, M. Grosveld, F., Hollis, M. (1992). LCR/MEL: A versatile system for high-level expression of heterologous proteins in erythroid cells. *Nucleic Acids Research* 20, 997-1003.

NOBLE, S., McGregor, M.S., Wentworth, D.E., Hinshaw, V.S. (1993). Antigenic and genetic conservation of the haemagglutinin in H1N1 swine influenza viruses. *Journal of General Virology* 74, 1197-1200.

ODAGIRI, T., Tobita, K. (1990). Mutation in NS2, a non-structural protein of influenza A virus, extragenetically causes aberrant replication and expression of the PA gene and leads to generation of defective interfering particles. *Proceedings of the National Academy of Sciences* 87, 5988-5992.

OLMSTED, R.A., Collins, P.L. (1989). The 1A protein of respiratory syncytial virus is an integral membrane protein present as multiple, structurally distinct species. *Journal of Virology* 63, 2019-2029.

OWEN, C.S. (1992). Comparison of spectrum shifting intracellular pH probes 5' (and 6')-carboxy-10-dimethylamino-3-hydroxy-spiro[7H-benzo[c]xanthene-7, 1'(3'H)-isobenzofuran]-3'-one and 2', 7'-biscarboxyethyl-5 (and 6)-carboxyfluorescein. *Analytical Biochemistry* 204, 65-71.

OXFORD, J.S., Schild, G.C. (1967). Inhibition of growth of influenza and rubella viruses by amines and ammonium salts. *British Journal of Experimental Pathology* 48, 235-243.

PAGANO, R.E., Martin, O.C., Kang, H.C., Haughland, R.P. (1991). A novel fluorescent ceramide analogue for studying membrane traffic in animal cells: accumulation at the Golgi apparatus results in altered spectral properties of the sphingolipid precursor. *Journal of Cell Biology* 113, 1267-1279

PAGANO, R.E., Sepanski, M.A., Martin, O.C. (1989). Molecular trapping of a fluorescent ceramide analogue at the Golgi apparatus of fixed cells: interaction with endogenous lipids provides a trans-Golgi marker for both light and electron microscopy. *Journal of Cell Biology* 109, 2067-2079.

PALESE, P., Compans, R.W. (1976). Inhibition of influenza virus replication in tissue culture by 2-deoxy-2,3-dehydro-N-trifluoroacetylneuraminic acid (FANA): mechanism of action. *Journal of General Virology* 33, 159-163.

PALESE, P., Tobita, K., Ueda, M. (1974). Characterization of temperature sensitive influenza virus mutants defective in neuraminidase. *Virology* 61, 397-410.

PASTERNAK, C.A., Micklem, K.J. (1981). Virally induced alterations in cellular permeability: a basis of cellular and physiological damage? *Bioscience Reports* 1, 431-448.

PATTERSON, S., Gross, J., Oxford, J.S. (1988). Intracellular distribution of influenza virus matrix protein and nucleoprotein in infected cells and their relationship to haemagglutinin in the plasma membrane. *Journal of General Virology* 69, 1859-1872.

PAYLER, D.K., Purdham, P.A. (1984). Influenza A prophylaxis with amantadine in a boarding school. *Lancet* i, 502-504.

PETRI, T., Dimmock, N.J. (1981). Phosphorylation of influenza virus nucleoprotein *in vivo*. *Journal of General Virology* 57, 185-190.

PINTO, L.H., Holsinger, L.J., Lamb, R.A. (1992). Influenza virus M2 protein has ion channel activity. *Cell* 69, 517-528.

PILARSKY, C., Koch-Brandt, C. (1992). Acidification slows the transport but does not influence the polarity of secretion of gp80 in polarized epithelial cell MDCK. *European Journal of Cell Biology* 59, 275-279.

PLOTCH, S.J., Bouloy, M., Ulmanen, I., Krug, R.M. (1981). A unique cap(m7GpppXm)-dependent influenza virion endonuclease cleaves capped RNA's to generate the primers that initiate viral RNA transcription. *Cell* 23, 847-858.

PONS, M.W. (1975). Influenza virus messenger ribonucleoprotein. *Virology* 67, 209-218.

PORTERFIELD, J. (1960). A simple plaque-inhibition test for the study of arthropod-borne viruses. *Bulletin of the World Health Organisation* 22, 373-380.

PRITCHETT, T.J., Brossmer, R., Rose, U., Paulson, J.C. (1987). Recognition of monovalent sialosides by influenza virus H3 hemagglutinin. *Virology* 160, 502-506.

PRIVALSKY, M.L., Penhoet, E.E. (1981). The structure and synthesis of influenza virus phosphoproteins. *Journal of Biological Chemistry* 256, 5368-5376.

PRYDZ, K., Hansen, S.H., Sandvig, K., van Deurs, B. (1992). Effects of brefeldin A on endocytosis, transcytosis and transport to the Golgi complex in polarized MDCK cells. *Journal of Cell Biology* 119, 259-272.

REAVES, B., Horn, M., Banting, G. (1993). TGN38/41 recycles between the cell surface and the TGN: Brefeldin A affects its rate of return to the TGN. *Molecular Biology*

of the Cell 4, 93-105.

REES, P.J., Dimmock, N.J. (1981). Electrophoretic separation of influenza virus ribonucleoproteins. *Journal of General Virology* 53, 125-132.

RICHARDSON, J.C., Akkina, R.K. (1991). NS2 protein of influenza virus is found in purified virus and phosphorylated in infected cells. *Archives of Virology* 116, 69-80.

RICHARDSON, C., Scheid, A., Choppin, P. (1980). Specific inhibition of paramyxovirus and myxovirus replication by oligopeptides with amino acid sequences similar to those at the N-termini of the F₁ or HA₂ polypeptides. *Virology* 105, 205-222.

RICHMAN, D.D., Yazaki, P., Hostetler, K.Y. (1981). The intracellular distribution and antiviral activity of amantadine. *Virology* 112, 81-90.

RINK, T.J., Tsien, R.Y., Pozzan, T. (1982). Cytoplasmic pH and free Mg²⁺ in lymphocytes. *Journal of Cell Biology* 95, 189-196.

RITTER, M., Steidl, M., Lang, F. (1991). Inhibition of ion conductances by osmotic shrinkage of Madin-Sarby canine kidney cells. *American Journal of Physiology* 261, C602-C607.

ROBERTS, P.C., Garten, W., Klenk, H-D. (1993). Role of conserved glycosylation sites in maturation and transport of influenza A virus hemagglutinin. *Journal of Virology* 67, 3048-3060.

RODRIGUEZ-BOULAN, E., Paskiet, K.T., Salas, P.J.I., Bard, E. (1984). Intracellular transport of influenza virus hemagglutinin to the apical surface of Madin-Darby canine kidney cells. *Journal of Cell Biology* 98, 308-319.

RODRIGUEZ-BOULAN, E., Sabatini, D. (1978). Polarized distribution of viral envelope proteins in the plasma membrane of infected epithelial cells. *Cell* 20, 45-54.

ROGERS, G.N., Daniels, R.S., Skehel, J.J., Wiley, D.C., Wang, X-F, Higa, H.H., Paulson, J.C. (1985). Host-mediated selection of influenza virus receptor variants. *Journal of Biological Chemistry* 260, 7362-7367.

ROGERS, G.N., Paulson, J.C. (1983). Receptor determinants of human and animal influenza virus isolates: differences in receptor specificity of the H3 hemagglutinin based on species of origin. *Virology* 127, 361-373.

ROGERS, G.N., Pritchett, R.J., Lane, J.L., Paulson, J.C. (1983). Differential sensitivity of human, avian and

equine influenza A viruses to a glycoprotein inhibitor of infection. Selection of receptor specific variants. *Virology* 31, 394-408.

ROMANOS, M.A., Hay, A.J. (1984). Identification of the influenza virus transcriptase by affinity-labeling with pyridoxal 5' phosphate. *Virology* 132, 110-117.

ROTH, M.G., Fitzpatrick, J., Compans, R.W. (1979). Polarity of influenza and vesicular stomatitis virus maturation in MDCK cells. Lack of a requirement for glycosylation of viral glycoproteins. *Proceedings of the National Academy of Sciences* 76, 6430-6434.

ROTH, M.G., Gething, M.J., Sambrook, J. (1989). Membrane insertion and intracellular transport of influenza virus glycoproteins. In 'The Influenza Viruses', pp.219-269. Edited by R.M. Krug, Plenum, New York.

RUBEN, F.L. (1987). Prevention and control of influenza: role of vaccine. *American Journal of Medicine* 82 suppl. 6A, 31-34.

RUIGROK, R.W.H., Aitken, A., Calder, L.J., Martin, S.R., Skehel, J.J., Wharton, S.A., Weis, W., Wiley, D.C. (1988). Studies on the structure of the influenza virus haemagglutinin at the pH of membrane fusion. *Journal of General Virology* 69, 2785-2795.

RUIGROK, R.W.H., Calder, L.J., Wharton, S.A. (1989). Electron microscopy of the influenza virus submembranal structure. *Virology* 173, 311-316.

RUIGROK, R.W.H., Hirst, E.M.A., Hay, A.J. (1991). The specific inhibition of influenza A virus maturation by amantadine: an electron microscopic examination. *Journal of General Virology* 72, 191-194.

RYAN-POIRIER, K.A., Kawaoka, Y. (1991). Distinct glycoprotein inhibitors of influenza A virus in different animal sera. *Journal of Virology* 65, 389-395.

SAKAGAMI, H., Nagata, K., Ishihama, A., Oh-hara, T., Kawazoe, Y. (1990). Anti-influenza activity of synthetically polymerised phenylpropenoids. *Biochemical and Biophysical Research Communications* 172, 1267-1272.

SANDVIG, K., Prydz, K., Ryd, M., van Deurs, B. (1991). Endocytosis and intracellular transport of the glycolipid-binding ligand shiga toxin in polarized MDCK cells. *Journal of Cell Biology* 113, 553-562.

SANSOM, M.S.P., Kerr, I.D. (1993). Influenza virus M2 protein: a molecular modelling study of the ion channel. *Protein Engineering* 6, 65-74.

SAUTER, N.K., Bednarski, M.D., Wurzburg, B.A., Hanson, J.E., Whitesides, G.M., Skehel, J.J., Wiley, W.C. (1989). Hemagglutinins from two influenza virus variants bind to sialic acid derivatives with millimolar dissociation constants: A 500-MHz proton nuclear magnetic resonance study. *Biochemistry* 28, 8388-8396.

SCHLEGEL, A., Omar, A., Jentsch, P., Morell, A., Kempf, C. (1991). Semliki Forest virus envelope proteins function as proton channels. *Bioscience Reports* 11, 243-255.

SCHULMAN, J.L., Palese, P. (1975). Susceptibility of different strains of influenza A virus to the inhibitory effects of 2-deoxy-2,3-dehydro-N-trifluoro-acetylneuraminic acid (FANA). *Virology* 63, 98-104.

SEARS, S.D., Clements, M.L., Betts, R.F., Maassab, H.F., Murphy, B.R., Snyder, M.H. (1988). Comparison of live attenuated H1N1 and H3N2 cold-adapted and avian-human influenza A reassortant viruses and inactivated virus vaccine in adults. *Journal of Infectious Diseases* 158, 1209-1219.

SEBESAN, S., Duus, J.Ø., Neira, S., Domaille, P., Kelm, S., Paulson, J.C., Book, K. (1992). Cluster sialoside inhibitors for influenza virus: synthesis, NMR and biological studies. *Journal of the American Chemical Society* 114, 8363-8375.

SEKSEK, O., Henry-Toullmé, N., Sureau, F., Bolard, J. (1991). SNARF-1 as an intracellular pH indicator in laser microspectrofluorometry: a critical assessment. *Analytical Biochemistry* 193, 49-54.

SEGAL, M.S., Bye, J.M., Sambrook, J.F., Gething, M-J.H. (1992). Disulfide bond formation during the folding of influenza virus hemagglutinin. *Journal of Cell Biology* 118, 227-244.

SELVAGGIO, A.M., Schwartz, J.H., Bengel, H.H., Alexander, E.A. (1986). Kinetics of the Na⁺-H⁺ antiporter as assessed by the change in intracellular pH in MDCK cells. *American Journal of Physiology* 251, C558-562.

SHAPIRO, G.I., Krug, R.M. (1988). Influenza virus RNA replication *in vitro*: synthesis of viral template RNA's and virion RNA's in absence of added primer. *Journal of Virology* 62, 2285-2290.

SHAW, M.W., Lamon, E.W., Compans, R.W. (1982). Immunologic studies of the influenza nonstructural protein NS1. *Journal of Experimental Medicine* 156, 243-254.

SKEHEL, J.J., Bayley, P.M., Brown, E.B., Martin, S.R., Waterfield, M.D., White, J.M., Wilson, I.A., Wiley, D.C. (1982). Changes in the conformation of influenza virus

hemagglutinin at the pH optimum of virus-mediated fusion. Proceedings of the National Academy of Sciences 79, 968-972.

SKEHEL, J.J., Schild, G.C. (1971). The polypeptide composition of influenza A viruses. Virology 44, 396-408.

SMITH, A.R., Bournsnel, M.E.G., Binns, M.M., Brown, T.D.K., Inglis, S.C. (1990). Identification of a new membrane-associated polypeptide specified by the coronavirus infectious bronchitis virus. Journal of General Virology 71, 3-11.

SPALTENSTEIN, A., Whitesides, G.M. (1991). Polyacrylamides bearing pendant α -sialoside groups strongly inhibit agglutination of erythrocytes by influenza virus. Journal of the American Chemical Society 113, 686-687.

STEINHAEUER, D.A., Holland, J.J. (1987). Rapid evolution of RNA viruses. Annual Reviews of Microbiology 41, 409-433.

STEINHAEUER, D.A., Wharton, S.A., Skehel, J.J., Wiley, D.C., Hay, A.J. (1991). Amantadine selection of a mutant influenza virus containing an acid-stable hemagglutinin glycoprotein: Evidence for virus-specific regulation of pH of glycoprotein transport vesicles. Proceedings of the National Academy of Sciences 88, 11525-11529.

STIENEKE-GRÖBER, A., Vey, M., Angliker, H., Shaw, E., Thomas, G., Roberts, C., Klenk, H-D., Garten, W. (1992). Influenza virus hemagglutinin with multibasic cleavage site is activated by furin, a subtilisin-like endoprotease. EMBO Journal 11, 2407-2414.

STRIDH, S. (1983). Determination of ribonucleoside triphosphate pools in influenza A virus-infected MDCK cells. Archives of Virology 77, 223-229.

STRIDH, S., Öberg, B., Chattopadhyaya, J., Josephson, S. (1981). Functional analysis of influenza RNA polymerase activity by the use of caps, oligonucleotides and polynucleotides. Antiviral Research 1, 97-105.

SUGRUE, R.J., Bahadur, G., Zambon, M.C., Hall-Smith, M., Douglas, A.R., Hay, A.J. (1990a). Specific structural alteration of the influenza haemagglutinin by amantadine. EMBO Journal 9, 3469-3476.

SUGRUE, R.J., Belshe, R.B., Hay, A.J. (1990b). Palmitoylation of the influenza A virus M2 protein. Virology 179, 51-56.

SUGRUE, R.J., Hay, A.J. (1991). Structural characteristics of the M2 protein of influenza A viruses: evidence that it forms a tetrameric channel. Virology 180, 617-624.

SUZUKI, Y., Nagao, Y., Kato, H., Matsumoto, M., Nerome, K., Nakajima, K., Nobusawa, E. (1986). Human influenza A virus hemagglutinin distinguishes sialyoligosaccharides in membrane-associated gangliosides as its receptor which mediates the adsorption and fusion processes of virus infection. *Journal of Biological Chemistry* 261, 17057-17061.

SWEET, C., Hayden, F.G., Jakeman, K.J., Grambas, S., Hay, A.J. (1991). Virulence of rimantadine-resistant human influenza A (H3N2) viruses in ferrets. *Journal of Infectious Diseases* 164, 969-972.

TARTAKOFF, A.M., Vassalli, P. (1983). Lectin-binding sites as markers of Golgi subcompartments: Proximal to distal maturation of oligosaccharides. *Journal of Cell Biology* 97, 1243-1248.

TAKATSY, G., Romvary, J., Farkas, E. (1967). Susceptibility of the domestic swine to influenza B virus. *Acta Microbiology Academy of Sciences Hungary* 14, 309-315.

THOMAS, J.A., Bucksbaum, R.N., Zimniak, A., Racker, E. (1979). Intracellular pH measurement in Ehrlich ascites tumor cells utilizing spectroscopic probes generated in situ. *Biochemistry* 18, 2210-2218.

TISDALE, M., Appleyard, G., Tuttle, J.V., Nelson, D.J., Nusinoff-Lehrman, S., Al Nakib, W., Stables, J.N., Purifoy, D.J.M., Powell, K.L., Darby, G. (1993). Inhibition of influenza A and B viruses by 2'-deoxy-2'-fluororibosides. *Antiviral Chemistry and Chemotherapy* 4, 281-287.

TOMINACK, R.L., Hayden, F.G. (1987). Rimantadine hydrochloride and amantadine hydrochloride use in influenza A virus infections. *Infectious Diseases Clinics of North America* 1, 459-478.

TSIEN, R.Y. (1989). Fluorescent indicators of ion concentration. In 'Methods in Cell Biology, Volume 30', pp.127-156. Edited by D. Lansing Taylor and Y-L Wang, Academic Press, New York and London.

TULIP, W.R., Varghese, J.N., Baker, A.T., van Donkelaar, A., Laver, W.G., Webster, R.G., Colman, P.M. (1991). Refined atomic structures of N9 subtype influenza virus neuraminidase and escape mutants. *Journal of Molecular Biology* 221, 487-497.

ULMANEN, I., Broni, B.A., Krug, R.M. (1981). The role of two of the influenza virus core P proteins in recognizing cap I structures (m7GpppNm) on RNA's and initiating viral RNA transcription. *Proceedings of the National Academy of Sciences* 78, 7355-7359.

UNDERWOOD, P.A. (1985). Receptor-binding characteristics

of strains of influenza Hong Kong subtype, using a periodate sensitivity test. Archives of Virology 84, 53-61.

VALCÁRCEL, J., Portela, A., Ortin, J. (1991). Regulated M1 mRNA splicing in influenza virus-infected cells. Journal of General Virology 72, 1301-1308.

VAN ERP, P.E.J., Jansen, M.J.J.M., de Jongh, G.J., Boezeman, J.B.M., Schalkwijk, J. (1991). Ratiometric measurement of intracellular pH in cultured human keratinocytes using carboxy-SNARF-1 and flow cytometry. Cytometry 12, 127-132.

VAN WYKE, K.L., Bean, W.J., Webster, R.G. (1981). Monoclonal antibodies to the influenza A virus nucleoprotein affecting RNA transcription. Journal of Virology 39, 313-317.

VARGHESE, J.N., Colman, P.M. (1991). Three dimensional structure of the neuraminidase of influenza virus A/Tokyo/3/67 at 2.2A resolution. Journal of Molecular Biology 221, 473-486.

VARGHESE, J.N., Laver, W.G., Colman, P.M. (1983). Structure of the influenza virus glycoprotein antigen neuraminidase at 2.9A resolution. Nature 303, 35-40.

VARGHESE, J.N., McKimm-Breschkin, L., Caldwell, J.B., Kortt, A.A., Colman, P.M. (1992). The structure of the complex between influenza virus neuraminidase and sialic acid, the viral receptor. Proteins: Structure, Function and Genetics 14, 327-332.

VEIT, M., Klenk, H-D., Kendal, A., Rott, R. (1991). The M2 protein of influenza A virus is acylated. Journal of General Virology 72, 1461-1465.

VEIT, M., Kretzschmar, E., Kuroda, K., Garten, W., Schmidt, M.F.G., Klenk, H-D., Rott, R. (1990). Site-specific mutagenesis identifies three cysteine residues in the cytoplasmic tail as acylation sites of influenza virus hemagglutinin. Journal of Virology 65, 2491-2500.

VEY, M., Orlich, M., Adler, S., Klenk, H-D., Rott, R., Garten, W. (1992). Hemagglutinin activation of pathogenic avian influenza viruses of serotype H7 requires the protease motif R-X-K/R-R. Virology 188, 408-413.

VIRTANEN, I., Ekblom, P., Laurila, P. (1980). Subcellular compartmentalization of saccharide moieties in cultured normal and malignant cells. Journal of Cell Biology 85, 429-434.

VOLLOCH, V., Housman, D. (1982). Terminal differentiation of murine erythroleukemia cells: physical stabilization of

end-stage cells. *Journal of Cell biology* 93, 390-394.

VON ITZSTEIN, M., Wu, W-Y., Kok, G.B., Pegg, M.S., Dyason, J.C., Jin, B., Phan, T.V., Smythe, M.L., White, H.F., Oliver, S.W., Colman, P.M., Varghese, J.N., Ryan, D.M., Woods, J.M., Bethell, R.C., Hotham, V.J., Cameron, J.M., Penn, C.R. (1993). Rational design of potent sialidase-based inhibitors of influenza virus replication. *Nature* 363, 418-423.

WAKAMIYA, N., Okuno, Y., Sasao, F., Ueda, S., Yoshimatsu, K., Naiki, M., Kurimura, T. (1992). Isolation and characterization of conglutinin as an influenza A virus inhibitor. *Biochemical and Biophysical Research Communications* 187, 1270-1278.

WALKER, J.A., Sakaguchi, T., Matsuda, Y., Yoshida, T., Kawaoka, Y. (1992). Location and character of the cellular enzyme that cleaves the hemagglutinin of a virulent avian influenza virus. *Virology* 190, 278-287.

WANG, C., Takeuchi, K., Pinto, L.H., Lamb, R.A. (1993). Ion channel activity of influenza A virus M2 protein: characterization of the amantadine block. *Journal of Virology* 67, 5585-5594.

WARD, C.W. (1981). Structure of the influenza virus hemagglutinin. *Current Topics in Microbiology and Immunology* 94, 1-74.

WARD, C.W., Dopheide, T.A. (1981). Evolution of the Hong Kong influenza A subtype. *Biochemical Journal* 195, 337-340.

WARNICK, J.E., Maleque, M.A., Bakry, N., Eldefrawi, A.T., Albuquerque, E.X. (1982). Structure-activity relationships of amantadine. 1. Interaction of the N-alkyl analogues with the ionic channels of the nicotinic acetylcholine receptor and electrically excitable membrane. *Molecular Pharmacology* 22, 82-93.

WATERFIELD, M.D., Gething, M.J., Scrace, G., Skehel, J.J. (1980). The carbohydrate side chains and disulphide bonds of the haemagglutinin of the influenza virus A/Japan/305/57 (H2N1). In 'Structure and Variation in influenza virus', pp.11-20. Edited by G. Laver and G. Air, Elsevier, North Holland, Australia.

WEBSTER, R.G., Brown, L.E., Jackson, D.C. (1983). Changes in the antigenicity of the haemagglutinin molecule of H3 influenza virus at acidic pH. *Virology* 126, 587-599.

WEBSTER, R.G., Campbell, C.H., Granoff, A. (1971). The *in vivo* production of 'new' influenza A viruses. *Virology* 44, 317-328.

WEIS, W., Brown, J.H., Cusack, S., Paulson, J.C., Skehel, J.J., Wiley, D.C. (1988). Structure of the influenza virus haemagglutinin complexed with its receptor, sialic acid. *Nature* 333, 426-431.

WHARTON, S.A., Belshe, R.B., Skehel, J.J., Hay, A.J. (1993). Role of virion M2 protein in influenza virus uncoating - specific reduction in the rate of membrane fusion between virus and liposomes by amantadine. *Journal of General Virology*, in press.

WHARTON, S.A., Hay, A.J., Sugrue, R.J., Skehel, J.J., Weis, W.I., Wiley, D.C. (1990). Membrane fusion by influenza viruses and the mechanism of action of amantadine. In 'Use of X-ray Crystallography in the Design of Antiviral Agents', pp.1-12. Edited by W.G. Laver and G.M. Air, Academic Press, Orlando, FL, USA.

WHARTON, S.A., Martin, S.R., Ruigrok, R.W.H., Skehel, J.J., Wiley, D.C. (1988a). Membrane fusion by peptide analogues of influenza virus haemagglutinin. *Journal of General Virology* 69, 1847-1857.

WHARTON, S.A., Ruigrok, R.W.H., Martin, S.R., Skehel, J.J., Bayley, P.M., Weis, W., Wiley, D.C. (1988b). Conformational aspects of the acid-induced fusion mechanism of influenza virus hemagglutinin. *Journal of Biological Chemistry* 263, 4474-4480.

WHITAKER, J.E., Haugland, R.P., Ryan, D., Dunn, K., Maxfield, F.R., Haugland, R.P. (1991). Dual excitation, pH sensitive conjugates of dextran and transferrin for pH measurement during endocytosis utilizing 514nm to 488nm excitation ratios. *Biophysical Journal* 59, 358a (abstract).

WHITE, J.M. (1990). Viral and cellular membrane fusion proteins. *Annual Reviews in Physiology* 52, 675-697.

WHITE, J.M., Wilson, I.A. (1987). Antipeptide antibodies detect steps in a protein conformational change: low-pH activation of the influenza virus hemagglutinin. *Journal Cell Biology* 105, 2887-2896.

WILEY, D.C., Skehel, J.J. (1987). The structure and function of the hemagglutinin membrane glycoprotein of influenza virus. *Annual Reviews in Biochemistry* 56, 365-394.

WILEY, D.C., Skehel, J.J., Waterfield, M. (1977). Evidence from studies with a cross-linking reagent that the haemagglutinin of influenza virus is a trimer. *Virology* 79, 446-448.

WILLEY, R.L., Maldarelli, F., Martin, M.A., Strebel, K. (1992). Human immunodeficiency virus type I vpu protein

regulates the formation of intracellular gp160-CD4 complexes. *Journal of Virology* 66, 226-234.

WILLIAMS, M.A., Lamb, R.A. (1986). Determination of the orientation of an integral membrane protein and sites of glycosylation by oligonucleotide-directed mutagenesis: influenza B virus NB glycoprotein lacks a cleavable signal sequence and has an extracellular NH₂-terminal region. *Molecular and Cellular Biology* 6, 4317-4328.

WILSON, I.A., Skehel, J.J., Wiley, D.C. (1981). Structure of the haemagglutinin membrane glycoprotein of influenza virus at 3A resolution. *Nature* 289, 366-373.

WRAY, S.K., Gilbert, B.E., Knight, V. (1985). Effect of ribavirin triphosphate on primer generation and elongation during influenza virus transcription *in vitro*. *Antiviral Research* 5, 39-48.

WRAY, S.K., Gilbert, B.E., Noall, M.W., Knight, V. (1985). Mode of action of ribavirin: effect of nucleotide pool alterations on influenza virus ribonucleoprotein synthesis. *Antiviral Research* 5, 29-37.

WRIGLEY, N.G. (1979). Electron microscopy of influenza virus. *British Medical Bulletin* 35, 35-38.

YE, Z., Pal, R., Fox, J.W., Wagner, R.R. (1987). Functional and antigenic domains of the matrix (M1) protein of influenza A virus. *Journal of Virology* 61, 239-246.

YOSHIMURA, A., Ohnishi, S-I. (1984). Uncoating of influenza virus in endosomes. *Journal of Virology* 51, 497-504.

ZEBEDEE, S.L., Lamb, R.A. (1988). Influenza A virus M2 protein: monoclonal antibody restriction of virus growth and detection of M2 in virions. *Journal of Virology* 62, 2762-2772.

ZEBEDEE, S.L., Richardson, C.D., Lamb, R.A. (1985). Characterisation of the influenza virus M2 integral membrane protein and expression at the infected cell surface from cloned cDNA. *Journal of Virology* 56, 502-511.

ZERIAL, A., Thuong, N.T., Helene, C. (1987). Selective inhibition of the cytopathic effect of type A influenza viruses by oligodeoxynucleotides covalently linked to an intercalating agent. *Nucleic Acids Research* 15, 9909-9919.

ZHIRNOV, O.P. (1990). Solubilization of matrix protein M1/M from virions occurs at different pH for orthomyxo- and paramyxoviruses. *Virology* 176, 274-279.

ZIMMERMAN, T.P., Deeprose, R.D. (1978). Metabolism of 5-amino-1- β -ribofuranosylimidazole-4-carboxamide and related

five-membered heterocycles to 5'-triphosphates in human blood and L5178Y cells. *Biochemical Pharmacology* 27, 709-716.

ZLYDNIKOV, D.M., Kubar, O.I., Kovaleva, T.P., Kamforin, L.E. (1981). Study of rimantadine in the USSR: a review of the literature. *Reviews of Infectious Diseases* 3, 408-421.